STUDIES OF MEMBRANE TRANSPORT AND LIQUID INTERFACES

by

James Laurence Mulligan B.Sc. ARCS

A thesis submitted for the degree of

Doctor of Philosophy of the University of London

and for

The Diploma of Membership of Imperial College

Physical Chemistry Section

Department of Chemistry

Imperial College of Science and Technology

London

December 1987

ABSTRACT

This thesis will describe work performed on lipid bilayers and supported liquid membranes with potential applications to electrochemical sensors , ion-selective electrodes and the study of interfacial polymerisation . The properties of a photo-polymerisable lipid have been studied on a Langmuir trough apparatus and coating characteristics of this lipid on various substrates have been investigated . The substrates studied include untreated polymer microfilters , silylated polyester filters , pure silica slides and gels .

The transference ratio of the substrates, (i.e. the ratio of the area of lipid monolayer covered substrate to the total substrate area), has been measured by an electronic feedback mechanism which keeps the surface pressure constant during the Langmuir-Blodgett dipping procedure .

As well as Langmuir trough studies , black lipid membranes of the polymerisable lipid have been used to investigate the electrochemistry of the lipid bilayers .

The transport of ions through liquid membranes, (e.g. K^+ transport through an organic solvent by means of chelation with valinomycin), has been studied by various means . The flux of halide ions, (e.g. counterions associated with a $KVal^+$ complex), has been followed on a rotating diffusion cell . A silver/silver halide ring electrode in the vicinity of the interface has been used as a potentiometric sensor for

the measurement of the membrane flux .

A.C. Impedance studies have also been employed , yielding information on the transfer of ions at the membrane / solution interface .

Potentiometric ring sensors have also been used to study interfacial polymerisation . For example , reactions forming polypeptide linkages yield hydrogen ions and chloride ions . These fluxes can be detected using the metal/metal oxide pH sensitive electrode and silver/silver chloride electrode respectively .

TO MY MOTHER AND THE MEMORY OF MY FATHER

ACKNOWLEDGEMENTS

I would like to thank :-

John Albery for his supervision.

Ian Lyle and Alec Smith and everybody at Port Sunlight.

The SERC and Unilever for providing the finance for this Ph.D.

Mike Pritchard for making the electrodes and technical asssistance in general , and John Hooper for making the electronics.

Dr.`s Riaz Choudhery , Bruce Lennox and Andrew Mount for their helpful suggestions and guidance.

Andy Mount , Ged O`Shea and Anne Williams for proof reading.

Christine , Bozena and Zoe for all their help.

All the members of the Albery research group past and present for a very enjoyable three and a half years.

Anne , again , for putting up with my ever changing moods during the writing of this thesis.

Bryan , Lyndon , Andy Marks , Postman Pat , Neil , Judith and particularly Jess the cat for being such good flat mates.

All the members of the "chemistry social club" whose names are too numerous to mention.

My family for moral support and encouragement.

CONTENTS

CHAPTER 3 EXPERIMENTAL METHODS

CHAPTER 4 STUDIES ON THE CREATION OF STABLE LIPID BILAYERS

LIST OF FIGURES

CHAPTER 1 INTRODUCTION

CHAPTER 2 THEORY

CHAPTER3 EXPERIMENTAL METHODS

CHAPTER 4 STUDIES ON THE CREATION OF STABLE LIPID BILAYERS

CHAPTER 5 THE DEVELOPMENT OF A NOVEL TECHNIQUE FOR STUDYING DIFFUSION THROUGH LIQUID MEMBRANES

LIST OF TABLES

CHAPTER 1 INTRODUCTION

1.1 The Importance of Membranes

Lipid bilayer membranes , and more generally liquid membranes , are of interest to academia and industry alike for their ability to separate selectively a wide range of molecules or ions from complicated mixtures .

Lipid bilayers can be used as a framework for a variety of enzyme systems[1] , and therefore are particularly applicable as a basis for electrochemical sensors . This thesis relates attempts to overcome the major downfall of lipid bilayers ; that is their intrinsic instability[1] . A general study of Langmuir-Blodgett coating is also instigated .

Following limited success in this field , a study of the diffusion of ions through liquid membranes was undertaken . This involved measuring the flux of halide ions by means of a rotating diffusion cell (RDC) , used in conjunction with an ion-selective arc electrode .

The techniques employed in following the diffusion of material through membranes can also be applied to following the formation of a polymeric membrane at a liquid-liquid interface .

1.2 Lipid Bilayers

1.2.1. Their occurrence in nature

Natural lipid bilayers , (e.g. cell and mitochondria membranes), consist of a bilayer structure with incorporated protein molecules[1,2](fig.1.1) . These membranes usually separate two aqueous regions , and the protein molecules

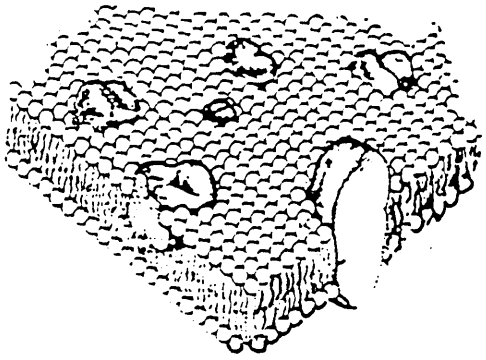

Figure 1.1 A Lipid Bilayer

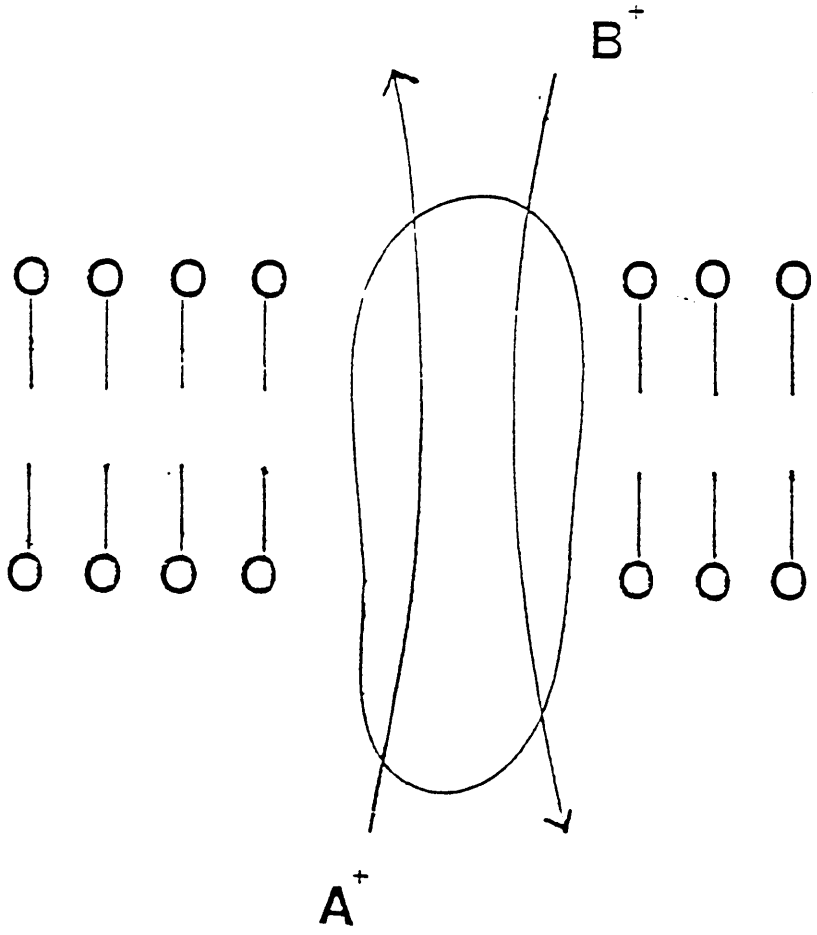

Figure 1.2 An Ion Pumping System

facilitate the passage of specific ions or molecules across the membrane , which would normally be prevented from transversing the bilayer due to the low relative permittivity of the central region (fig.1.2) . An example of this is the sodium / potassium pump which occurs at cell membranes . Sodium ions (A^+) , are shuttled out of the cell and potassium ions (B^+) , into the cell , a mechanism which is required for various metabolic processes[3]. The protein carrier molecule in this example is ATPase .

The specificity of these systems arises due to the presence of sites in the protein molecule which will house species of a particular size and arrangement[3] . The housing of the ion or molecule , in the protein is directly analgous to enzyme catalysis . Another important feature of the pumping systems is the ability of the protein to alter its structure . Consequently species are transported from one side of the membrane to the other[4,5]

1.2.2. Lipid Bilayer Arrangements

Lipid Bilayers can exist in essentially two forms (fig. 1.3) :-

vesicles - these are roughly spherical arrangements of bilayer . They are generally very stable as their structure is energetically favourable , i.e. it forms spontaneously . The problem with vesicles arises from their size ,(in the order of microns) . This results in limiting their use , as there is not easy access of , for example electrodes , to both sides of the membrane . They have been used , however , as drug delivery systems[6] , and as model cell membranes[7] .

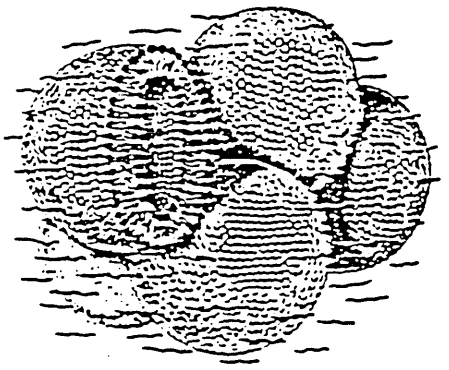

Figure 1.3 Lipid Vesicles

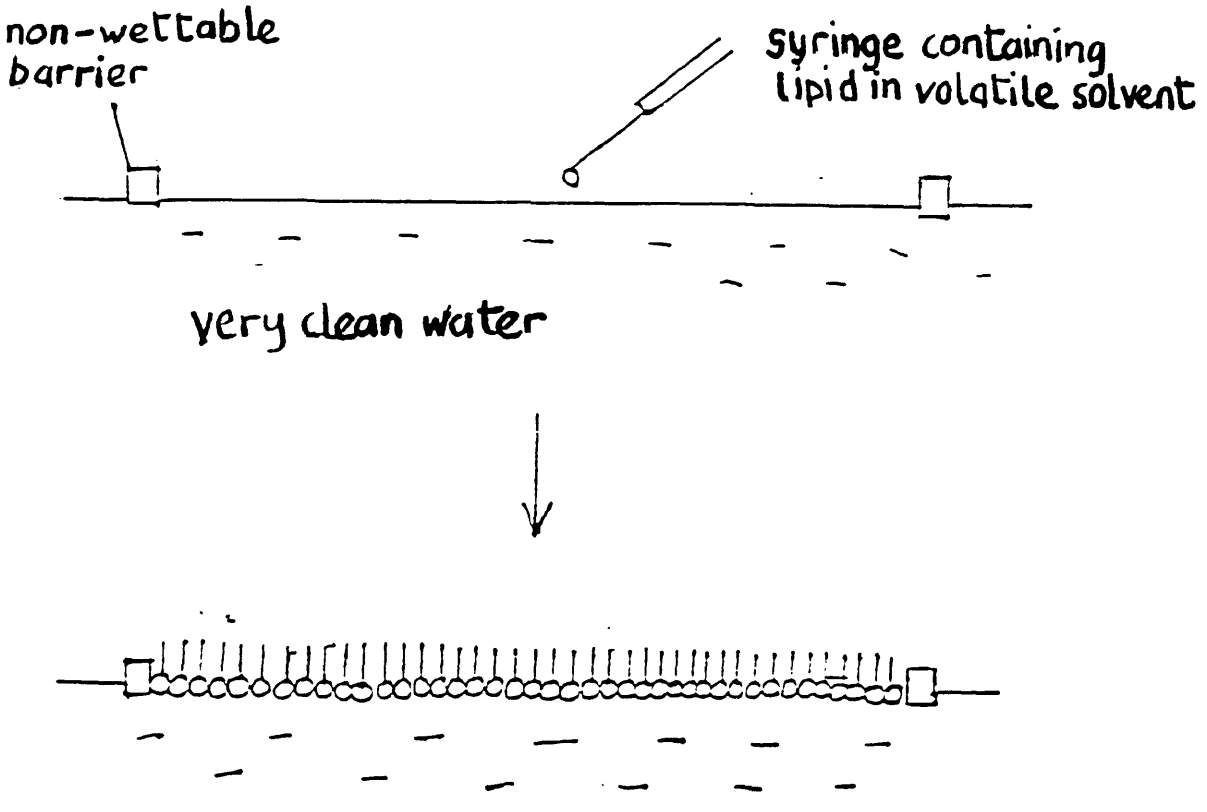

Figure 1.4 Monolayer Formation

planar lipid bilayers - these are , obviously , planar membranes . This arrangement allows easy access of , for example , electrodes to either side of the membrane and so planar bilayers may be used in electrochemical sensors . The drawback of a planar arrangement is that they are inherently unstable .

1.2.3. The stabilisation of planar bilayers

As described above planar bilayer membranes must be formed in order to obtain easy measurement of diffusional , electrochemical and other properties . The main techniques of forming lipid bilayers are as follows .

1.2.3.1. The Langmuir-Blodgett Technique

The ability of oil molecules to spread evenly over a water surface has been known for over two centuries[8] , but it was not until the 1890`s that the characteristics of monolayers were investigated[9,10] . A big step in the study of monolayers at the air-water interface was the discovery that only oils with polar head groups spread on water[11] . Irving Langmuir explained this observation[12] and related Π/A isotherms to the orientation of the molecules forming the monolayer . His observations were backed up by the experimental observation that the cross-sectional area of a fatty acid molecule on a water surface is independent of its chain length[12].

Langmuir's studies on monolayers were extended by a co-worker Katherine Blodgett[13] . In this work glass slides were coated with sections of monolayer by the movement of the slide vertically through the water surface . The success of

this procedure depends on having a constant surface pressure , and therefore a constant molecular cross-sectional area , during the coating of the substrate , i.e. the glass slide . This difficulty was overcome by having the monlayer of interest separated from a monolayer of piston oil by a thread . The piston oil monolayer was in equilibrium with piston oil in the water and so could readily expand to counteract the contraction of the other monolayer by removal of molecules by adsorption onto the substrate . These experiments have been made easier to perform with the advent of sophisticated electronics which can control the area of the monolayer very accurately .

Blodgett noticed three types of deposition X,Y and Z (fig. 1.6) . Y deposition involves coating of the substrate on the upward and downward motions . X and Z depositions involve coating on only the downward or upward motion respectively . Although fig. 1.6 suggests that a series of bilayers are formed only for Y type deposition it has been observed that bilayers are formed even when X and Z deposition occur[14,15] , so evidently rearrangement of molecules on the substrate surface is possible .

The success of deposition is measured in terms of the deposition ratio[16] , Which is the ratio between the area of monolayer removed from the water surface , to the geometric area of the substrate . For easy measurement of substrate area , it must obviously be smooth . This is also important because if the monolayer is deposited on a water filled

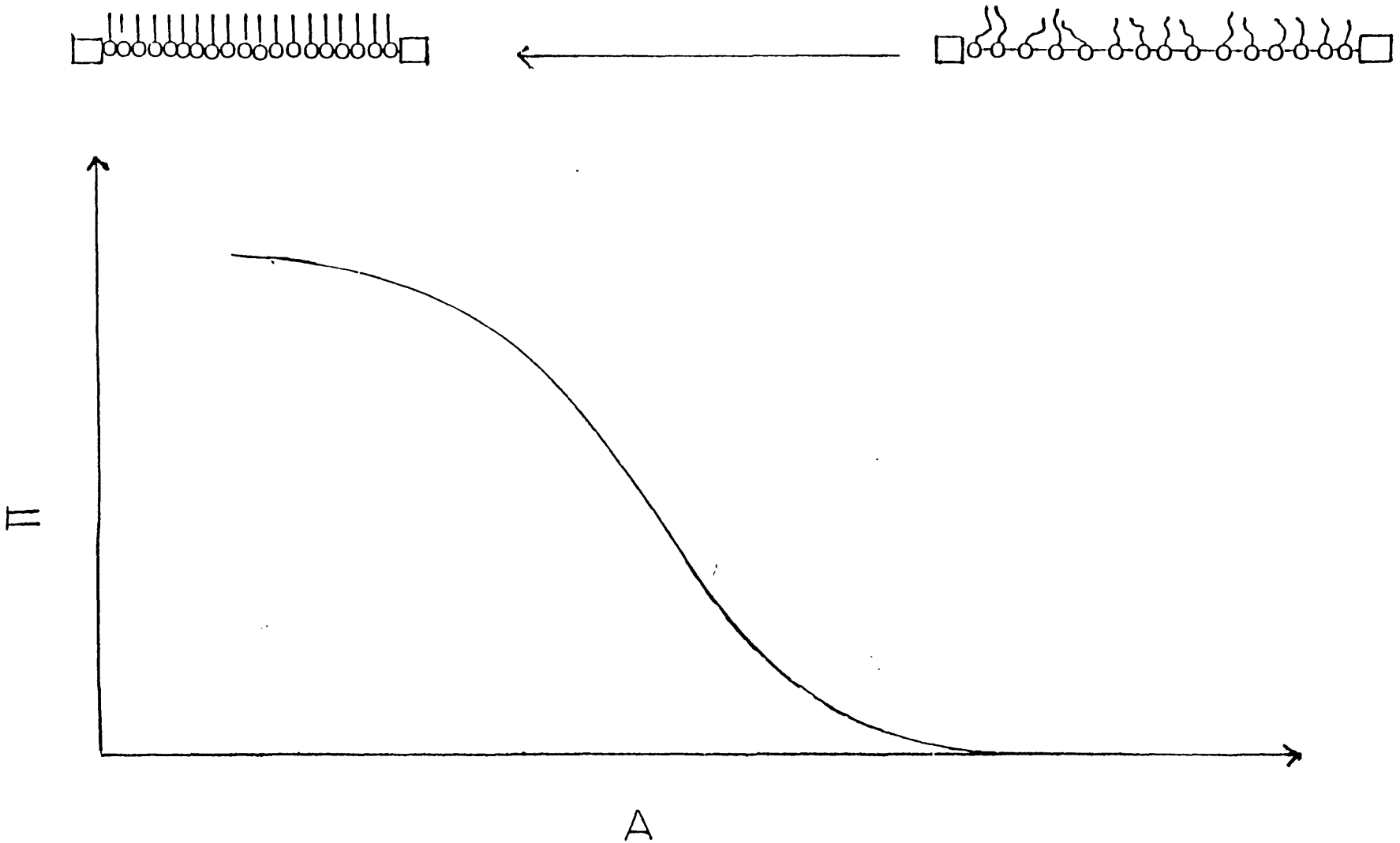

Figure 1.5 A Π / A Isotherm

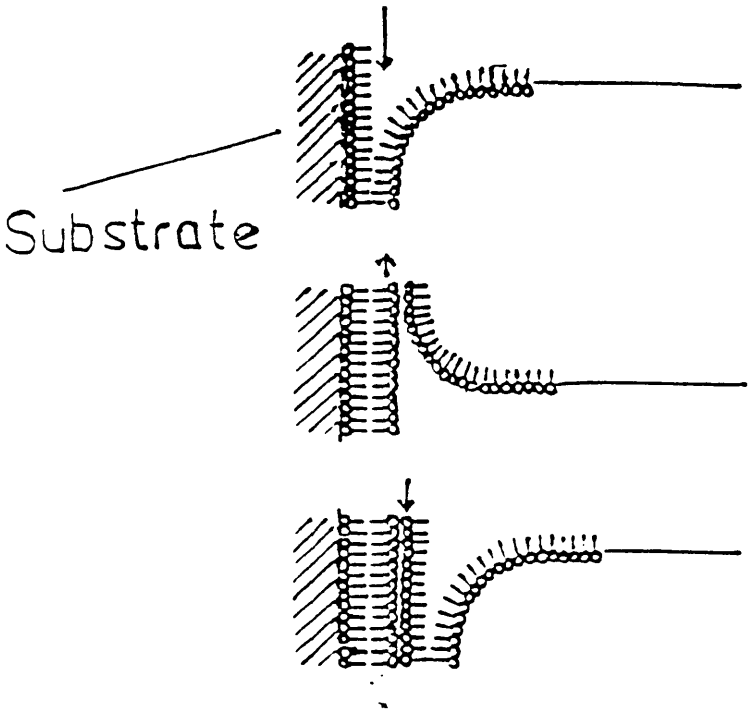

Figure 1.6 Y-Type Deposition

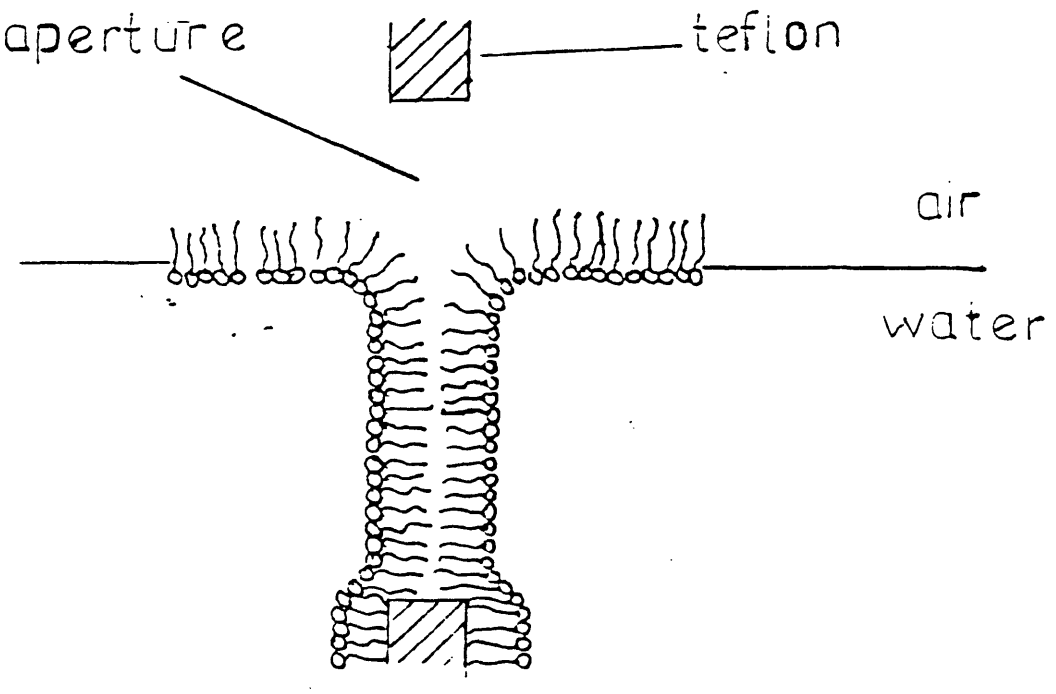

Figure 1.7 The Montal-Mueller Method

indentation , the drying out of the substrate will probably result in the collapse of the monolayer .

There have been numerous modifications to the Langmuir-Blodgett technique : Montal and Mueller[17] devised a technique for forming a bilayer by the movement of a teflon substrate , with an aperture , through the air-water interface (fig. 1.7) Tredgold and Elgamal[18] used a conventional Langmuir-Blodgett technique to form a monolayer coated substrate and then coated a second monolayer in a method similar to that used by Montal and Mueller . Kossi and Leblanc[19] also used a conventional Langmuir-Blodgett method to form the first monolayer , but then used a novel touching method to coat the second onto the substrate (fig. 1.8) . Heckman et al[20] developed a replacement to the Langmuir trough . In the funnel technique (fig 1.9) , a monolayer is spread on water contained in a PTFE funnel . The monlayer is then compressed by simply allowing the water to be steadily released from a tap at the bottom of the funnel . The surface pressure of the monlayer in the straight of the funnel is obtained from a Π/A isotherm of the surfactant . Deposition of material onto the substrate is carried out by allowing the water level to drop by the appropiate amount . Deposition analagous to the downward Langmuir-Blodgett dipping is performed by pumping water back into the funnel by means of a peristaltic pump .

1.2.3.2. Black Lipid Membrane Formation

Lipid bilayers can also be prepared in one step processes as well . Black lipid membrane is the term given to

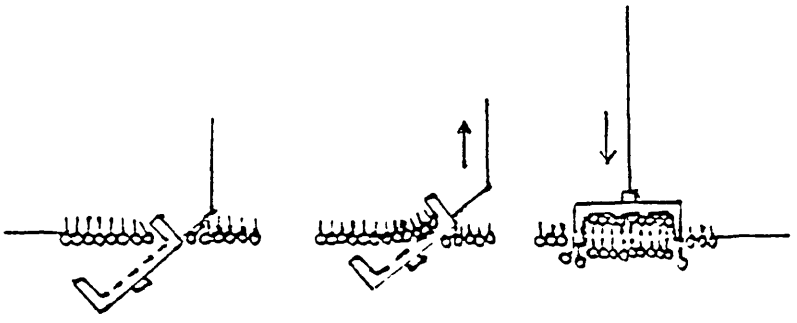

1.8 The Kossi and LeBlanc Method

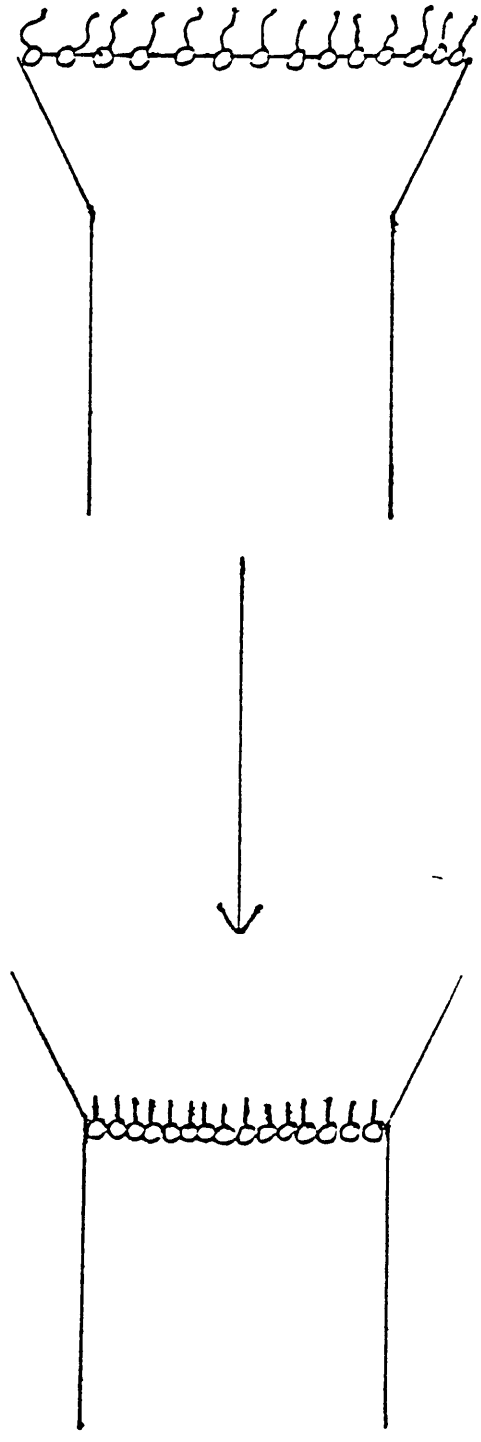

Figure 1.9 The Funnel Technique

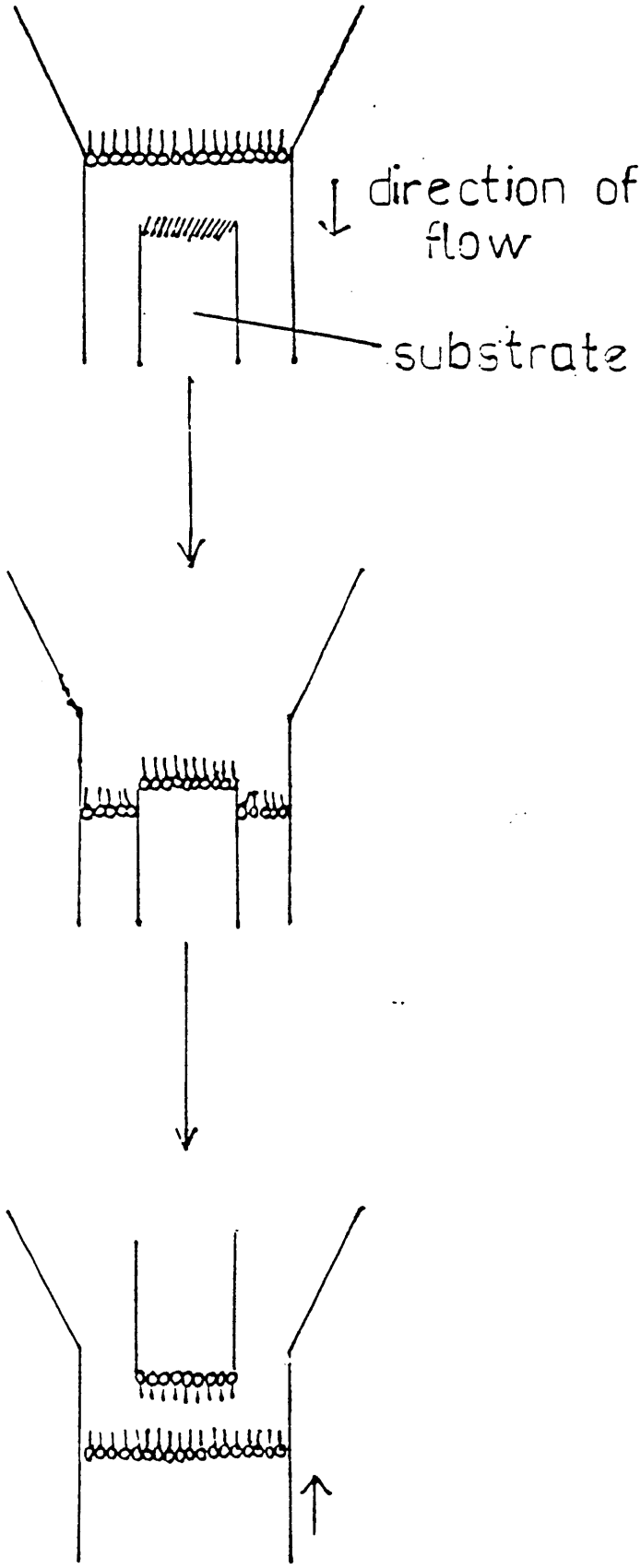

Figure 1.10 The Coating of a Substrate

a bilayer formed by placing a small drop of lipid solution in a small orifice submerged in an aqueous phase . The formed membrane thins , due to the removal of the solvent , over a period of minutes . This technique was first employed as recently as the 1960's [21] . The lipid can be applied by a syringe , brush or similar device . The support is usually an inert , polymeric material (e.g. PTFE , a polyester microfilter) and the orifice (or collection of orifices in the case of microfilters) is at most a few millimetres in diameter . A similar result is obtained if a loop or mesh of metallic or polymeric material is dipped into a lipid solution and then exposed to air . An everyday example of this phenomenon is the formation of soap bubbles (vesicles) in children's toys . An important experimental point in black lipid membrane formation , is that bilayers consisting of pure lipid will almost certainly collapse spontaneously on formation . To increase stability components are added to the lipid solution . The most common strenghthener is oxidised cholesterol which incorporates itself into the bilayer structure but is also unreactive and does not allow the passage of ions through the membrane[21] .

1.2.3.3. Miscellaneous Techniques

Guy and Fleming[22] have used a rotating diffusion cell to study diffusion through a lipid impregnated Millipore filter. In this technique the structure of the lipid layer is not very well defined , and consequently of limited use . Regen et al[23] used the property of lipids to congregate at water-oil interfaces to modify the surface of a hydrophobic

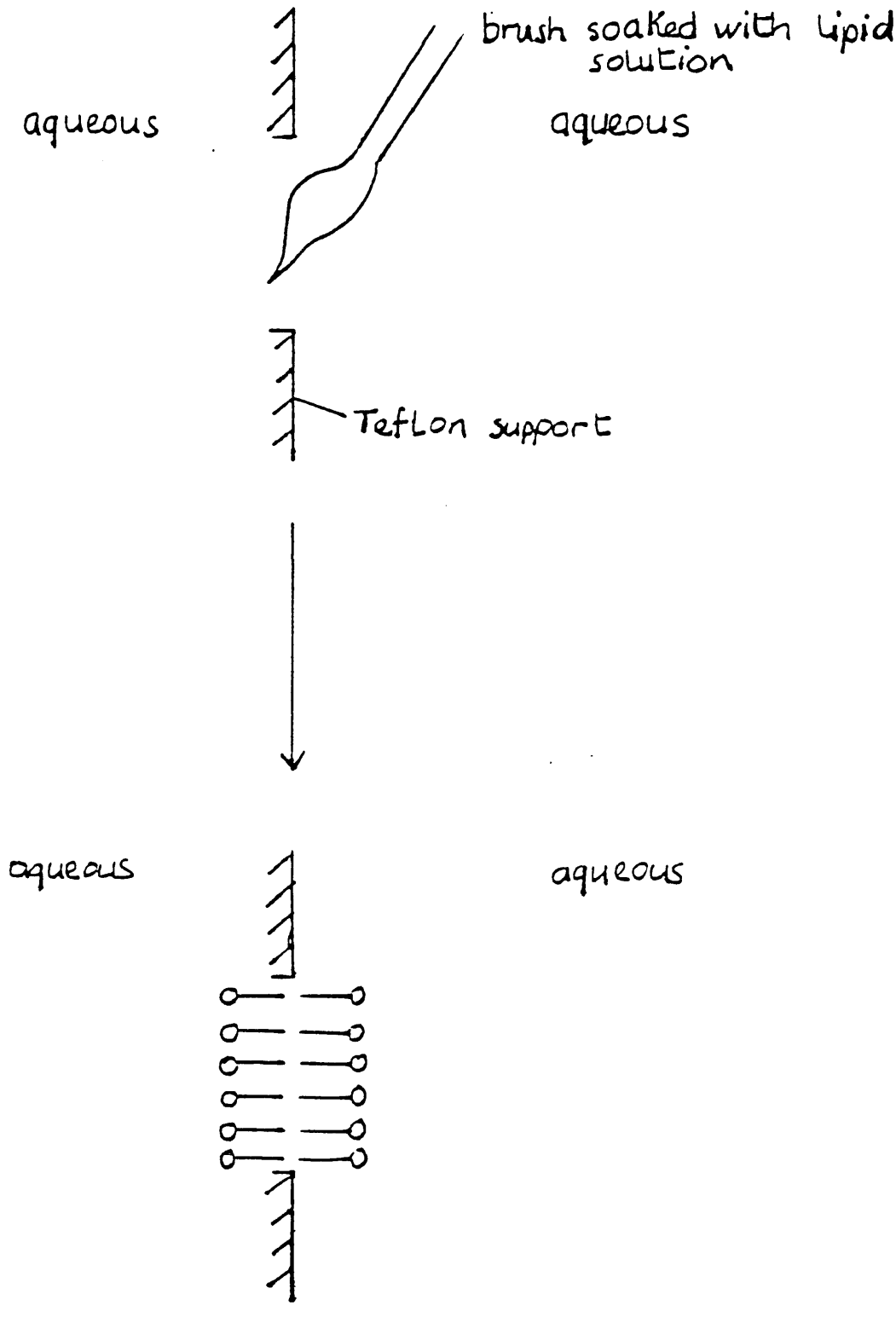

1.11 BLM Formation

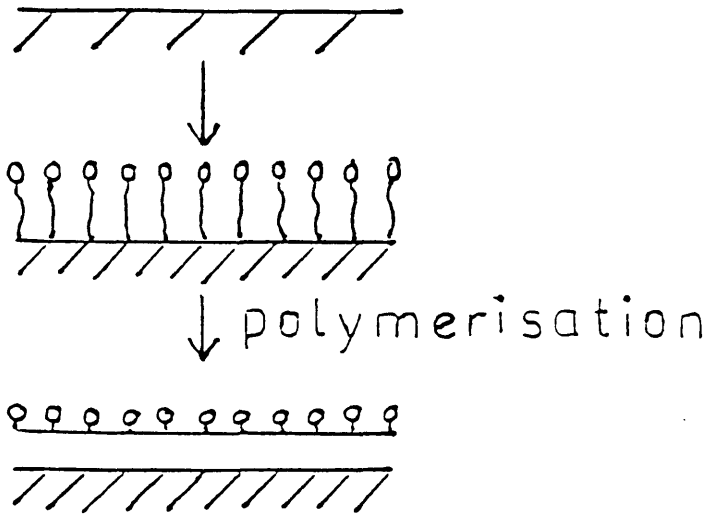

Figure 1.12 Coating Polymers with Lipids

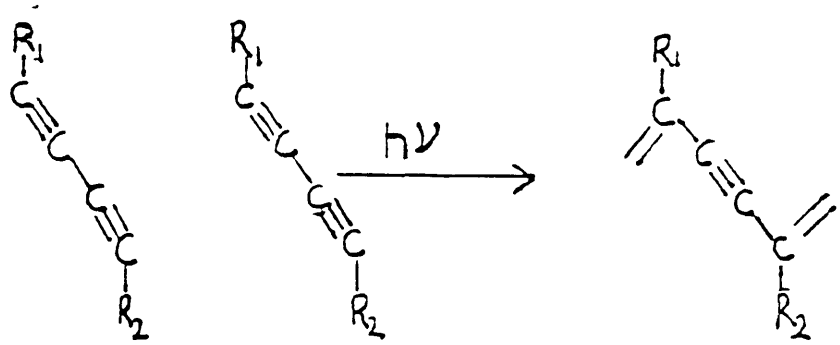

Figure 1.13 The Reaction Mechanism of Diactylenic Polymerisation

polymer . This subject will be dealt with , in more detail , in chapter 4 .

1.2.4. The Stabilisation of Lipid Bilayers

The previous sections have described various methods of forming lipid bilayer structures . The common feature with synthesised lipid bilayers is their poor stability[2,24] . A variety of methods have been employed to increase their durability :-

1.2.4.1.Supporting the Bilayers on a Substrate

Placing the lipid structure on a substrate (e.g. polymer , gel etc.) has already been discussed . The problem with this technique is that the substrate must be permeable to the target molecule , and so a solid polymer or a single crystal , which would be prefered for their Langmuir-Blodgett coating characteristics , cannot be used .

1.2.4.2.Incorporation of Large Molecules

Incorporating large molecules into the lipid structure also strengthens them . Oxidised cholesterol has been discussed for black lipid membranes . The protein molecules also stabilise the structure[1] , but , in general the bilayers formed do not have long term stability i.e. more than days .

1.2.4.3.Lipid Polymerisation

Polymerisation of the lipid molecules has been employed to stabilise the structure[2,24] . A degree of synthetic preparation is required for this technique . Tables 1.1a) and 1.1b) summarise the possible polymerisations. When the polymerisable group is part of the hydrophillic head group its amphiphillic nature is usually diminished[2] .

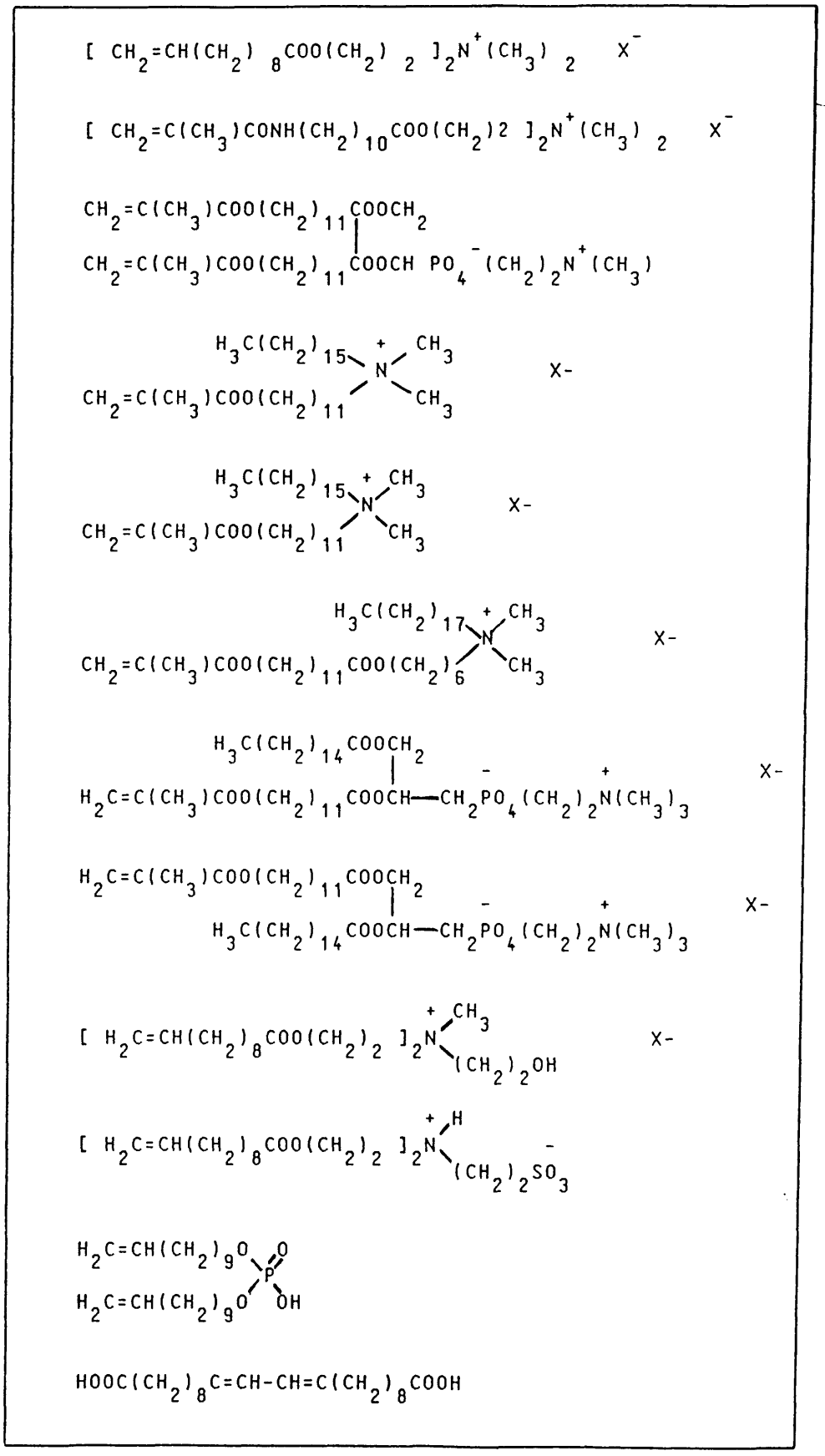

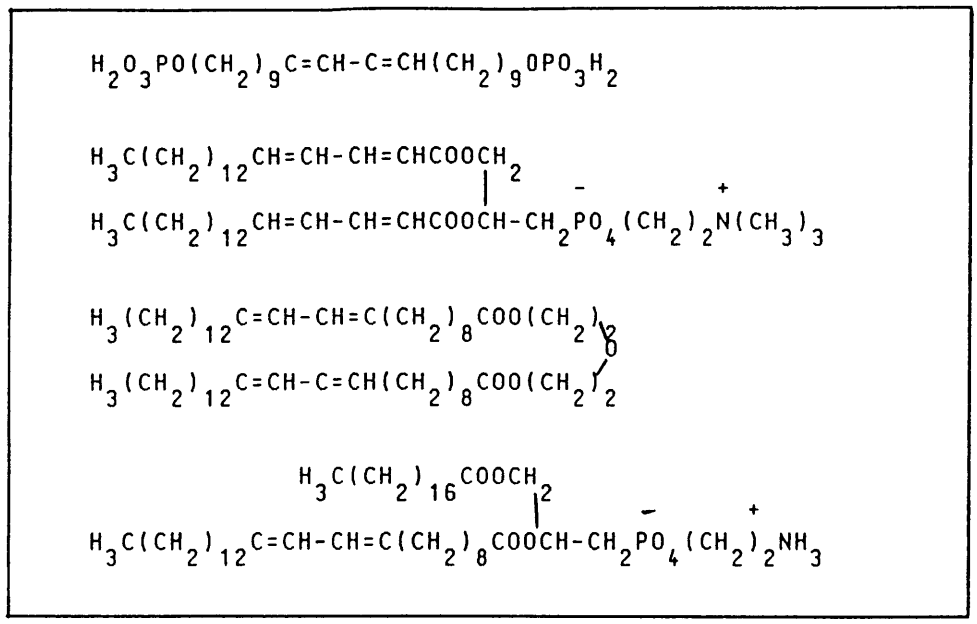

Table 1.1 a) Polymerisable Lipids with Reactive Tail Groups

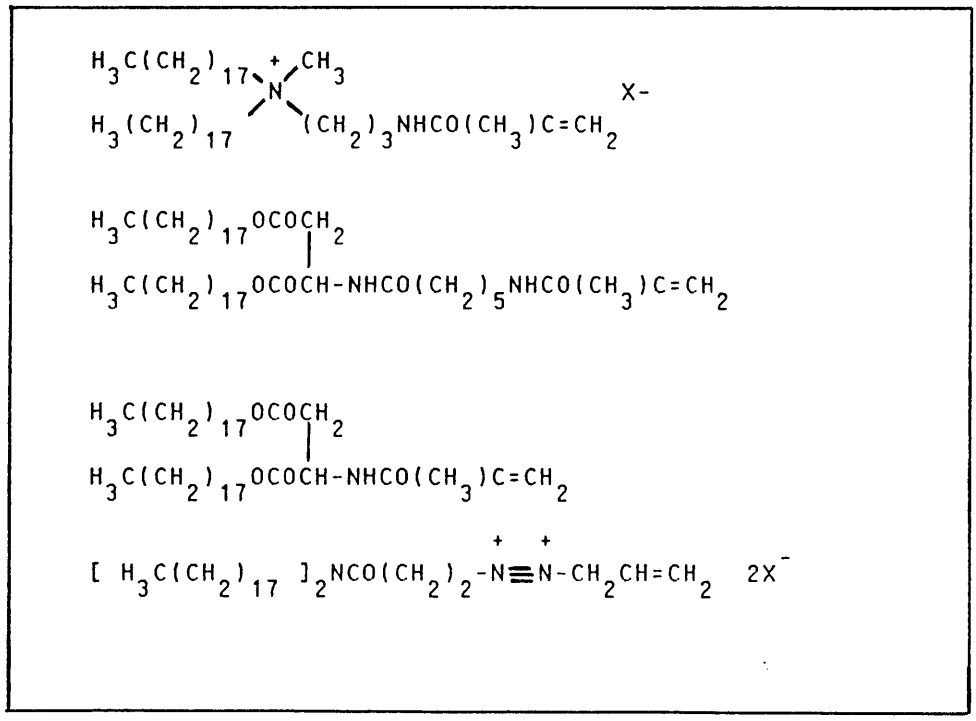

Table 1.1 b) Polymerisable Lipids with Reactive Head Groups

Polymerisation of the hydrophobic tails affects the mobilty of the lipids[25] , which is important when considering the incorporation of protein molecules[2] . It is possible to alleviate the problems of the mobility of the lipids by adding unpolmerisable species into their structure . This reduces the degree of polymerisation and so the amount of non-polymerisable material present should be minimised .

The range of polymerisable lipids that have been most extensively studied are ones with a diacetylene moeity in the hydrophobic chain . This is mainly due to the ease of polymerisation (UV light) . There is also an extensive knowledge of the behaviour of diacetylenes due to their interest in various branches of chemistry and physics[27] . Diacetylenic lipids have much lower phase transition temperatures[28] . They also undergo shrinkage[26] during a topochemical[2,28] polymerisation and are coloured[2,28] . The topochemical nature of the reaction means that experiments using these lipids must be performed on a Langmuir trough , or similar apparatus , where the molecular area can be controlled . Diacetylenes are polymerised via a blue species to the final red product (see fig. 1.16) in a time of the order of minutes[2,28] .

The most common range of lipids a with a polymerisable head group are those with a double bond . These can be polymerised either by UV irradiation or by a radical initiator such as azoisobutyronitrile[29] . This polymerisation cannot be controlled like the diacetylenic reaction (it is not topochemical) but is important for any application where the fluidity of the lipid structure is important e.g.

biomimetic studies .

1.2.5.Studies on Lipid Bilayers

Electrical studies can yield valuable information about lipid bilayers . The measurement of A.C. impedance using , for example , a Wayne-Kerr bridge can yield the resistance and the electrical capacitance of the membrane . The resistance of the bilayer gives an indication of the regularity of its structure - a low resistance generally indicates the incomplete formation of the bilayer[21] . The capacitance will give a semi-quantitative measure of bilayer thickness assuming the bilayer acts as a parallel plate capacitor :-

$$C = \varepsilon_0 \varepsilon_r A / d \qquad (1.1)$$

The relative permittivity must be assumed . It has been observed that the membrane thickness , d , increases if solvent is present in the membrane[29] .

Measuring A.C. impedance spectra , i.e. the change in the real and imaginary components as the frequency of the A.C. signal changes , is not particularly applicable to pure lipid bilayers as the flux of material through the membrane is too low to enable satisfactory measurement of the current passed . For membranes with proteins incorporated however , the impedance spectra would give information on the diffusion characteristics of both ions going into the membrane and passing through the membrane .

The diffusion and permeabilty of non-electrolytes has also been studied[30] , particularly water[31] . The effect of subjecting the bilayer to various compounds has been studied:

polypeptides , such as gramicidin , form channels in the lipid bilayer which reduce their electrical resistance[32] . Other molecules also act as carriers as well , but in general ions of the alkali and alkaline earth metals are most readily transported[32] .

General bilayer stability[33] and electrical breakdown[34,35] yields interesting information on the stability of bilayers and how strong they are with respect to natural membranes . Fluorescence studies can be used to yield information on the flexibility of the hydrophobic chains[21]

The effect of ultra-sound on lipid bilayers is of significance as it is often used to create vesicles[1] . Ultrasound can be used to speed up the thinning (the removal of solvent) of lipid bilayers[36] . The photoeffects of lipid bilayers are important as they play an important role in photosynthesis[21] . Although studies of the biochemistry of lipid bilayers are still important most work is concentrated on utilizing the membranes for technological advances[30] e.g. solar energy conversion or electrochromism .

1.3 Ion-Selective Electrodes

1.3.1. Introduction

The operation of ion-selective electrodes (ISE's) relies on the creation of a semi-permeable membrane i.e. a membrane that selectively affects the transport of ions across it . Ostwald created the concept of semi-permeable membranes[38] to explain observations on biological membranes . More detailed theories on the electrical properties of

MOLECULE	ION SHUTTLED
VALINOMYCIN	K^+ (OTHER ALKALI METALS)
CROWN ETHERS	ALKALI METALS
QUATERNARY ALKYL AMMONIUM SALTS	HALIDES (ESP. Cl^-) , NITRATES
ALKYL PHOSPHATES	Ca^{2+}

Table 1.2 a) Carrier Molecules

MOLECULE	ION SHUTTLED
RHODOPSIN	H^+
ATPase	K^+ , Na^+ AND H^+
ATPase (Mg DEPENDANT)	Mg^{2+} , H^+
CROWN ETHER (STACKS)	Co^{2+} , H^+

Table 1.2 b) Channel Formers

biological membranes[39,40] arose around the turn of the century and the search for a model for biological membranes started in earnest after this time . Sucess was limited until the creation of a stable lipid bilayer[21] , but the theories developed were applied to thicker membranes .

There are two basic types of ion-selective membranes - solid membranes , often made of crystalline material and liquid membranes , which consist of an oil (e.g. long chain hydrocarbon) . The most studied ion-selctive membrane is the glass electrode membrane . It was observed that this consists of a solid membrane selective for protons and sodium ions as early as the 1930`s[41] . Other solid ion-selective membranes were not prepared until the 1960`s[42,43] . Work on liquid membranes with dissolved ion exchanger started around this time[44] and the first operational ion-selective electrode based on a liquid membrane was prepared in the late 1960`s[45].

In the last twenty years there has been a vast increase in the amount and diversity of research work into ion-selective electrodes . Biological species can be placed in the membrane to react with target molecules producing ionic species (and therefore an electrical signal) . Enzymes are particularly suitable for this operation because of their selectivity[47] . Bacterium electrodes[47] and electrodes with tissue replacing the enzyme[48] have been sucessfully employed.

As well as altering the properties of the membrane , novel applications of the ion-selective process have been investigated :-

Microelectrodes are in principle normal ISE`s but are reduced in scale to the order of micrometres . The dimensions of these devices allows for measurement of intracellular ionic concentrations . A variety of ion-selective membranes have been employed in microelectrodes . Glass membranes have been used to measure pH and sodium ion concentrations[49] . Other solid membranes for chloride ion concentration and liquid membranes for potassium , chloride and calcium ion concentrations have also been employed[51] .

Ion-selective membranes have also been incorporated into electronic components . Ion-selective field effect transistiors (ISFET) are basically field effect transistors[52] with an ISE membrane and a test solution replacing the gate[38,53,54] , (fig. 1.15) . ISFET`s work by the principle that the magnitude of the drain current , I_D , passed between the source and drain contacts depends on the electron density of a n-type channel formed in the p-type semi-conductor . This electron density is in turn dependent on the value of the gate voltage , V_G , which takes on a value set by the activity of the target ions in the test solution . An ISFET can be calibrated so that the value of V_G which results in a specific value of I_D gives the activity , (or concentration) , of the target species .

ISFET`s have been used to measure pH[55] , halide ions[53] , potassium ions and calcium ions[55] . Penicillin concentrations have also been measured[57] , by means of an ISE incorporated with an enzyme .

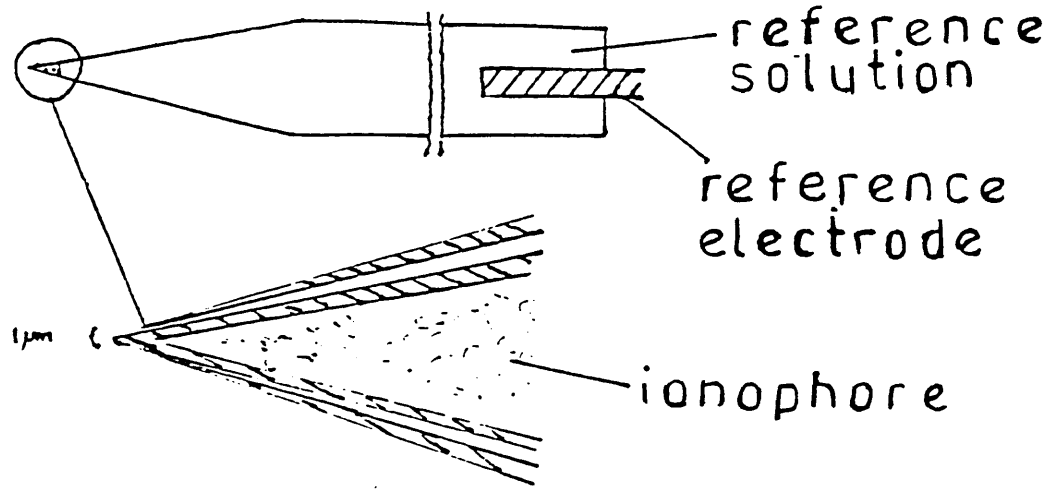

Figure 1.14 A Micro-electrode

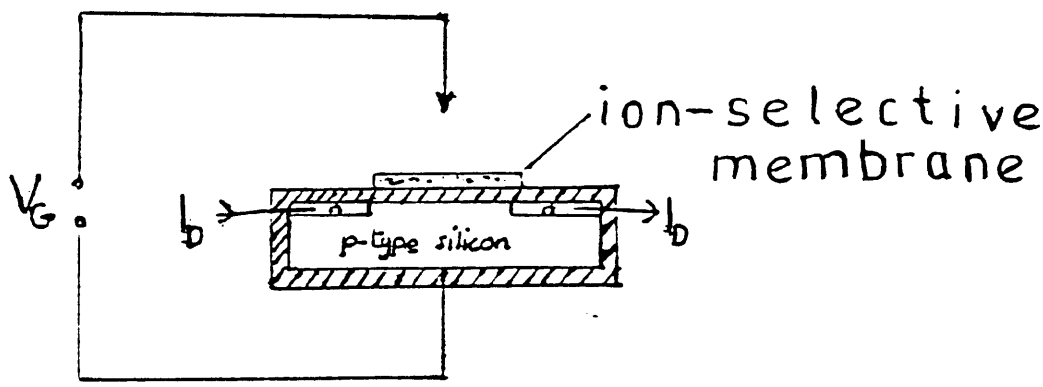

Figure 1.15 An Ion-Selective Feild Effect Transistor (ISFET)

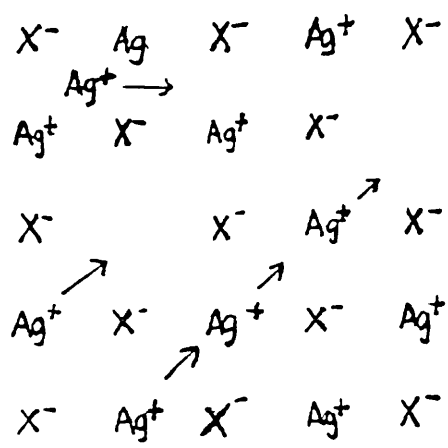

Figure 1.16 The frenkel Mechanism

1.3.2. The Basic Concept of ISE`s

Fundamentally , an ion-selective electrode consists of a reference solution with a known concentration of the ion of interest , separated from the solution to be analysed by a semi-permeable membrane . Both solutions have reference electrodes in them (e.g. calomel) . The E.M.F. of the cell is given by :-

$$E = E_{REF} + \Delta\phi_m - E_{ANAL} \qquad (1.2)$$

Where E_{ANAL} and E_{REF} are the potential of the reference electrodes in the analysis and reference solutions respectively . $\Delta\phi_m$ is the membrane potential and is of basic importance in the use of the ISE .

The ISE potential can defined :-

$$E_{ISE} = E_{REF} + \Delta\phi_m \qquad (1.3)$$

If the solution to be analysed and the reference solution are simply different concentrations of the analyte , A , with the appropriate counterion , the membrane potential is given by :-

$$\Delta\phi_m = RT/ZF \ln [a_{A,ANAL} / a_{A,REF}] \qquad (1.4)$$

substituting into 1.3

$$\Delta\phi_m = C + RT/ZF \ln a_{A,ANAL} \qquad (1.5)$$

C is a constant independant of the activity of the analyte in either solution . Hence the membrane potential is proportional to the activity of the analyte . Unfortunately , the system described is too simple for practical applications, and the effect of interfering ions must be considered .

If the solution to be analysed contains an interferent ion, B , 1.4 becomes :-

$$\Delta\phi_m = \frac{RT}{ZF} \ln \frac{a_{A,ANAL} + k_s a_{B,ANAL}}{a_{A,REF}} \qquad (1.6)$$

k_s is the selectivity coefficient of the ISE for A ions with respect to B ions . If the activity of B is very low and the selectivity coefficient very small then 1.6 reduces to 1.7 .

$$dE_{ISE} / d \ln a_A = RT/ZF \qquad (1.7)$$

Conversely , if the selectivity coefficient , or the activity of B high with respect to that of A a similar equation to 1.4 is obtained but the membrane potential will be constant irrespective of the concentrations of A or B .

1.3.3 Ion-Selective Membranes

1.3.3.1. Solid Membranes

These membranes have fixed ion-exchange sites to facilitate the movement of particular species across the membrane . The membranes can exist in various forms :- single crystal , pressed pellet , enclosed in a polymeric framework etc. . A variety of ions have been studied with solid ion-selective membranes (Table 1.4)

Silver halide membranes have been used to measure both silver and halide (Cl , Br , I) concentrations [38,58] . The silver ions carry a current by a Frenkel mechanism[58] and the amount of silver ions , in the defects , available for the passage of current is dependent on the external silver concentration . As silver halides are sparingly soluble , the halide concentration affects the silver concentration . $dE_{ISE}/ d \log[X^-]$ is approximately 56 mV[38] . The membranes may be used in single crystal or pressed pellet form or can

ISE MEMBRANE	ION SENSED
AgX (Cl, Br , I ONLY)	Ag^+ , X^-
Ag_2S	S^{2-}
MS / Ag_2S (or Ag_2Se Ag_2Te, HgS, HgTe)	Pb^{2+} , Cd^{2+} , Zn^{2+}
LaF_3	F^-

Table 1.3 Ions Studied with Solid ISE Membranes

GLASS COMPOSITION	ION SENSED
15% Li_2O, 25% Al_2O_3 60% SiO_2	Li^+
11% Na_2O, 18% Al_2O_3 71% SiO_2	Na^+ (H^+)
27% Na_2O, 5%Al_2O_3 68% SiO_2	K^+
28.8% Na_2O, 19.1% Al_2O_3 52.1% SiO_2	Ag^+

Table 1.4 Ions Studied with Glass Electrodes

be precipitates in a silicone rubber matrix .

Other halide salts may be used for the same purpose , in particular mercury halides[59,60] , as well as other silver salts , such as silver thiocyanate[61] . Silver halide ISE`s may also be used to detect cyanide ions as these act as complexing agents and affect the dissolution of silver ions[62,63] .

A similar mechanism for ion-selectivity exists for the monoclinic silver sulphide membrane . As this material has , almost , exclusively silver ions as the current carrying species[64,65] and a low solubility the sulphide ISE is a particularly reliable sensor .

A set of ISE`s can be formed with mixtures of silver sulphide and other non-conducting sulphides[60] (Table 1.3) . In these membranes the activity of the metal affects the sulphide activity which in turn produces an effect on the silver ion activity altering the electrode response .

The range of silver halide ion-selective membranes do not include silver fluoride . Fluoride ion-selectivity can be obtained from a lanthanum trifluoride membrane though . Lanthanum trifluoride has a hexagonal structure with alternate layers containing a mixture of ions then solely fluoride ions . Thus fluoride ions are mobile in the crystal structure which facillitates isotropic conduction and fluoride ion selectivity[67,68] .

1.3.3.2. Glass Electrodes

Glass electrode membranes are unusual for ISE membranes in that they do not result in net transfer of the target ions

across the membrane[63] . The membrane potential results from the transfer of ions from the solution into the membrane which are located in interstitial sites (chelated to oxygen atoms on the silica / aluminate backbones) . Glass elctrodes are selective not only for protons but also for the alkali metals and silver ions (Table 1.4) . The relative selectivities are dependent on the composition of the glass , due to the fact that aluminates have a negative charge and silicates do not and so a high amount of aluminate favours ions with a high charge density (i.e. small ions) .

1.3.3.3. Liquid Membranes

Ion-selective electrodes with liquid membranes can be broken into two categories : membranes with ion-exchanging ions to prefer selectivity and membranes with uncharged ionophores .

1.3.3.3.1.Liquid membranes with ion-exchanging ions .

The ion exchanging ions must be very hydrophobic to be soluble in a membrane of low dielectric constant . As a general rule the more hydrophillic the target ion , the more hydrophobic the ion exchanger must be[70,71] . A list of ion exchanging ions and their respective determinands is shown in table 1.5a .

1.3.3.3.2.Liquid Membranes with Ionophores

Ionophores must have polar regions to coordinate to , and thus stabilise , the determinand ions . As well as this property , ionphores have to dissolve in oily liquids and so must have long aliphatic chains or aromatic groups . Cyclic species (e.g. valinomycin , crown ethers) are particularly

ION-EXCHANGING ION	ION SENSED
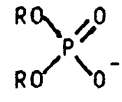 (R= ALKYL, ARYL)	Ca^{2+}
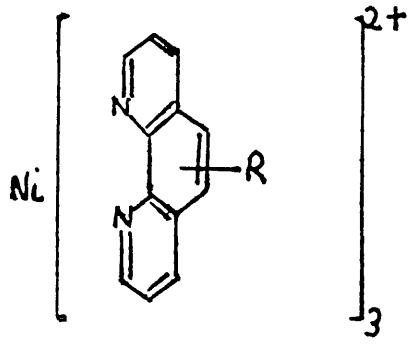	NO_3^- , BF_4^-
$P(C_{12}H_{25})_4^+$	ReO_4^-
$H_3CN(C_{12}H_{25})_3^+$	Cl^-
$N(C_{10}H_{21})_4^+$	NO_3^- , Cl^-
$HN(C_{10}H_{21})_3^+$	HCO_3^-
BPh_4^-	Cs^+ , NR_4^+
$B(p\text{-}PhCl)_4^-$	K^+, acetylcholine

Table 1.5 a)Ion-Exchanging Ions used in Liquid Membranes

IONOPHORES	IONS SENSED
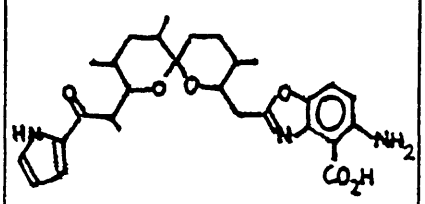	Ca^{2+}
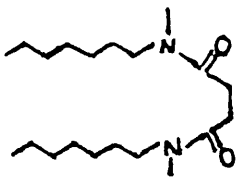	Mg^{2+}
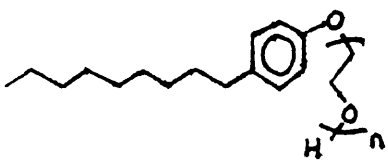	Ba^{2+}
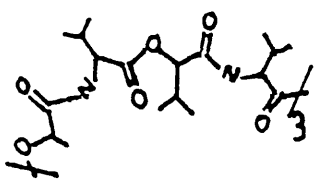	K^{+}
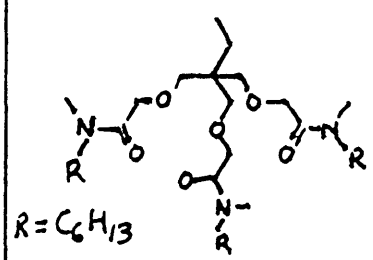	Na^{+}
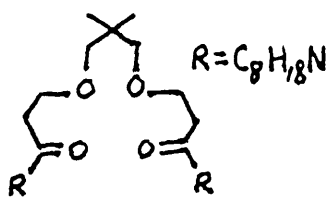	UO_2^{2+}

Table 1.5 b)Ionophores used in Liquid Membranes

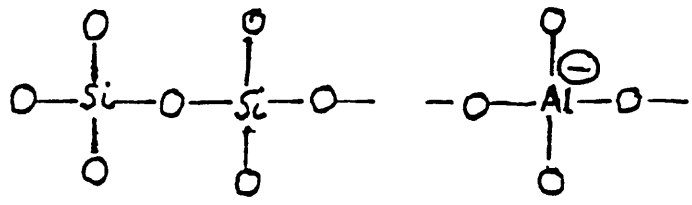

Figure 1.17 The Structure of Silicates and Aluminates

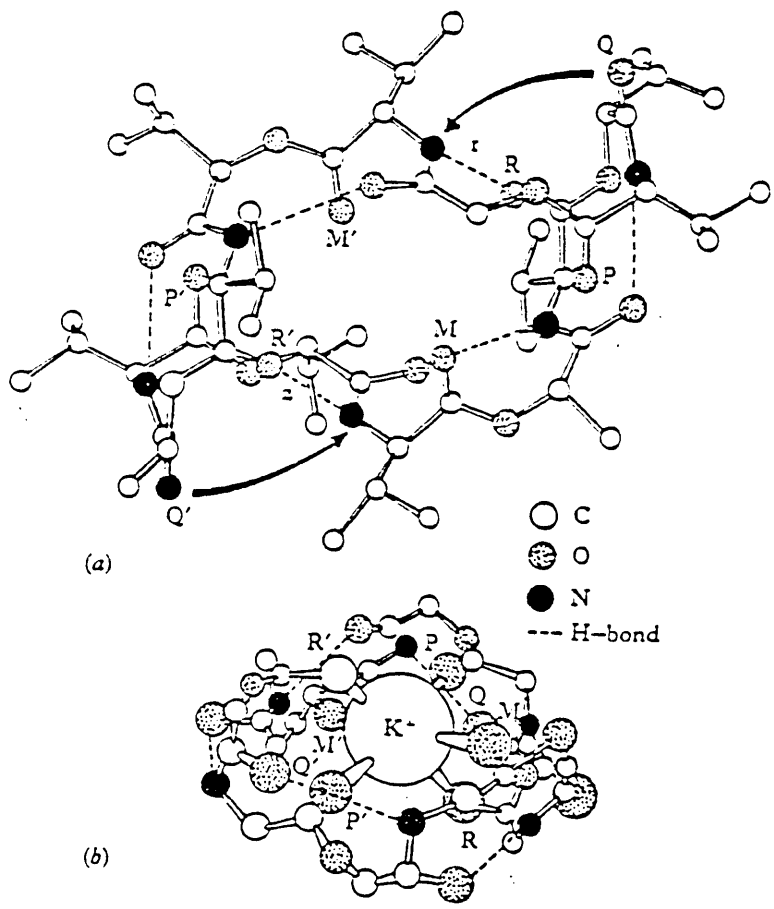

Figure 1.18 Valinomycin a) Unchelated b) Bound to a K^+ ion

applicable for use as ionophores , as they generally have good size selective properties . A summary of ionophores and their respective determinands is shown in table 1.7b .

1.4. Interfacial Polymerisation

Since the pioneering work of Staudinger and Carothers[72,73] interest in polymer chemistry has blossomed . The combination of interfacial and polymer chemistry has been particularly fruitful[72,73,74] . The interface provides a means of selecting the reagents , i.e. surface active monomeric species . This also controls the nature of the polymerisation and manipulation of the reaction conditions can produce variations in the finished polymer[74] .

Polymers can be produced by a wide range of processes[74,75] but there are three basic methods .

1.4.1.Free Radical Additions

These polymerisations result from the cleveage of weak bonds by heat or irradiation . e.g. 2,2'- bisazoisobutyronitrile

$$(CH_3)_2C(CN)N{=}NC(CN)(CH_3)_2 \longrightarrow 2\ (CH_3)_2C(CN)\cdot + N_2$$

This reaction is followed by an addition involving the free radical formed .

1.4.2. Ionic Additions

These polymerisations are similar to free radical additions but the active species cannot be formed simply by heating . Generally , an initiator molecule is used e.g.

$$BF_3.OH_2 + CH_2{=}C(CH_3)_2 \longrightarrow (CH_3)_3C^+ + BF_3OH^-$$

$$(CH_3)C^+ + CH_2=C(CH_3)_2 \longrightarrow (CH_3)_3\overset{+}{C}CH_2C(CH_3)_2 \longrightarrow \longrightarrow$$

1.4.3. Condensation Polymerisation

These polymerisations result from simple elimination (or ring opening) reactions , e.g.esterification , amidations etc.

$$HOOCRCH_2OH + HOOCR`CH_2OH \longrightarrow HOOCRCH_2OCOR`CH_2OH \longrightarrow$$

1.4.3.1. Interfacial Condensation Polymerisation

When the reacting species in a condensation polymerisation consists of one molecule soluble in an aqueous phase and the other in an organic phase , but not water , then polymerisation can occur at a water-oil interface . An example of this type of polymerisation is the nylon rope trick[75,76,77] , where a diacyl chloride , soluble in non-aqueous solvents such as carbon tetrachloride , reacts with a diamine , soluble in water .

1.4.3.2. The Reaction Kinetics of Interfacial Polymerisation

The rate of polymerisation can be defined as the rate of removal of either of the monomers . For two species A and B reacting in this manner this is descibed mathmatically :-

$$-d[A]/dt = k[A][B] \qquad (1.8)$$

This assumes that the rate of reaction is independent of chain length (generally true[75,76]) and that any catalysts , such as acids or bases , are in excess .

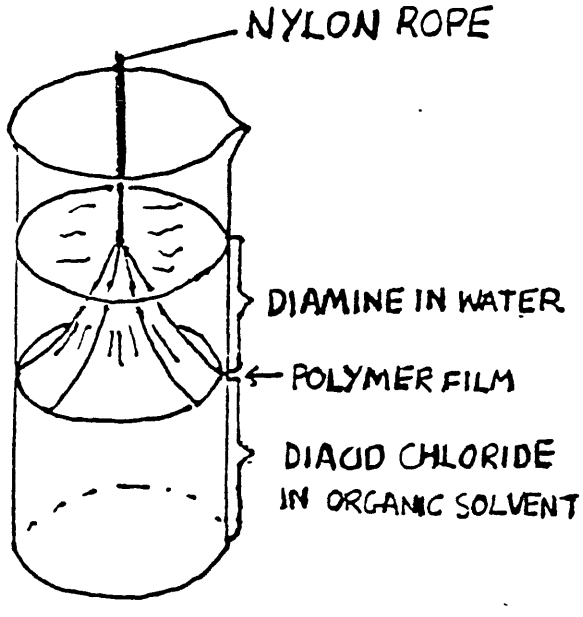

1.19 The Nylon Rope Trick

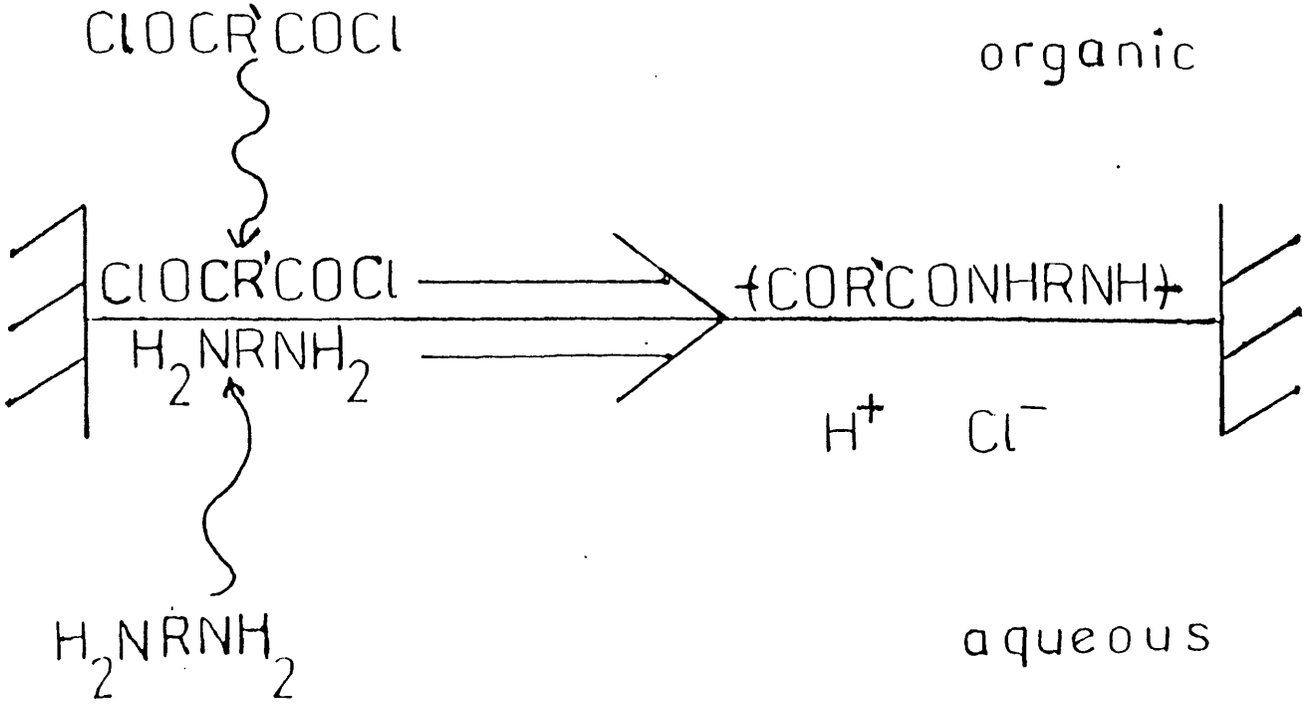

Figure 1.20 The Mechanism of Interfacial Polymerisation

The rates of reaction tend to be fast[78,79] and thus difficult to measure . At moderate temperatures though , kinetic studies can be employed . The absence of heating is advantageous as well as convenient , since the cost of operation is brought down as well the extent of side reactions .

1.4.3.3 Measuring the Rates of Polymerisation

The measurement of the rate of polymerisation usually involves following the removal of one of the monomer units . For interfacial polymerisation this usually involves the monomer in the aqueous phase as the concentration of particles in this phase tends to be more easily measured[74] .

Various methods have been employed to obtain the magnitude of monomer concentration at various times after the initiation of polymerisation :-

- Titration of an acidic or basic species can be employed[74] . This tends to involve the removal of aliquots from the aqueous phase .

- Spectrophotometric analysis of monomer units has also been performed[78] .

- Radioactive labelling of atoms present in the functional groups of the monomers has also been succesfully employed[80] .

- The measurement of the conductivity of the aqueous phase has been utilised as a means of obtaining the change of monomer concentration[81] . This technique is only applicable for ionic species and the creation of charged side products may affect the analysis unless their rate of production is

proportional to the rate of polymerisation .

The techniques mentioned are generally referred to as end group analysis , (i.e. the functional groups at the end of monomer chains are monitored) and can also be used to measure the degree of polymerisation ($\overline{DP}$) or number average molecular weight (M_n)[75,76] which give a measure of the average chain length . This value is important as long chain polymers , (at least over fifty monomer units) , are required for the strength and robustness needed for commercial polymers .

1.4.3.4 The Mechanism of Interfacial polymerisation

The generally recognised mechanism of interfacial condensation polymerisations[74,75] is that the reaction initially begins at the interface and then spreads into the bulk of the organic phase . This is a result of the fact that monomer in the aqueous phase tends to be more soluble in the organic phase than vice versa[74] . This results from the fact that long chain monomers are used to produce commercially useful polymers . The hypothesis is substantiated by the observation that optimum polymerisation conditions do not involve eqivalent amounts of monomer , (as is the case for homogeneous polymerisations[75,76]) but excess amounts of the aqueous monmer[74] . Moreover the rate of polymerisation tails off in a manner suggesting that diffusion of the reactants through a formed membrane is occurring[81] .

There are three types of polymer film growth observed for interfacial condensations[74] .

i) Rapid polymer precipitation followed by swelling of

the polymer film . Fast polymerisation rates are observed initially but tail off due to the slow diffusion of monomer through the swollen polmer film .

ii) Rapid precipitation but no swelling due to repulsion of the solvent by the polymer . Low concentrations of monomer are required to avoid the low percentage yields , i.e. polymerisation is terminated when extensive polymerisation occurs .

iii) Slow precipitation which results in little swelling. This mechanism results when the formed polymer is partly soluble in the organic phase and is only applicable for low molecular weight polmers .

1.4.3.5 Factors Affecting the Rate of Polymerisation

The factors affecting rate of interfacial polymerisation can be summarised as follows[74] :-

1) Chemical reaction rate .

2) Precipitation rate of the polymer .

3) Impurities in the reactants and solvents .

4) Transfer rate of the aqueous monomer across the interface .

5) Partition coefficient of the reactants .

6) Concentration of the reactants .

7) Mass transport .

8) Side reactions .

9) Viscosities of the solvent and the polymer .

Some of the factors are inter-related . The chemical reaction is generally facille so 1) does not generally

figure in the kinetic analysis . Other factors can be investigated if mass transport can be controlled .

1.4.3.5.1 The Effect of Impurities

In general , interfacial polymerisations are not affected by impurities unless they are surface active[71] . This is not surprising as they interfacial concentration of non-surfactants will be neglible . Significant increases in the rate of polymerisation occur when surfactant molecules are present in the reaction cell , even at low concentrations[82] . This is due to the lowering of interfacial tension which allows easier transfer of monomer from the aqueous to the organic phase . Significant amounts of surfactant will lead to the formation of emulsions and so increase the interfacial area .

1.4.3.5.2 The Effect of the Organic Solvent

The nature of the organic phase affects the rate of polymerisation . As the interfacial tension decreases , i.e. the organic solvent becomes less hydrophobic , the reaction rate increases[82] . Another factor related to this is the optimum reaction ratio , (the ratio of the concentrations of aqueous and organic phase monomers) . For more hydrophobic monomers , a greater concentration ratio is required for the optimum rate of polymerisation . This is due to the lowering of the partition coefficient of the aqueous monomer in the organic phase .

E.g. The optimum reaction ratio for the production of 6,10-nylon[77] .

solvent	reactant ratio
cyclohexane	17
p-xylene	8
carbon tetra-chloride	6.5
chloroform	1.7

1.4.3.5.3 The Effect of Side Reactions

Side reactions are usually unimportant for interfacial polymerisations as the polymerisation process is very fast even at moderate temperatures[74] .The most important side reaction in interfacial polymamidation is the hydrolysis of acid halides[74,80] . Even this reaction is unimportant for long chain acid halides[80,83] . The hydrolysis is most pronounced at high pH values[80,83] , but for long chained monomers , as used most frequently , there is at best a conversion of acid halide to carboxylic acid of a few percent in the polymerisation reaction time[80] . The data for acid chloride hydrolysis comes from experiments where no polymerisation is atempted and so this value can be assumed to be lower when the acid halide has to diffuse through the polymeric film to reach the aqueous phase .

1.5 Plan of this Thesis

After this introductory chapter , the rest of this thesis will be laid out as follows . Chapter two will outline briefly the background theory of the experimental methods

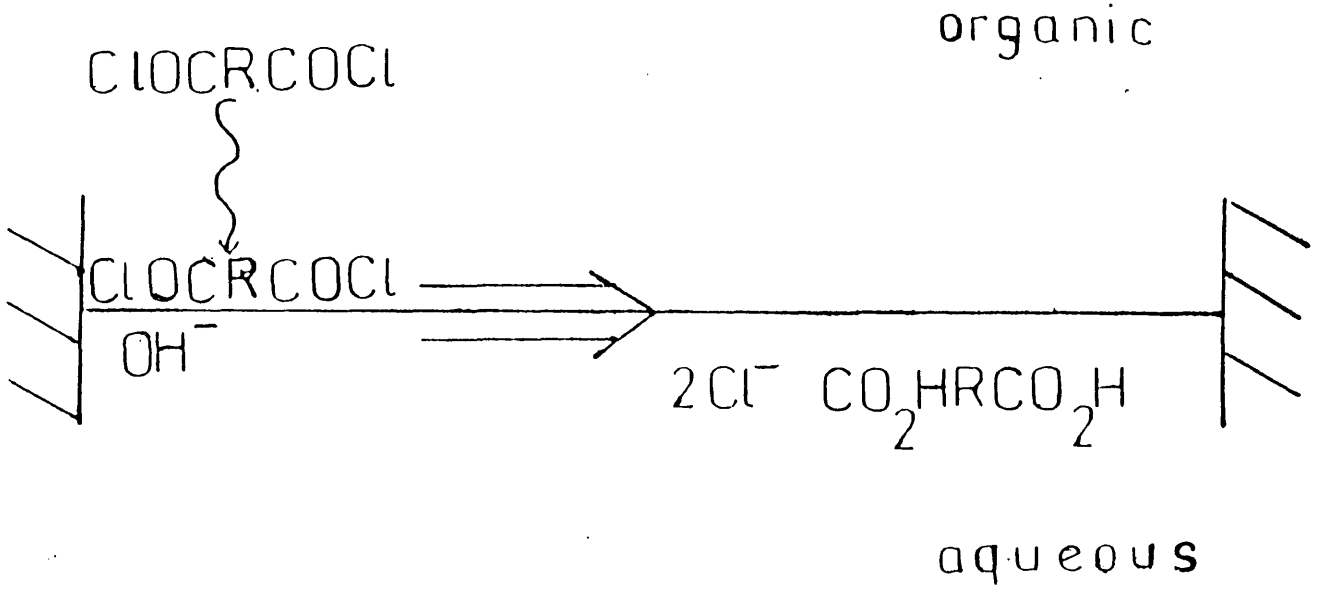

Figure 1.21 The Hydolysis of Acid Halides

employed in this study . Chapter three will consist of a description of the standard procedures performed .

Chapter four will give an account of work aimed at creating stable lipid bilayers , both the novel techniques used and the results obtained . The conclusions drawn from this work and suggestions for future experimentation are also included in this chapter . Chapter five will describe the use of a rotating diffusion cell to measure the flux of ions passing through a liquid membrane and chapter six the use of the cell to follow interfacial polymerisations . Both chapters will outline future work in the relevant subject fields .

CHAPTER 2 THEORY

This chapter will give a brief outline to the background theory of the expeimental techniques used . Fuller accounts of the techniques mentioned can be obtained from the relevant literature .

2.1 THE ROTATING DIFFUSION CELL (R.D.C.)

2.1.1 The Mathematical Model

The mathematical principles governing the rotating diffusion cell (R.D.C.) are analagous to those governing the ring disc electrode[84,85,86] .

When a planar disc is rotating in a fluid , flow patterns are set up (fig. 2.1) which describe how fluid is sucked towards the disc and then flung radially outwards near the disc surface . The flow patterns can be described mathematically by separating the polar coordinates of the velocity (fig. 2.2)

rotational comp. $V_{\phi}=r\omega G(\gamma)$ (2.1)

radial comp. $V_{r}=r\omega F(\gamma)$ (2.2)

normal comp. $V_{z}=-(\omega\upsilon)^{1/2}H(\gamma)$ (2.3)

ω=rotation speed (rad s^{-1}) υ=kinematic viscosity ($cm^{2}s^{-1}$)

$\gamma=z/z_{H}$ a dimensionless distance variable

$z_{H}=(\upsilon/\omega)^{1/2}$ the hydrodynamic length

The functions F , G and H (fig. 2.2b) describe the respective velocity components . It can be deduced that at the disc surface (i.e. z=0) fluid rotates with the disc , meanwhile away from the disc surface fluid is thrust radially outwards .

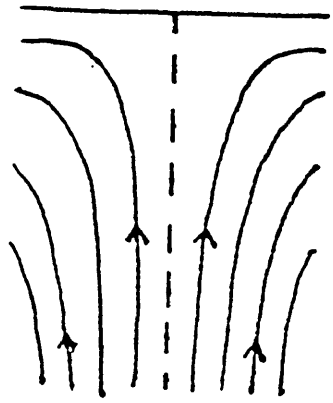

2.1 Flow Patterns at a Rotating Disc

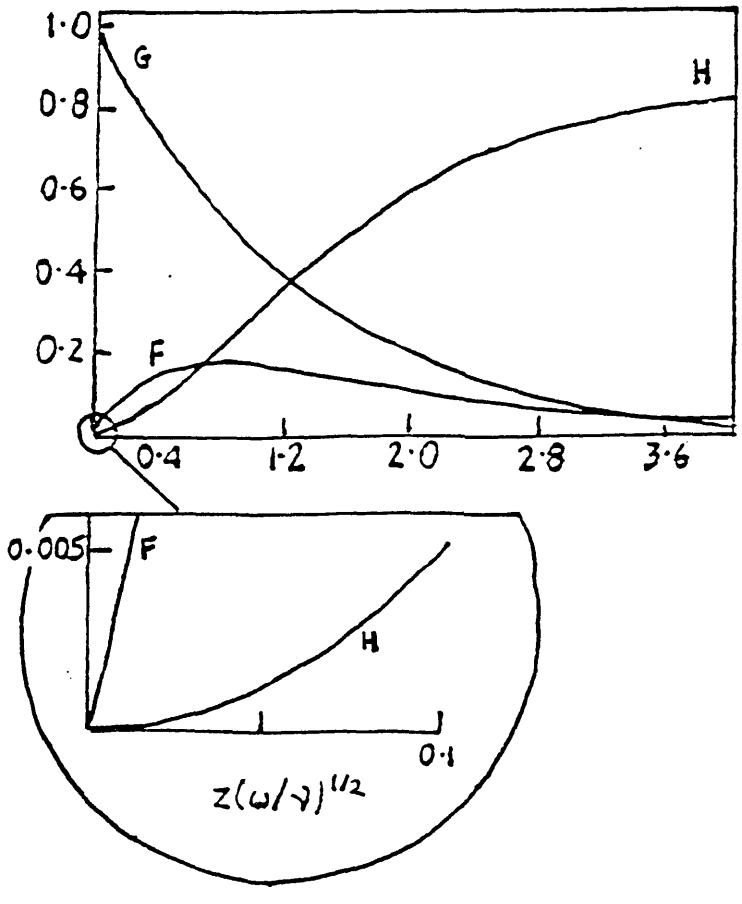

2.2 The Polar Coordinate Representation of a Rotating Disc

Two main features arise from this mathematical treatment

i) F , G and H depend only on z

ii) V_z is independent of r , which means the whole of the disc is uniformly accessible to the bulk fluid .

Steady state transport to a rotating disc can be described by the equation[87]

$$\frac{\delta c}{\delta t} = D \frac{\delta^2 c}{\delta z^2} - V_z \frac{\delta c}{\delta z} = 0 \qquad (2.4)$$

c = conc. of species (mol cm^{-3})

D = the diffusion coefficient (cm^2 s^{-1})

From equation 2.4 the velocity component is found to be

$$V_z = 0.51\omega^{3/2}\upsilon^{-1/6}z^2 \qquad (2.5)$$

On integration

$$\left(\frac{\delta c}{\delta z}\right)_{z=0} = c_\infty - c_o \qquad (2.6)$$

c_o and c_∞ are the concentrations of a species at the disc and in the bulk respectively

The steady state flux of a species is given by Fick's Law

$$j = D \left(\frac{\delta c}{\delta z}\right)_{z=0} = \frac{D(c_\infty - c_o)}{z_D} \qquad (2.7)$$

$$z_D = 0.643\upsilon^{1/6}D^{1/3}\omega^{-1/2} \qquad (2.8)$$

From figure 2.3 it can be observed that z_D can be regarded as the diffusion layer thickness i.e. when $z < z_D$ diffusion is the main mode of transport , and when $z > z_D$ convection is the main mode of transport .

Another expression for the flux of species can be obtained by analogy to the rotating disc electrode . The flux of species when mass transport is rate determining

can be given by :-

$$j = c_\infty k_D \qquad (2.9)$$

where k_D is the mass transfer rate constant

$$k_D = D / z_D \qquad (2.10)$$

combining 2.8 , 2.9 and 2.10

$$j = 1.554 c_\infty D^{2/3} \upsilon^{-1/6} \omega^{1/2} \qquad (2.11)$$

This is reffered to as the Levich equation and a plot of flux versus the square root of the rotation speed as a Levich plot .

However , if there is another step in the transference of material from one side of the filter disc to the other , independent of mass transfer , e.g. an interfacial reaction , diffusion through a liquid membrane , then the overall rate constant is given by :-

$$1 / k = 1 / k_D + 1 / k' \qquad (2.12)$$

k' is the rate constant for the other process . The smaller of k_D and k' is rate determining .

$$\frac{c_\infty}{j} = \frac{0.643 D^{-2/3} \nu^{1/6}}{\omega^{1/2}} + \frac{1}{k'} \qquad (2.13)$$

A plot of the reciprocal of the flux versus the reciprocal of the square root of the rotation speed is a straight line and reffered to as a Koutecky-Levich plot.

Contributions to the value of k' for the diffusion of material through the liquid membrane come from interfacial resistances , (e.g. chelation) , and from the diffusion of the complex through the membrane . This will be expanded in more detail in chapter 5

A similar situation arises when a two-phase system is

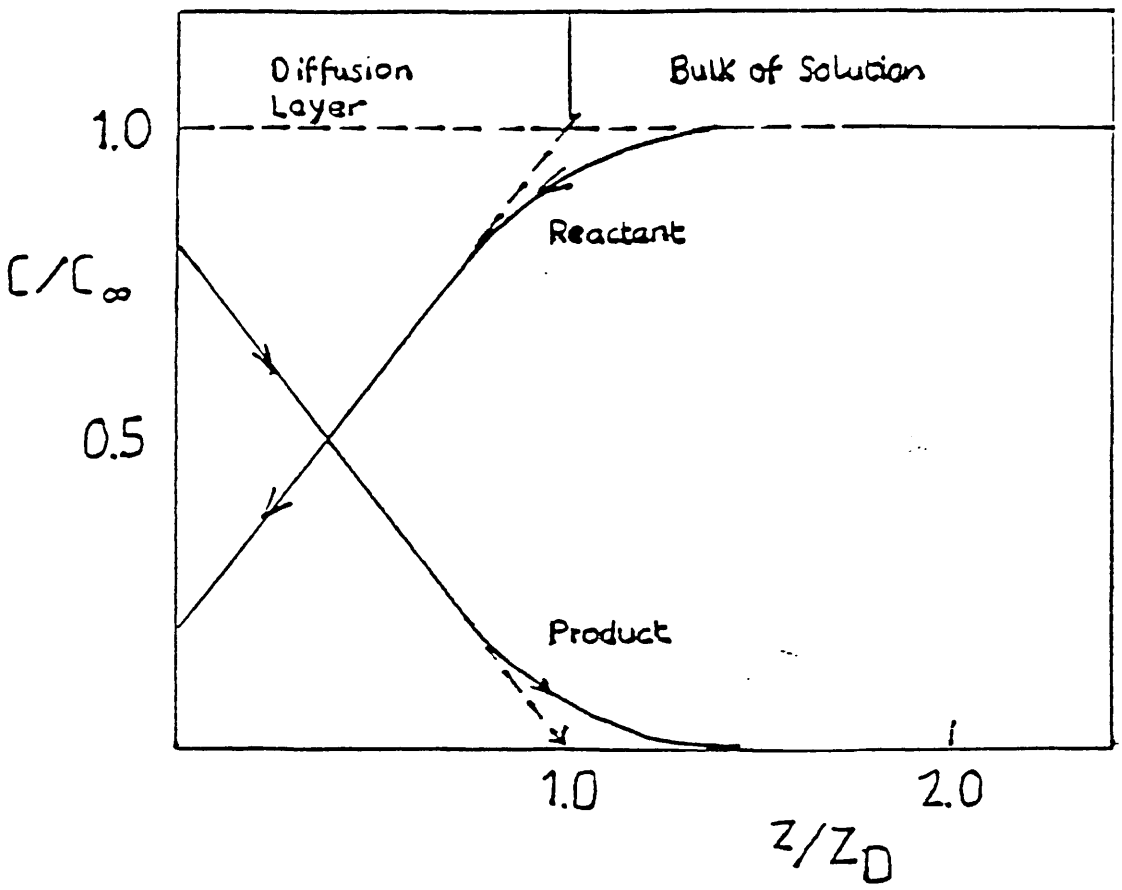

2.3 c / c_∞ versus z / z_D

set up . The terms contributing to the flux are mass transport , interfacial resistance and diffusion through a soaked Millipore filter , which in general lead to higher values .

2.2 The Arc Electrode System

2.2.1 The general Technique

Experiments performed on a rotating diffusion cell require a means by which the molecules fluxing through the Millipore filter disc can be quantitatively detected . Positioning an arc electrode on the collapsed part of the filter , concentric to the porous disc , provides a means of detection , as long as the presence of the fluxing species (ion) effects a change in the potential of the electrode .

The basis of the arc electrode technique is the same as that of the rotating ring disc electrode (R.R.D.E.)[84]. The flow patterns of a R.R.D.E. are the same as the R.D.E. , (fig. 2.8) . A set fraction of material generated at the disc reaches the ring , or arc , which is given by the collection efficiency, N_o . An analytical solution of N_o has been obtained by Albery and Bruckenstein[88,89] .

$$N_o = 1 - F(\alpha/\beta) + \beta^{2/3}(1-F(\alpha)) - (1+\alpha+\beta)^{2/3}\{1-F([\alpha/\beta][1+\alpha+\beta])\} \qquad (2.14)$$

where

$$F(\theta) = 3^{1/2}/4\pi \ln\{(1+\theta^{1/3})^3/(1+\theta)\} + 3/2\pi \arctan[(2\theta^{1/3}-1)/3^{1/2}] + 1/4 \qquad (2.15)$$

$\alpha = (r_2/r_1)^3-1 \quad \beta=(r_3/r_1)^3-(r_2/r_1)^3$

r_1 , r_2 and r_3 are defined in figure 2.11

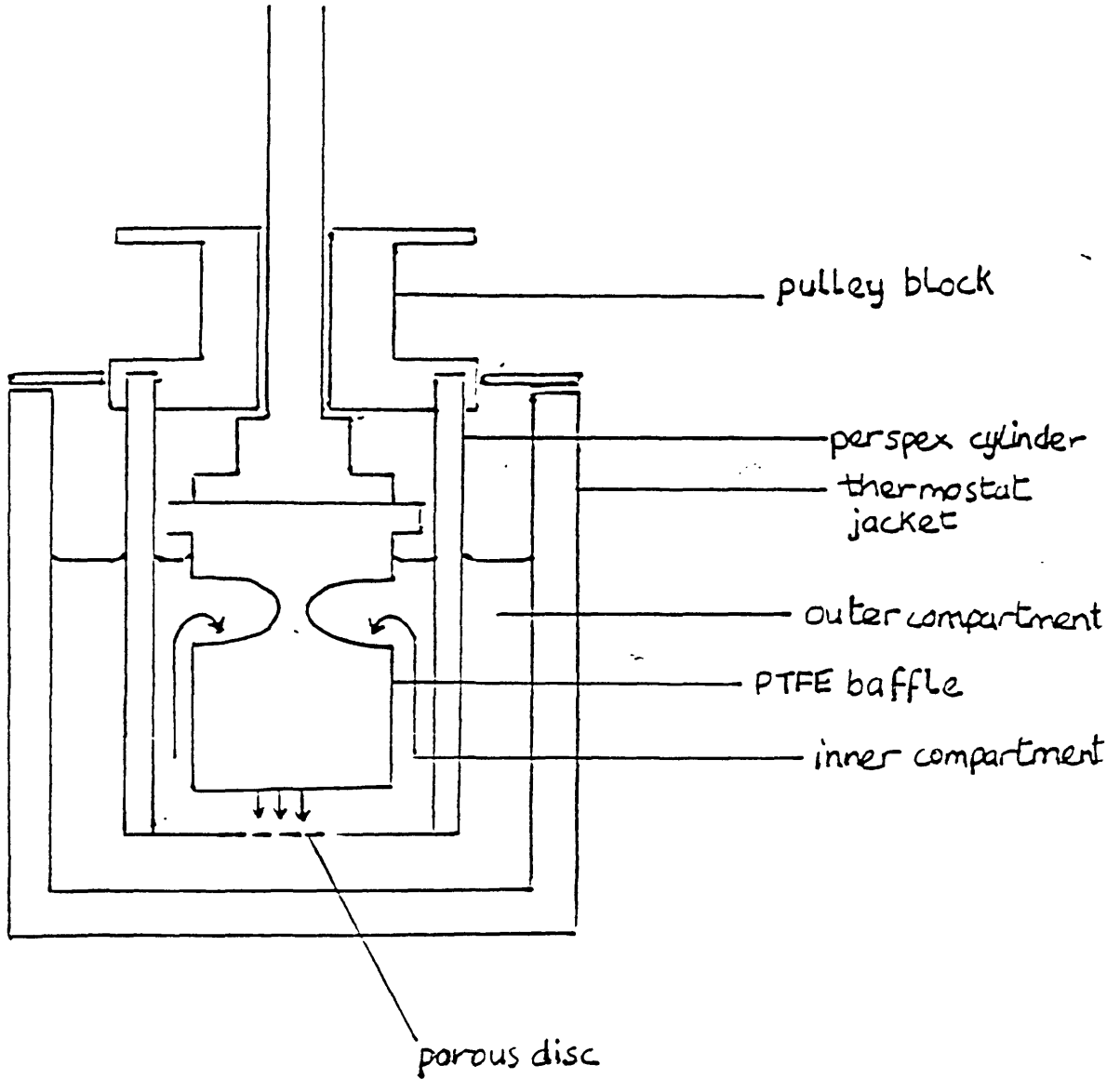

2.4 A Rotating Diffusion Cell (RDC)

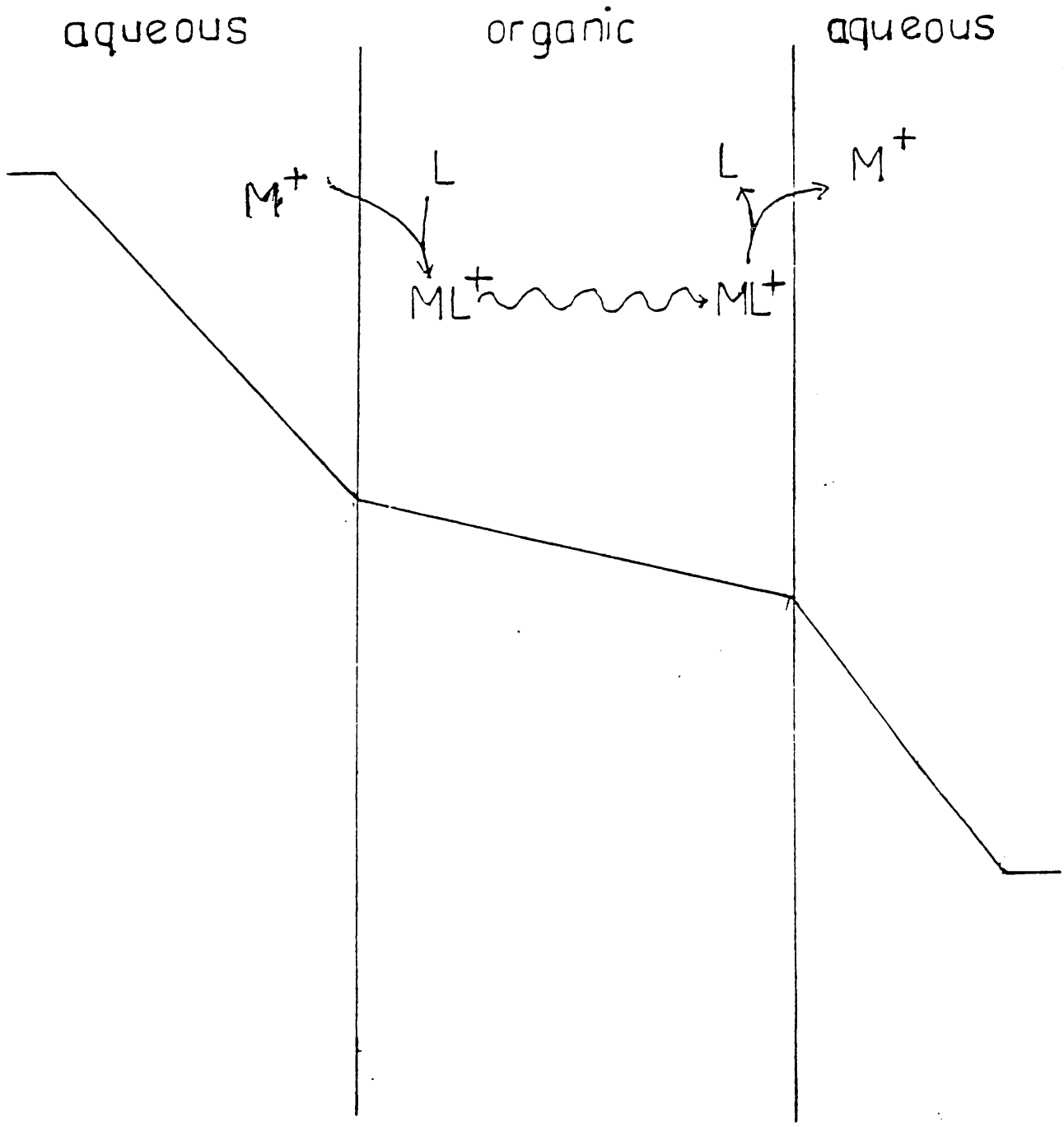

2.5 A Liquid Membrane System

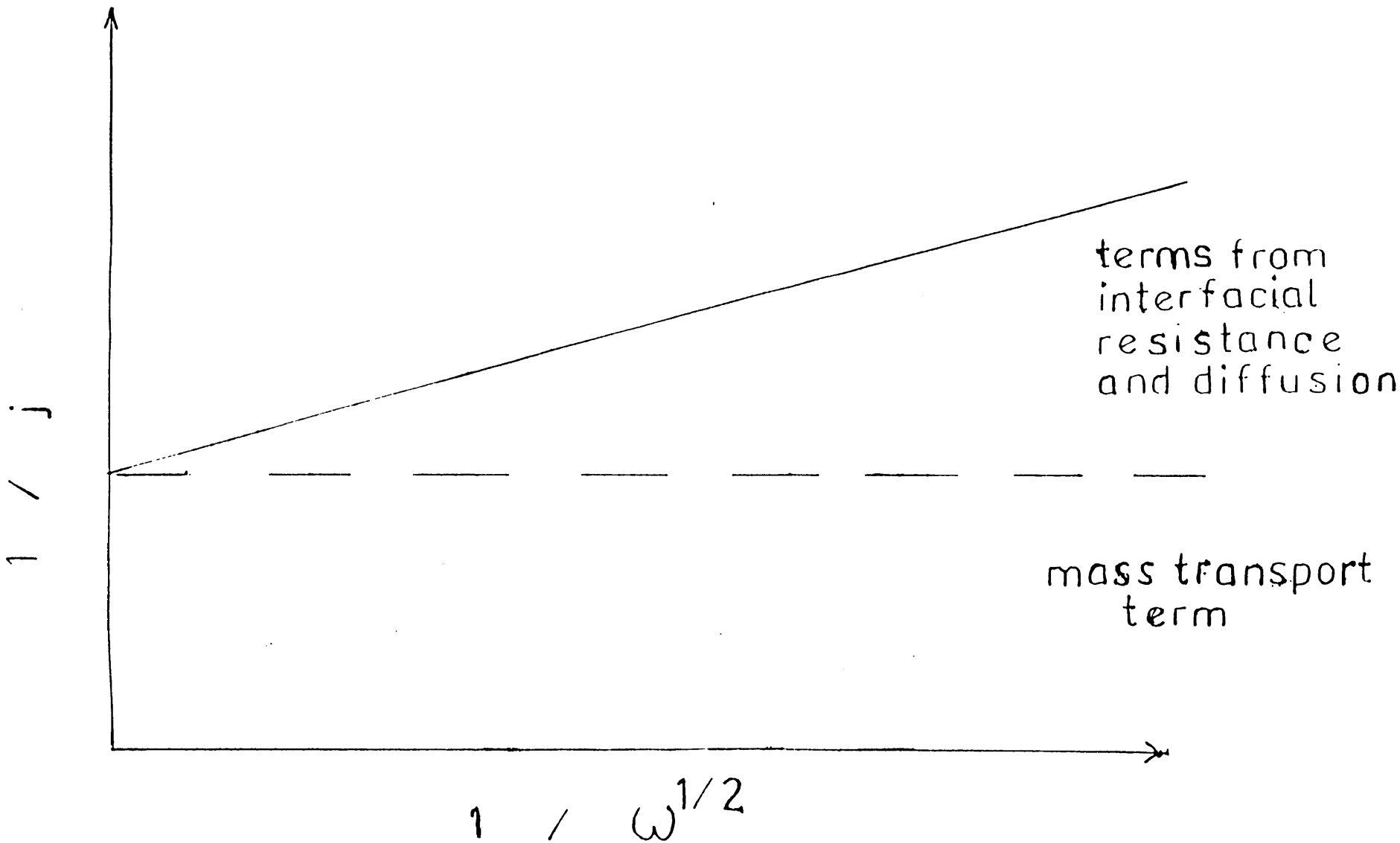

2.6 A Koutecky-Levich Plot for Liquid Membranes

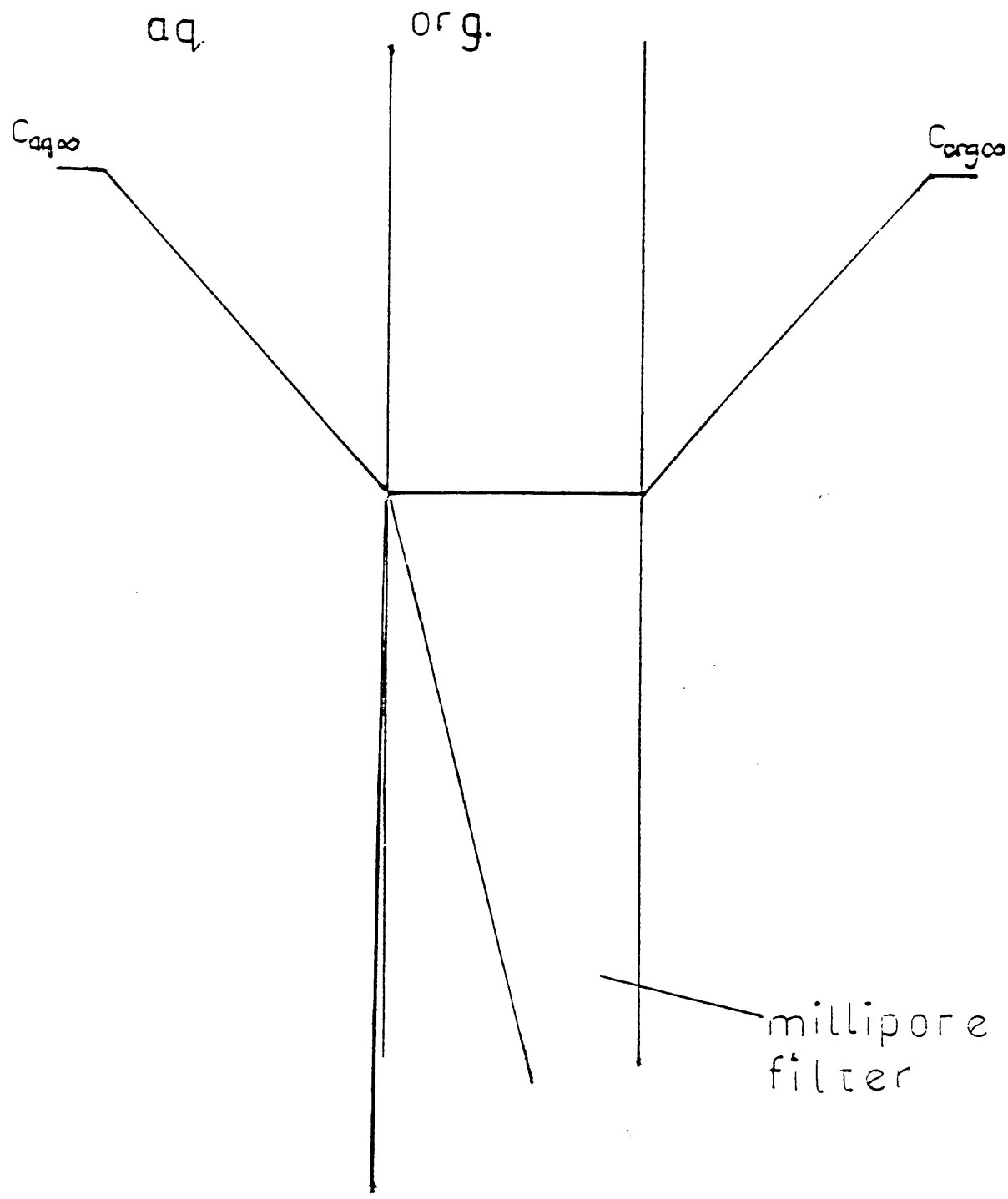

2.7 A Liquid-Liquid Interfacial System

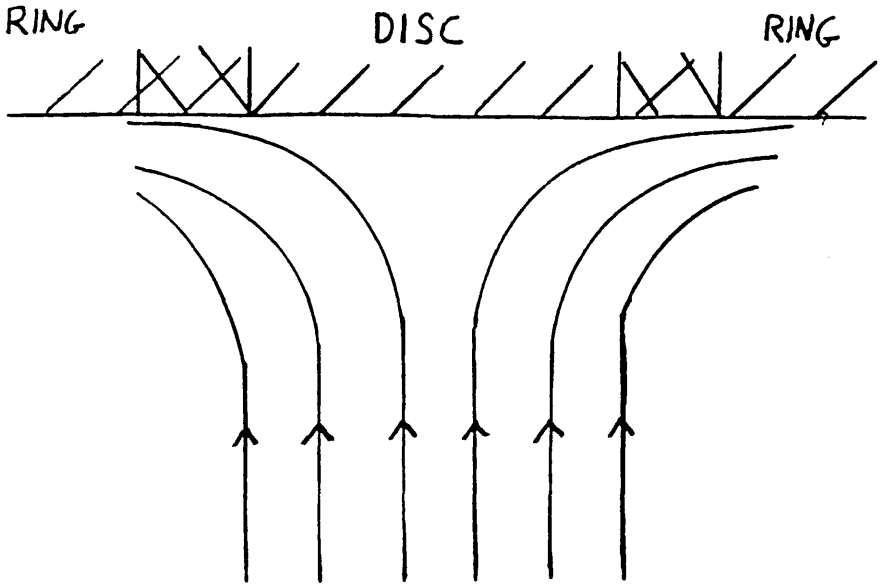

2.8 Flow Patterns for a RRDE

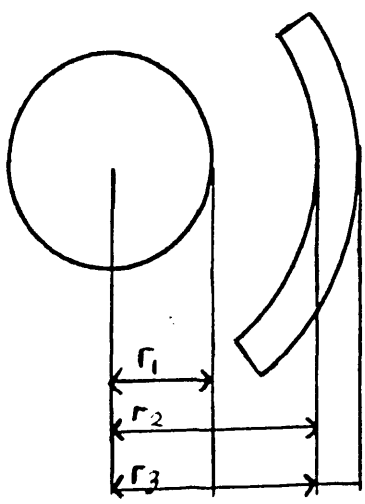

2.9 An Arc Electrode

From 2.14 it can be deduced that N_o is solely a function of electrode geometry , and does not vary with rotation speed .

The main difference between the R.R.D.E. and the R.D.C. with the arc electrode is that the electrode is not a complete ring for interfacial chemistry studies . This can be taken account of if needs be , but in the case of potentiometric sensors , no compensation is necessary as the potential of the arc is independent of area .

2.2.2 The Silver/Silver Halide Arc Sensor

A silver/silver halide arc electrode can be produced galvanostatically , (see section 3.4.2) . The electrode consists of a porous silver halide layer covering the silver metal surface . Silver halides are sparingly soluble in water therefore the concentration of the ions adjacent to the electrode can be given by the solubility product :-

$$K_{SP} = [Ag^+][X^-] \qquad (2.16)$$

The potential of the electrode is dependent on the silver/silver ion couple and can be expressed by the Nernst equation

$$E = E^{\ominus}_{Ag/Ag^+} + 2.3\frac{RT}{F}\log_{10}[Ag^+]$$

$$= E^{\ominus}_{Ag/Ag^+} + 2.3\frac{RT}{F}\log_{10}K_{SP} - 2.3\frac{RT}{F}\log_{10}[X^-] \qquad (2.17)$$

Which means the potential of the electrode is dependent on the halide ion concentration .

A number of assumptions have been made in order to obtain 2.21 :-

i) There is no direct electron transfer between silver and silver halide . This has been shown to be valid assumption in the case of thin , porous silver halide films[90,91] .

ii) The kinetics of silver halide association and dissociation are fast enough for the equilibrium concentrations of ions close to the electrode to be maintained .

iii) Silver Halide is always present i.e. it does not totally dissolve off the electrode .

Due to the hydrodynamics of the R.D.C. , (see section 2.2) , the concentration of halide at the arc will be proportional to the flux of ions either diffusing from the inner compartment , or being created at the interface . The mathematics of this relationship have been solved[92,93] . From equation 2.13 of reference 92 an expression for the flux of X^- species can be obtained where X^- is the only species in the outer compartment that affects the electode potential and the mass transfer limited current approaches infinite values :-

$$j = - \frac{i^{\infty}_{arc}}{N_0 F} \exp \left[- \frac{\Delta E_{arc} F}{RT} - 1 \right] \qquad (2.18)$$

where

$$\Delta E_{arc} = (E_{arc})_{iarc=0} - (e_{arc})_{j,iarc=0}$$

i.e. the difference in arc potential from the value when no halide fluxes.

where N_0 is the collection efficiency for the arc electrode , j is the flux of X^- at the filter disc . i^{∞}_{arc} is the mass transport limited current at the arc electrode . It is important to note that the X^- must be the majority charge carriers for the above condition to be met . Therefore the concentration of the X^- must be well above the square root of the solubility product of the relevant silver halide .

Therefore the flux of halide ion at the disc of a R.D.C. can be evaluated by measuring the potential of a silver / silver halide arc electrode with respect to its potential when no species flow from the disc to the ring (i.e. $\omega=0$) . A measurable ΔE_{arc} can be produced when the value of jF is comparable to or greater than i^{∞}_{arc,Ag^+} . Using low concentrations of silver in the bulk solution reduces the value of the mass transport controlled current and so enables measurement of low fluxes .

2.3 A.C Impedance Studies

A.C.impedance measurement over a range of frequencies , (i.e. impedance spectra) , can yield a vast amount of information about membranes , e.g. diffusional properties , the effect of adsorption , double layer charging .

A simple circuit diagram is shown in fig 2.10a , consisting of a capacitance (C_A) in parallel with a resistor (R_B) and this combination in series with another resistor (R_A) . The real and imaginary components may be calculated :-

For the parallel CR circuit

$$1/Z_P = 1/R_B + \omega C_A i \qquad (2.19)$$

rearranging this gives

$$Z_P = \frac{R_B}{1+(R_B\omega C_A)^2} - \frac{R_B^2\omega C_A i}{1+(R_B\omega C_A)^2} \qquad (2.20)$$

And therefore the real and imaginary components for the whole circuit are :-

$$Z' = R_A + R_B \,/\, 1+(R_B\omega C_A)^2 \qquad (2.21)$$

$$Z'' = R_B^2\omega C_A \,/\, 1+(R_B\omega C_A)^2 \qquad (2.22)$$

eliminating ω

$$(Z' - R_A - R_{B/2})^2 + Z''^2 = (R_{B/2})^2 \qquad (2.23)$$

This is the equation of a circle hence fig.2.10b . When $Z''=0$ $Z' = R_A$ and R_A+R_B therefore the radius of the semicircle is $R_{B/2}$. The peak of the circle (Z'' is a maximum) occurs at a frequency which equals $1 / R_BC_A$.

This theory can be extended to an actual membrane which will usually have an equivalent circuit (i.e. the representation of the cell by means of electrical components) , consisting of numerous CR parallel components representing various processes :-

i) Bulk membrane geometric capcitance and resistance , R_b, C_G.

ii) Double layer capacitance and charge transfer (across the double layer) resistance , C_{dl},R_{ct} .

iii) Warburg diffusional impedances , C_w,R_w

iv) Impedance due to adsorption of molecules on the membrane.

v) Interfacial reaction impedance .

The resulting impedance spectra consist of , in general , a number of semicircles . The positioning of particular semicircles depends on the value of the time constant , τ ,

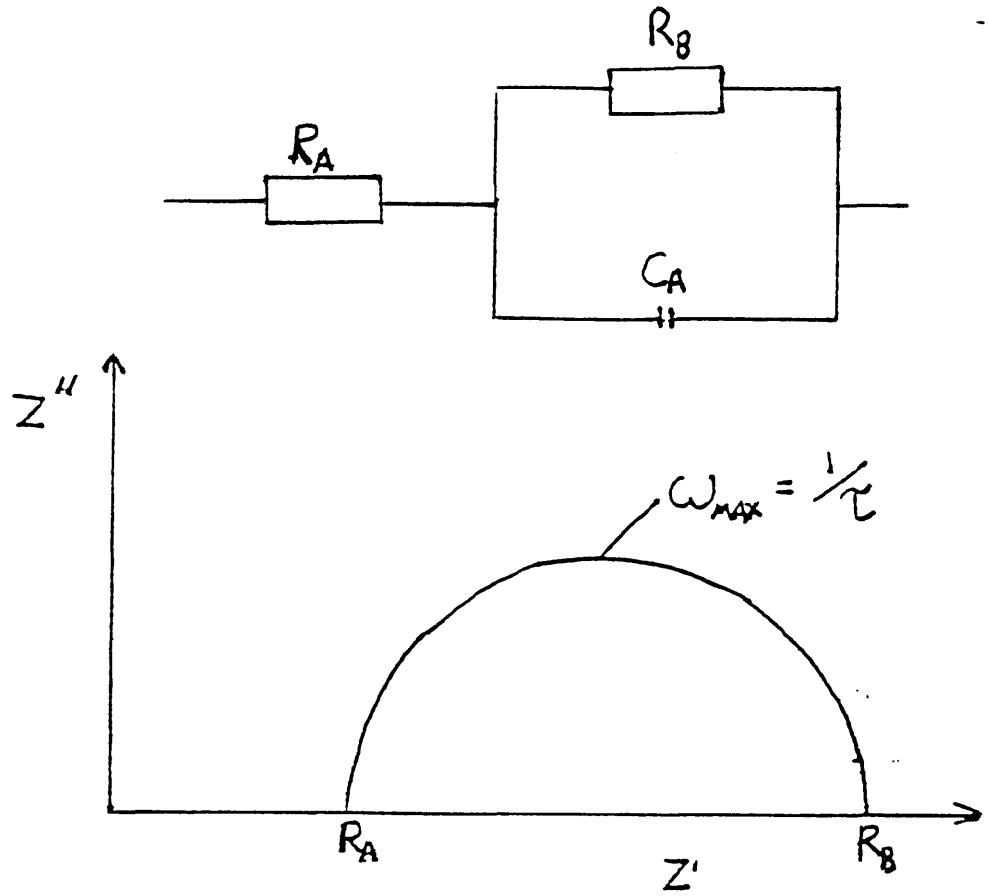

2.10a A CR circuit

b The resultant Impedance spectrum

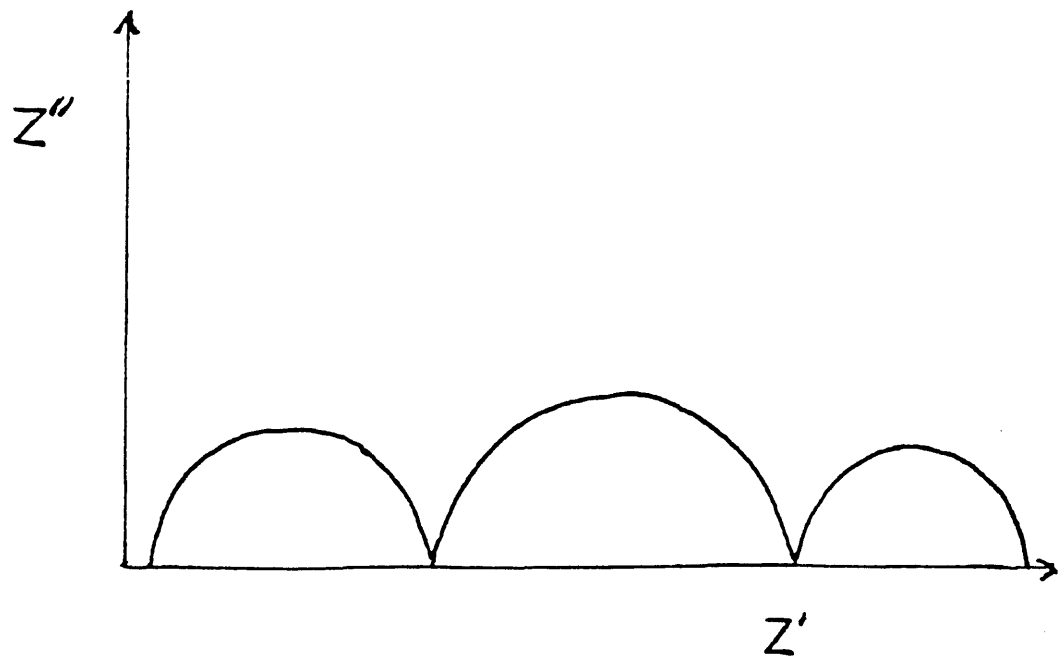

2.11 The Typical Impedance Spectrum of a Membrane

which is the product of resistance and capacitance . If τ is small then the semicircle is observed in the high frequency range , and vice versa .

Sometimes the resistance of the solution , R_s , is appreciable . When this is the case , R_s is equivalent to R_A in the previous example . The main exception to the above is the Warburg diffusional impedance . This describes a diffusional term in the transfer of ions across the double layer . The real and imaginary terms of the Warburg impedance are equal , i.e. a straight line at $\pi/4$ radians is observed . Warburg impedance generally occurs along with charge transfer /double layer terms . A more extensive account of the theory of A.C. impedance spectra can be obtained from the literature[94] .

From the value of the charge transfer resistance of a membrane a value of the exchange current may be obtained using the equation[94] :-

$$i_o = RT / nFR_{ct} \qquad (2.24)$$

R , T , n and F have their usual significance and i_o is the exchange current .

CHAPTER3 EXPERIMENTAL METHODS

3.1 Chemicals and Apparatus

3.1.1 Chemicals and Solvents

The photo-polymerisable lipid (fig. 3.1) was prepared by the organic chemistry section of the Unilever research laboratory at Port Sunlight . It was purified by column chromotography , using chloroform/acetic acid followed by methanol/acetic acid mixtures as eluents .

All solvents were AnalR , or equivalent , grade . Chemicals were supplied by Sigma apart from the non-polymerisable lipids , which were obtained from Lipid products . Aqueous solutions were prepared using doubly deionised water , purified by passage through a Millipore Milli-Q system .

3.1.2 Apparatus Manufactured "In-House"

The rotating diffusion cell was manufactured by Mr. Michael Pritchard and the associated electronics by Mr. John Hooper . The Langmuir trough assembly and associated electronics were built by Kathy Snook . The arc electrodes were manufactured in the thin membrane laboratory in the electrical engineering department of Imperial college .

3.1.3 Recording Devices

Chart recorders X-Y Bryans 60000 series

Y-t Gould BS 273

Digital multimeter Fluke 8010A

Impedance measurements were obtained using a Wayne Kerr bridge Solartron Schlumberger controlled by a Torch micro-computer .

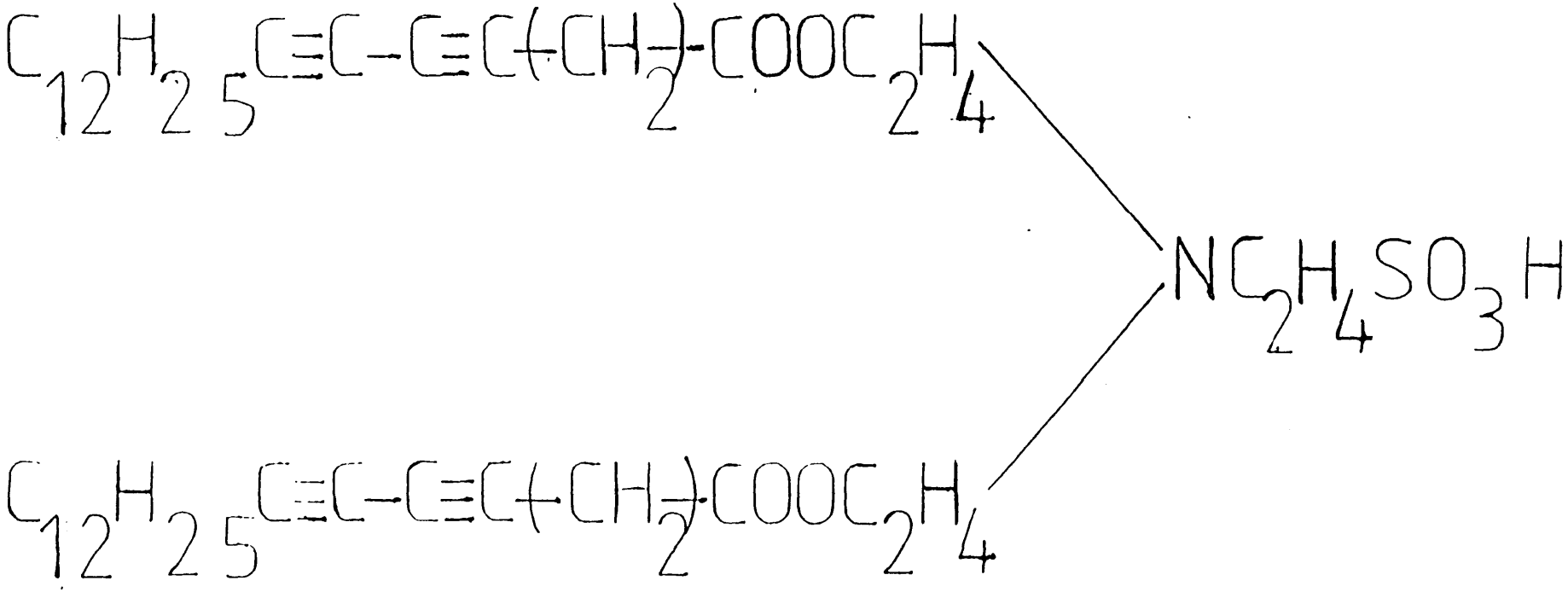

3.1 The Diacetylenic Lipid Used in This Study

3.1.4 Controlling Devices

The Langmuir trough controlling electronics have been described elsewhere[95] . Their basic operation is as follows - The surface pressure of a monolayer was measured by means of a displacement transducer , which could be calibrated to measure the change in weight of a Willhelmy plate (fig. 3.2). Molecular area was measured by employing a precision stepper motor to drive the movable barrier . The area swept by the barrier was obtained by the calibration of a digital , or graph , output from the motor . The surface pressure of a monolayer was kept constant by means of a comparative logic circuit (fig 3.3) . This circuit checks to see if the transducer output was within a specified window ($\pm \Delta\Pi = \pm \Delta 0.2$ dynes cm^{-1}) of a selected reference value , usually the transducer output at the initiation of the constant pressure experiment .

For the black lipid membrane studies current/voltage relationships were obtained by means of a potentiostat , the input voltage of which was supplied by a triangular wave generator .

The potential of the arc electrodes was followed with respect to a saturated calomel electrode (S.C.E.)

A.C. impedance measurements were performed using a Solartron phase sensitive device (p.s.d.) . A four electrode system was employed and the electrochemical cell was controlled potentiostatically ,with the reference electrode input being the difference between two S.C.E.

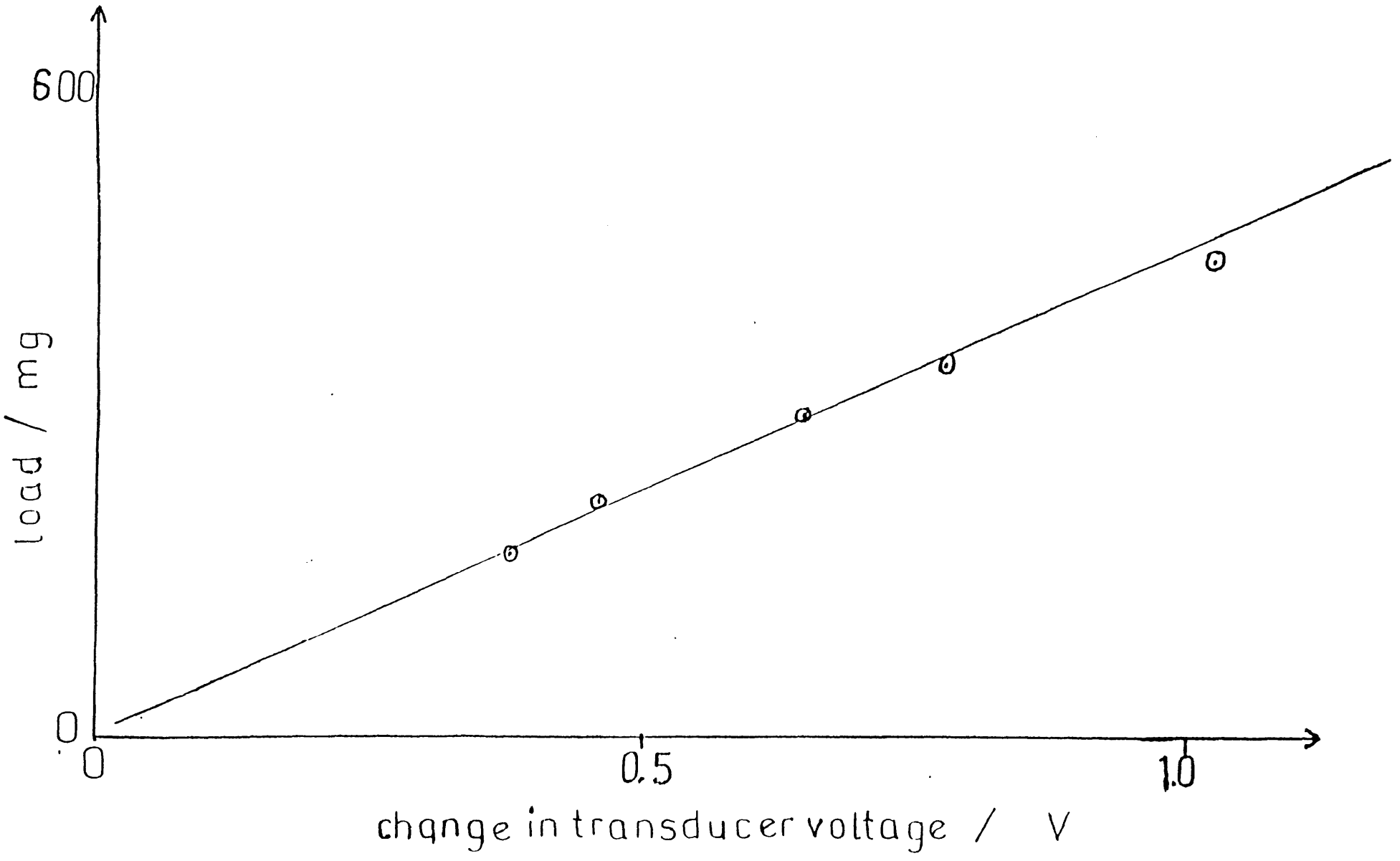

3.2 Calibration Curve for the Displacement Transducer

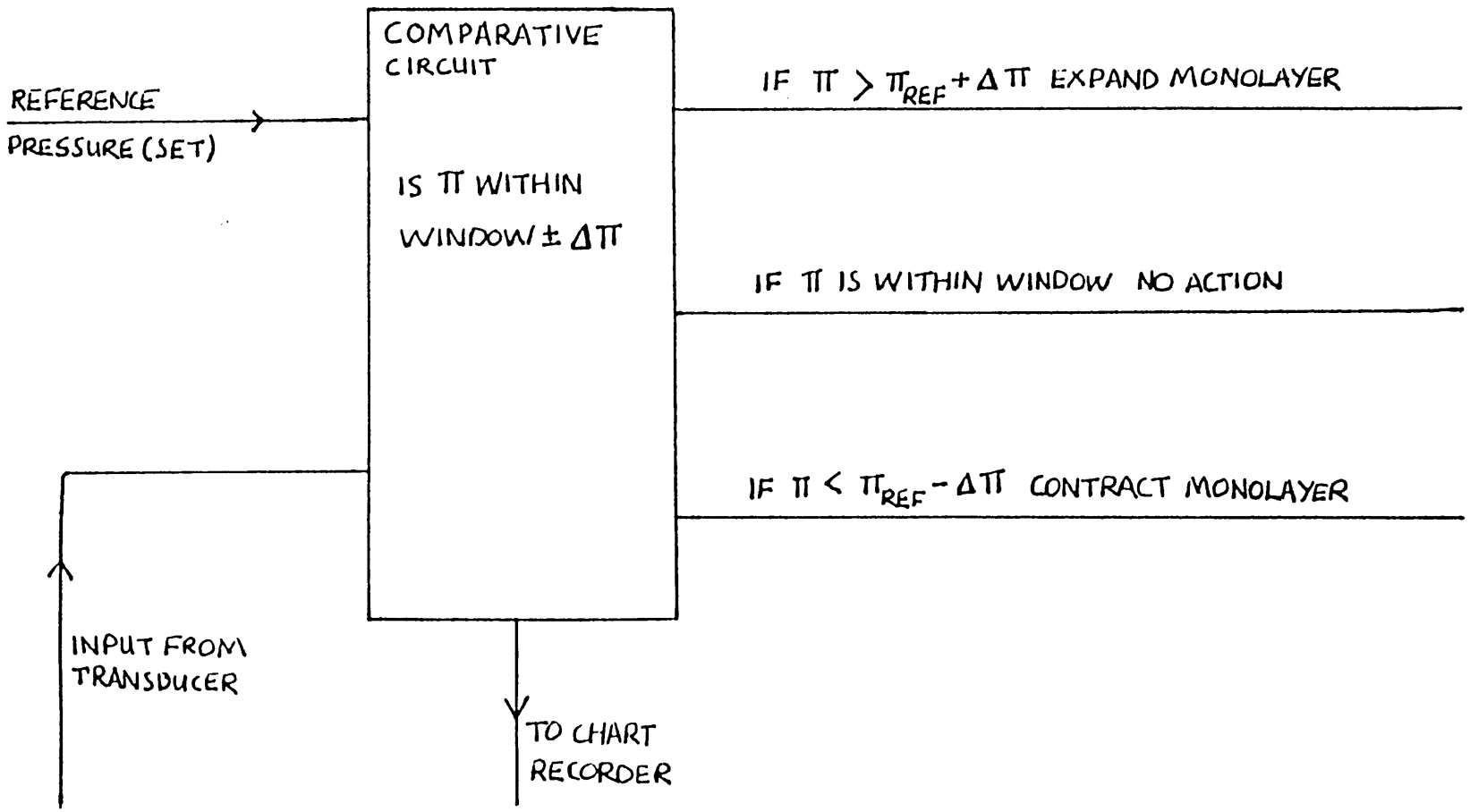

3.3 The Logic Circuit for the Constant Surface Pressure Mode Electronics

references on either side of the membrane . The two current carrying electrodes were made of platinum gauze .

3.1.5 Miscellany

i) Silver paint was supplied by Johnson Matthey .

ii) Microfilters were obtained from-

Millipore GSWP0047 polyester filters

Nucleopore polycarbonate filters

iii) Silica slides were provided by Optiglass

iv) PTFE components were supplied by Fluorochem .

v) Hamilton microsyringes were obtained from V.A.Howe .

3.2 Langmuir-Blodgett Experiments

The Langmuir trough was located in a dust-free , thermostated environment . The general procedure of these experiments was as follows :-

3.2.1 Cleaning Procedure

Experiments performed at the water-air interface are particularly vulnerable to contamination by foreign matter , and meticulous procedures were followed at all times . The Langmuir trough was always left full of doubly distilled water when not in use . This water was removed before an experiment by means of an aspirator , the glass nozzle of which had been cleaned by acid treatment . The Langmuir trough and barriers were then cleaned with a series of solvents , (n-heptane , ethanol and water) , using ashless filter paper held by tweezers . Doubly distilled water was then placed in the trough until a meniscus of roughly two millimetres was visible . The surface of the water was cleaned by moving a barrier across the trough and

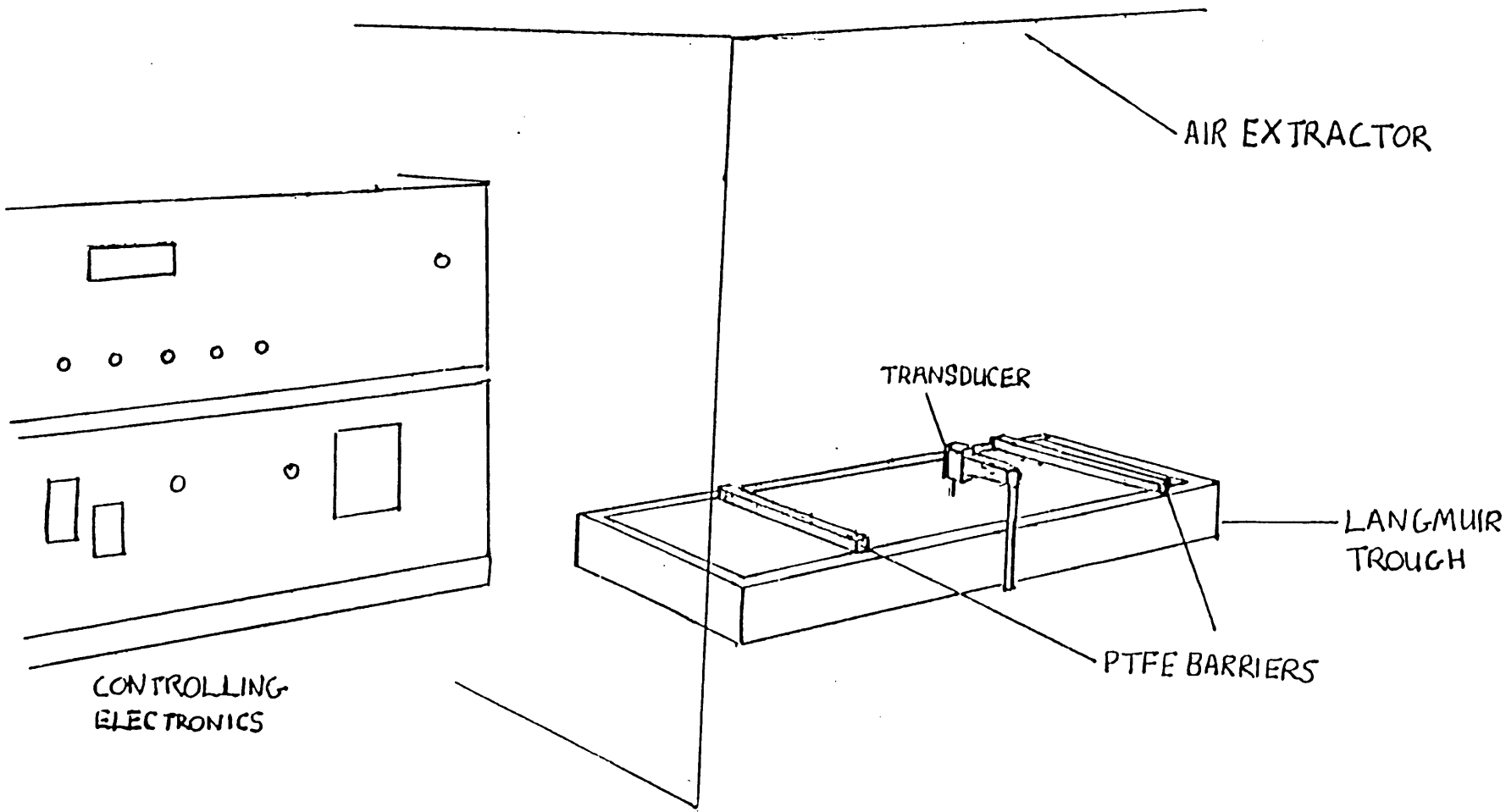

3.4 The Langmuir Trough

simultaneously holding the aspirator nozzle to the water surface to remove any particles collected by the barrier .

3.2.2 The Spreading Procedure

The Wilhelmy plate were made out of ashless filter paper , cut from a stainless steel template . It was suspended from a displacement transducer . After the transducer reading had settled , usually 10-15 minutes , one of the barriers was moved across the water surface . This procedure should result in no change in the transducer reading , i.e. no change in the surface tension of the water surface as it is clean . If this was not the case the trough would be emptied and the cleaning procedure repeated .

The Wilhelmy plate was now calibrated with a known weight , approximately 20 mg , and the surface pressure could then be calculated by the equation :-

$$\pi = \frac{F}{l} = \frac{y \,.\, f \,.\, 0.9814}{\text{plate perimeter}} \qquad (3.1)$$

π surface pressure in dynes cm-1 (=mN m-1)

y chart recorder divisions

f calibration weight / resultant displacement (mg div^{-1})

0.9814 is the acceleration due to gravity in units of cm s^{-2}

The plate perimeter was determined by the size of the template as the thickness of a wet filter was found to be constant experimentally[95] .

The spreading solution , lipid in a volatile solvent , was prepared so that a reasonably small volume (approximately 100µl) , gave a molecular area of roughly one nm^2 per molecule . The small volume reduces the time

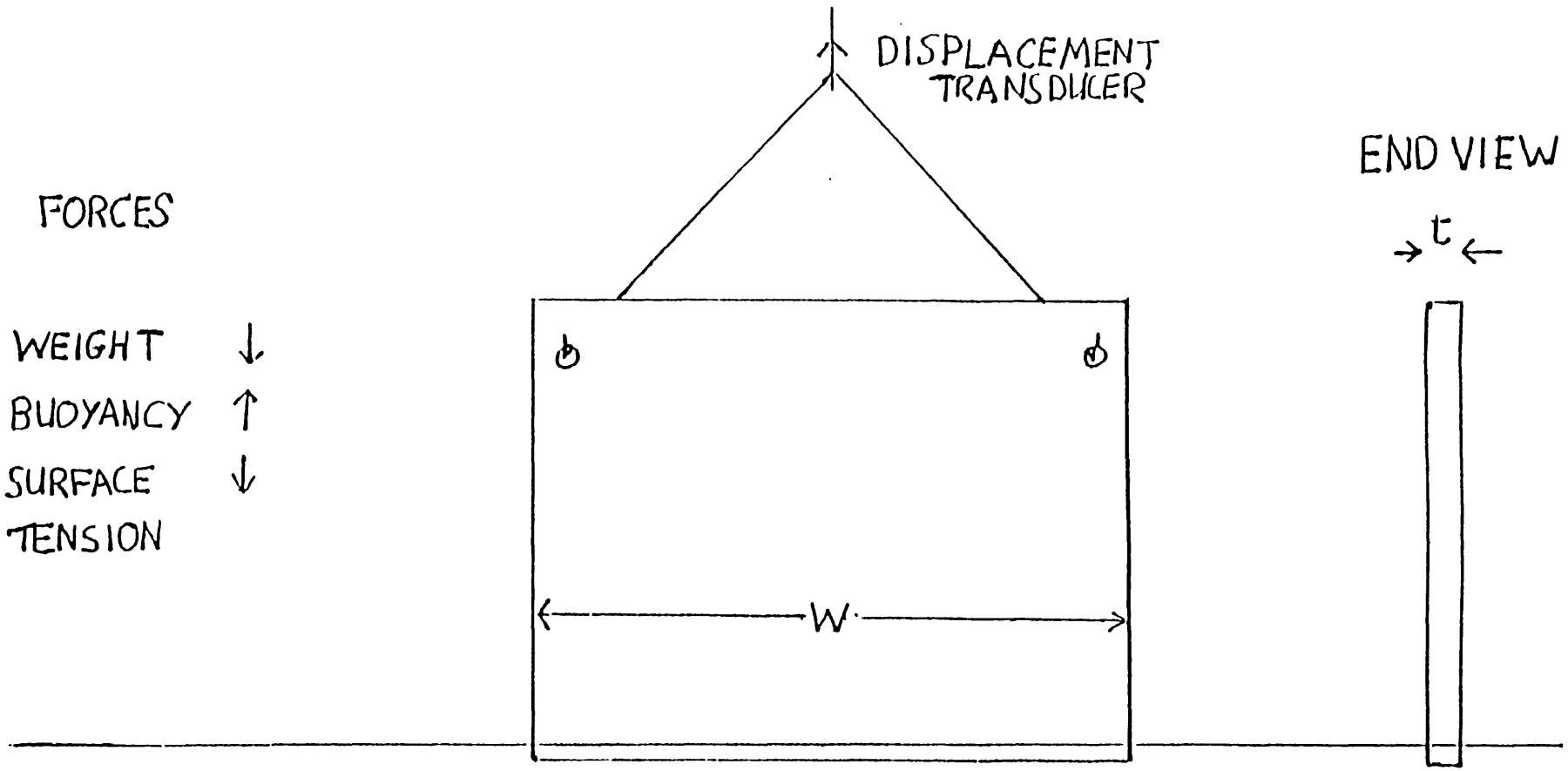

3.5 A Wilhelmy Plate

needed for evaporation of the solvent , and the initial molecular area enables a complete π / A isotherm to be obtained in one experiment (fig. 3.7) .

Spreading the monolayer consisted of :-

i) forming a droplet of solution at the head of the syringe .

ii) touching the surface of the water with this droplet .

iii) allowing the solvent to evaporte . This period increased gradually as the amount of lipid on the surface became larger , and was followed by noting surface pressure reading (fig. 3.6) . The surface pressure rises on addition of the spreading solution but drops as the solvent evaporates .

3.2.3 Measurement of a π/A Isothem

After the spreading procedure had been completed the monolayer was left untouched for a few hours to allow the solvent to fully evaporate . When recording the isotherm the area of the monolayer is reduced at a very slow rate , (barrier movement in the order of mm per second) , to make sure the structure of the lipids is the equilibrium one .

Surface pressure is measured from 3.1 . Molecular area is obtained from the calibrated digital output . An important point to remember when calculating the area of the monolayer is that the Wilhelmy plate is wetted by the water , (i.e. it has a positive meniscus) . The area of wetting must be added to the area between the barriers of the Langmuir trough . For filter paper plates the area of wetting is simply twice the area of the template , (i.e. both sides of the Wilhelmy plate are wetted) .

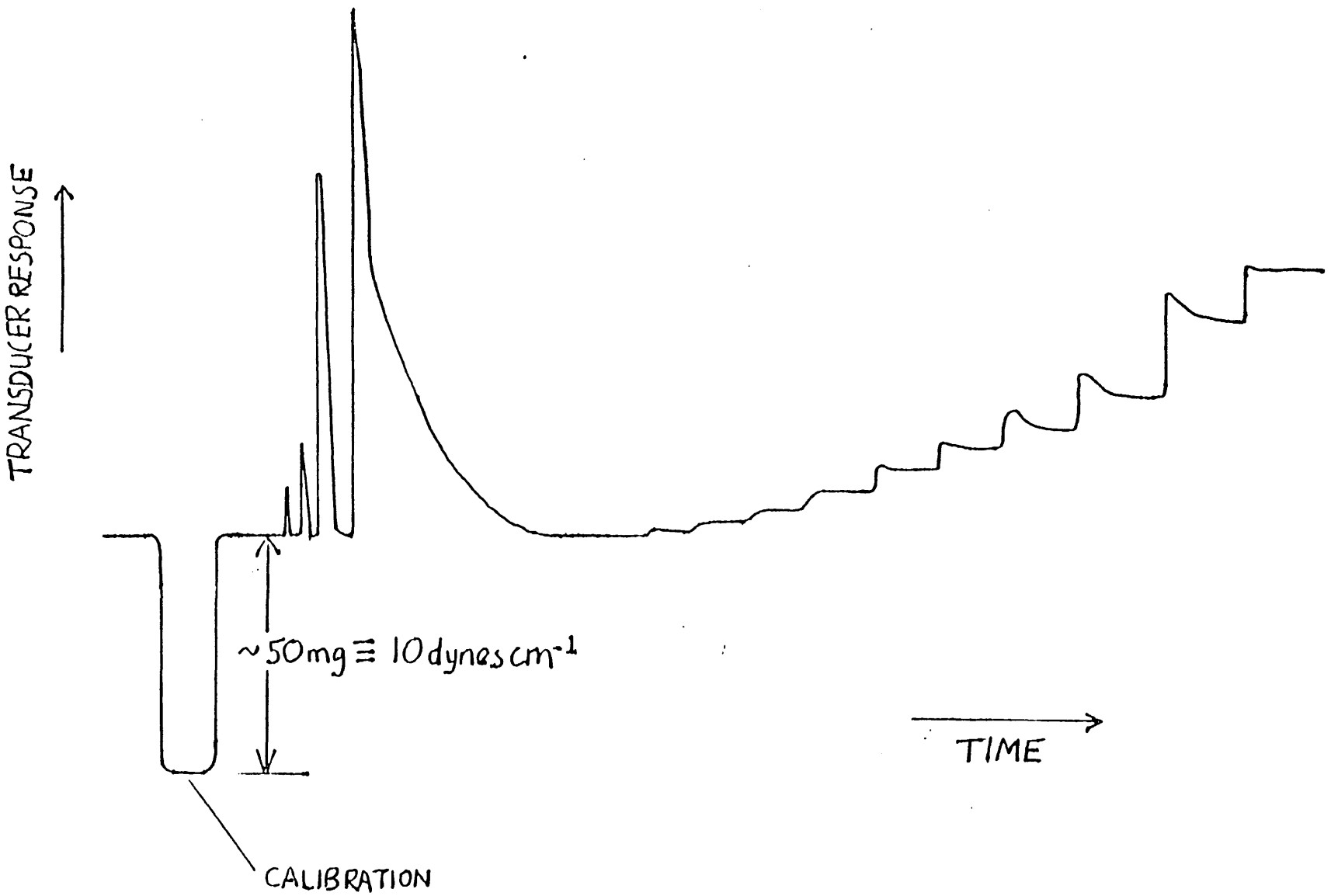

3.6 A Chart Recorder Output from a Langmuir Trough Experiment

3.2.4 The Photo-Polymerisation Procedure

The monolayer was usually polymerised on the Langmuir trough . Because the polymerisation reaction is topochemical[2,28] , U.V. irradiation was exposed to compressed monolayers . On polymerisation the monolayer shrinks[2,28] , but this was counteracted by employing the constant pressure mode of the electronics . The reading of the area swept by the barrier to keep the surface pressure constant was a measure of the shrinkage .

3.2.5 The Langmuir-Blodgett Coating Procedure

Langmuir-Blodgett dipping was carried out , usually after the polymerisation of the monolayer , by means of the carriage (fig. 3.7) . The apparatus facillitates slow vertical movement (from 0.06 to 15 mm per second) . Generally a slow upward and a relatively fast downward movement were employed . Slow speeds were counter productive for downward coatings as a negative meniscus forms .

3.3 Black Lipid Membranes

Black lipid membranes are formed when solutions of lipids are placed onto a small orifice that is submerged in an aqueous phase . Black lipid membranes of the diacetylenic lipid (fig. 3.1) were prepared as follows :-

3.3.1 The Cell

A Millipore membrane was used as the orifice (collection of orifices) . The Millipore membrane was supported on a perspex cylinder and wa treated in such a way

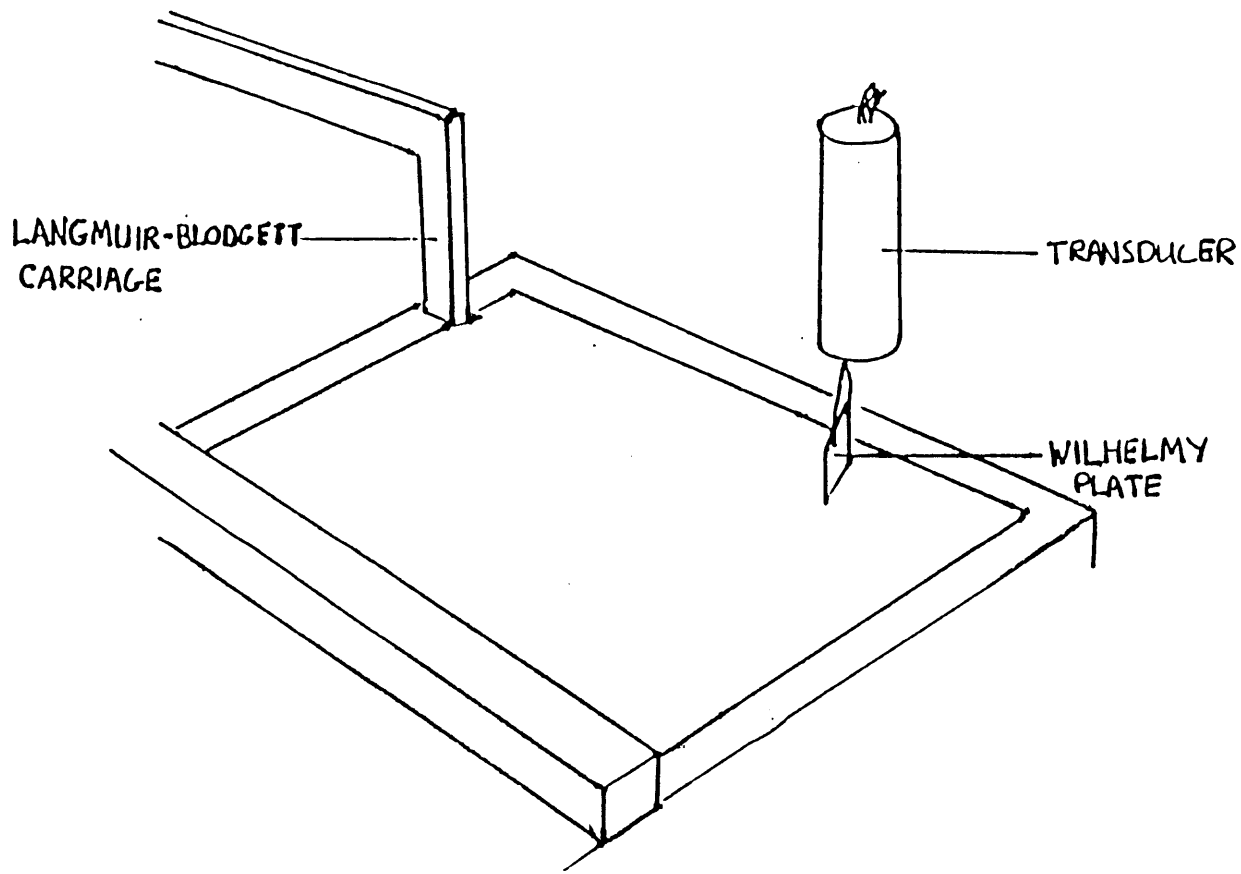

3.7 The Langmuir-Blodgett Carriage

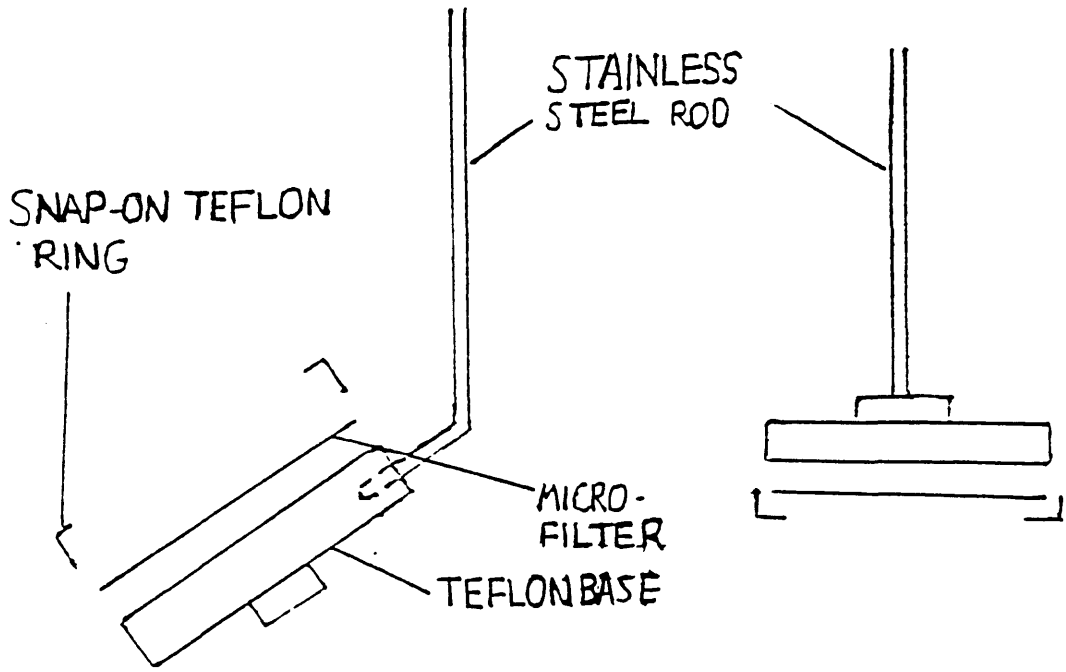

3.8 The Microfilter Support

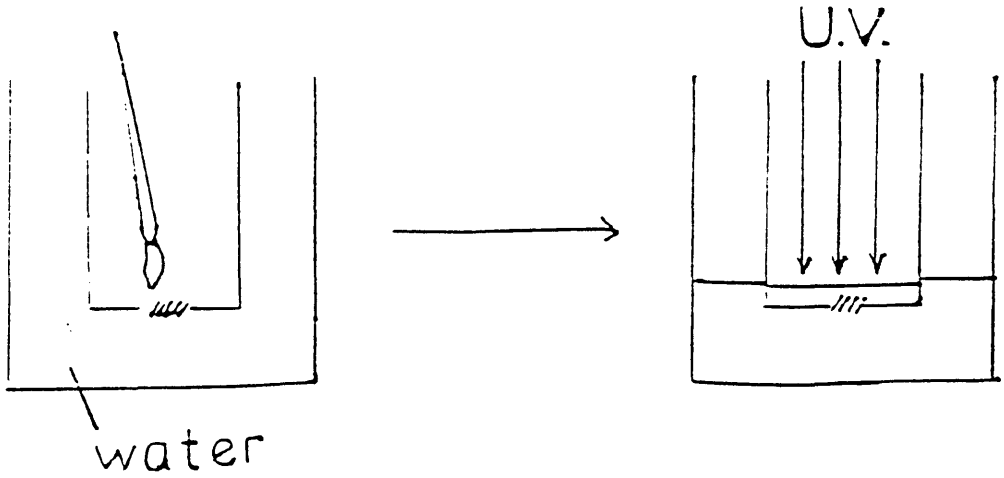

3.9 The Brush Technique

that all the pores outside a small central region , diameter roughly one millimetre , were collapsed - see section 3.4.1 for the details of this procedure .

3.3.2 The Bilayer Forming Solution

A solution of the lipid in a large chain alkane , e.g. dodecane , was prepared at a concentration of 1mM . Oxidised cholesterol , (oxidised by bubbling oxygen through a dodecane solution for six hours) , was added to the solution in a one to ten ratio with the lipid .

3.3.3 Forming the BLM

A few millilitres of the solution prepared was applied to the porous region of the Millipore membrane by means of a pencil brush . An aqueous solution of potassium chloride (0.01M) was placed on either side of the wet Millipore filter . A dose of U.V. irradiation would generally be applied soon after the formation of the BLM .

3.3.4 Testing the BLM

The integrity of the resultant bilayer was tested by means of a Wayne Kerr bridge . The resistance of a bilayer should be in the order of $M\Omega\ cm^{-2}$, and assuming the bilayer acts as parallel plate capacitor its thickness can be obtained from :-

$$\text{Thickness} = A\varepsilon_o\varepsilon_r / C \qquad (3.2)$$

A is the effective area of the Millipore filter .

C is the capacitance of the bilayer .

ε_o the permittivity of free space .

ε_r the relative permitivity which must be assumed .

The current-voltage characteristics of the formed bilayer

were obtained . This will be discussed further in chapter 4 .

3.4 The Rotating Diffusion Cell (R.D.C.)

The basic design of the R.D.C. has been described elsewhere[85,96] . The cell basically consists of two compartments separated by a Millipore filter (fig.2.4) .

3.4.1 The Manufacture of the Cell

The cell relies on the creation of a central porous disc surrounded by an impermeable region . This is achieved by attaching a Millipore filter to a perspex cylinder . The cell is then rotated in a lathe at moderate frequency (roughly five hertz) , and a collapsing solution , one part 1,2-dichloroethane , one part 1,4-dioxane and one part n-heptane is applied by means of a coarse pencil brush . Solution is placed roughly 0.75 cm from the centre of the Millipore filter and then radially outwards . The cell is then soaked in doubly distilled water for a few hours and then dried in a dessicator .

3.4.2 Production of the Arc Electrodes

After collapsing the pores on the outside of the Millipore filter a stainless steel template was then fitted onto the cell . A thin silver film , thickness approximately 100 nm , was then sputtered onto the surface of the filter , in a region where the pores had been collapsed .

Values of the radii , r_1 , r_2 and r_3 where obtained from a photographic enlargement of the completed cell . The values of the collection efficiency N_0 and the area of the porous part of the disc were then calculated .

Photograph of uncleared (TOP) and cleared (BOTTOM)

Millipore filters.

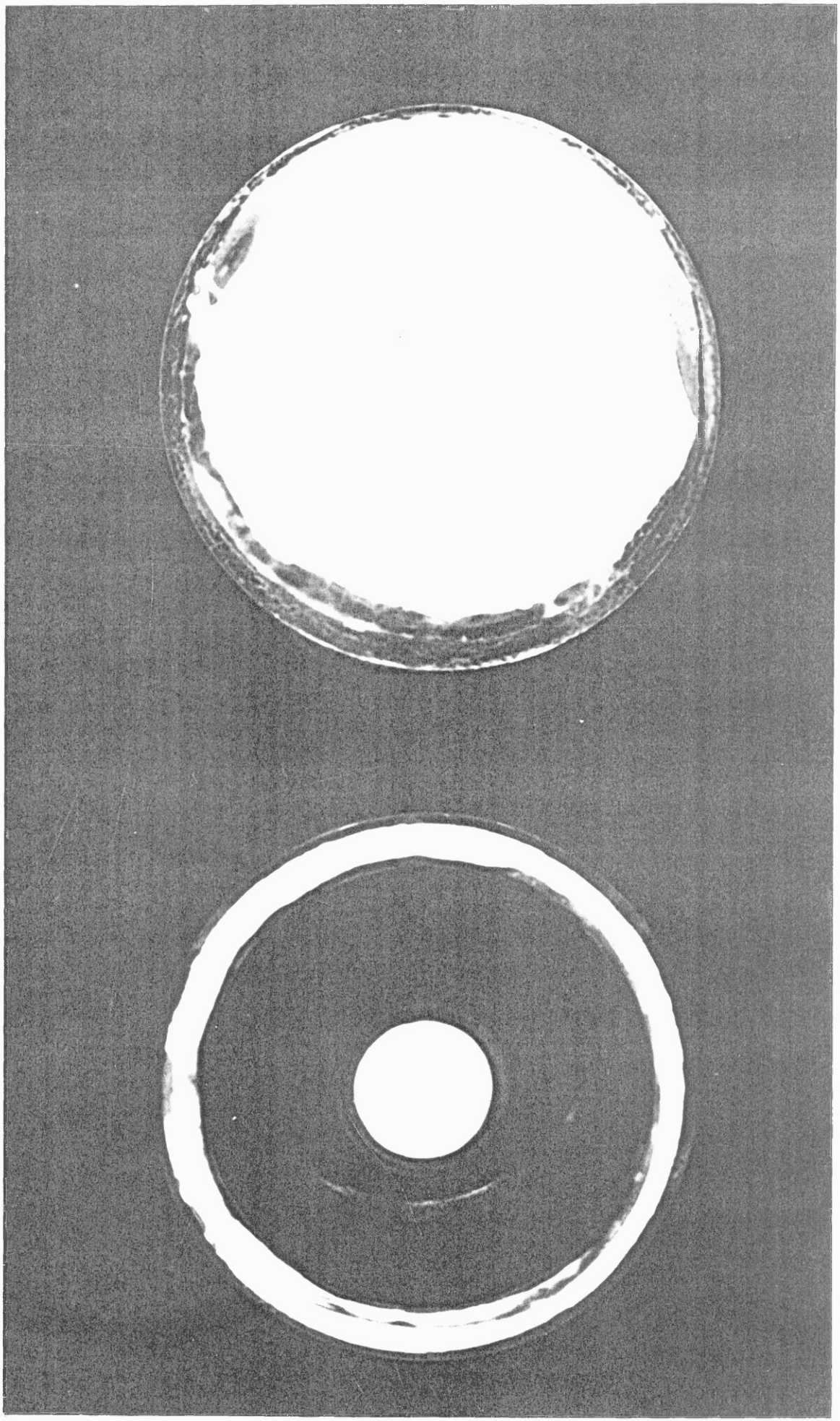

The silver / silver halide electrodes were prepared by anodising the arc . Aqueous solutions of HX (10^{-2}M) were used and a current of 100 μA was passed for roughly one minute .

3.4.3 Experimental Procedure

Before setting up an interfacial system the Millipore filter was washed with n-heptane . After this procedure it was then soaked in n-heptane , (for the interfacial polymerisation experiments) ,for a few minutes . Alternatively , the filter was soaked in a liquid membrane forming solution , (e.g. valinomycin in diphenyl ether) , overnight . With the filter wet , with heptane or diphenyl ether , solutions were placed into the inner and outer compartments .

Electrical contact with the arc was made by means of silver paint . The paint connected the arc to the rotating pulley block , and was insulated from the solutions with perspex cement . Carbon brushes were used as contacts to the pulley block .

CHAPTER 4 STUDIES ON THE CREATION OF STABLE LIPID BILAYERS

4.1 The Design of a Lipid Bilayer Amperometric Sensor

A number of criteria have to be satisfied before lipid bilayers can be an integral part of electrochemical sensors .

i) The formation of a resistive structure , (the basic structure of the membrane has to be resistive otherwise the incorporation of protein molecules will be pointless).

ii) Membrane stability is also very important . Bilayers are intrinsically unstable[1] , and working sensors must be relatively long-lived .

iii) The bilayers must be able to have protein molecules incorporated into them . This implies a degree of flexibility in the lipid chains , as well as particular dimensions , (i.e. the membranes must be very thin) .

iv) The membranes must be portable . The ability to remove the bilayers from aqueous solution would be advantageous , if not essential .

v) Ease of preparation is another important factor . The method of preparation must result in bilayers of consistent structure and quality , which over-elaboration would inhibit.

vi) The cost of preparing the lipid bilayer membrane is important . Highly expensive membranes will have little or no use . Most of the sensing functions of lipid bilayer membranes are attainable by other means . Although an amperometric sensor has the advantage of being " on-line " , this could well be deemed unnecesary if the cost of preparation is high .

4.2 Bilayer Preparation

4.2.1 The Stabilisation of Lipid Bilayers

Formation of stable lipid structures was a primary concern of this work . The incorporation of proteins and various improvements to a finished sensor could only be investigated after this had been achieved .

It was decided that supporting the lipid structures on a solid substrate was a pre-requisite as unsupported bilayers can only be formed with very small dimensions . This also allows the bilayer to be portable .

Polymerisation of the lipid structure was also used as an aid to stability . This helps to retain an exact bilayer structure , as an unpolymerised bilayer is liable to rupture with mechanical stress or jolting . It was decided that the diacetylenic lipid , (fig. 3.1) , would be used . This lipid has been polymerised in vesicle form , and the resultant structure allows the incorporation of protein molecules by simple incubation[97] . This polymerisation is topochemical and thus lipids need to have an ordered structure before the stabilisation can occur . The easiest way of achieving this is to use a Langmuir trough type of apparatus and so form lipid monolayers at the air-water interface . Liquid-liquid interfaces are less easy to control .

4.2.2 Langmuir Trough Experiments

Surface pressure is defined as the reduction of surface tension of a pure water surface by the adsorption of surface active material . The surface pressure therefore gives an

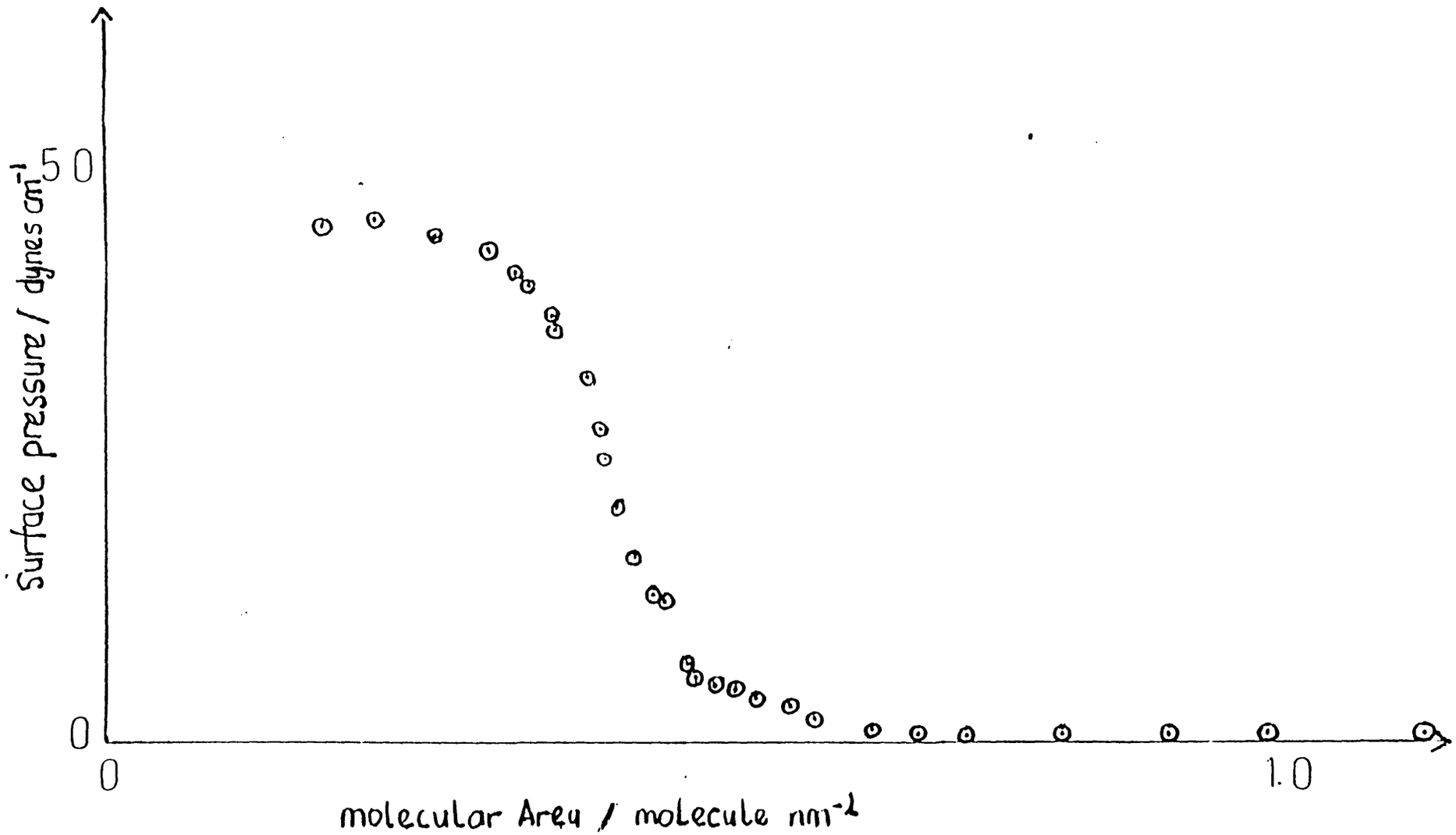

4.1 A π/A Isotherm of the Diacetylenic Lipid

indication of the sort of processes occuring at the air-water interface .

A typical isotherm is shown in figure 4.1 . The isotherm is analagous to the pressure/volume isotherm for a gas , (i.e. Boyle's Law) , in that it shows the physical state of the molecules in the monolayer at particular surface pressures . At high molecular areas the molecules are fluid , in a gaseous or liquid-like state , and are not organised into a regular structure . The point of inflexion is indicative of a change of state to a solid , crystalline arrangement . At this point the molecules are interacting strongly , and consequently large changes in surface pressure occur for slight changes in molecular area . A kink in the isotherm at this stage indicates a change in molecular packing . In general , the new molecular arrangement will be one with a lower average molecular area .

Generally the isotherms are reversible . This rule is broken at the collapse point when the monolayer structure becomes unstable and folds in on itself . The shape of the π/A isotherms are dependent on many variables including pH , (if the head group has a labile proton) , temperature , (particular packing arrangements may have high activation energies) , ionic strength , (for charged species) and the material the trough is made from .

4.2.3 The Funnel Technique

Heckman et al.[20] have reported a replacement for the Langmuir trough . This consists of a funnel arrangement in which the lipid monolayer is compressed by the removal of

water , very slowly , out of a tap at the bottom of the funnel , (fig. 1.9) . The funnel is designed in such a way that the lipid monolayer is compressed from the fluid type phase , when the funnel is full to the brim , to a crystalline structure in the straight part of the funnel . The funnel technique was preferred to a conventional Langmuir trough design because of the ease of construction , cheapness and ease of use .

The funnel was prepared for use in a method similar to that for a Langmuir trough , (section 3.2) . Initially a glass funnel was used ; the surface of the glass inside the funnel had been treated with dichlorodimethyl silane to make it hydrophobic , as a hydrophobic surface is suggested[20] to repel the head groups of the lipid .

The water was removed from the funnel at a very slow rate , (of the order of millilitres per hour) . When the monolayer was located in the straight part of the funnel it was irradiated with U.V. light for approximately one hour . The substrate , (a microfilter supported on a perspex cylinder) , was coated by the method shown in figure 1.10 . The water level was allowed to drop below the microfilter to coat the first monolayer . The funnel was then emptied and cleaned . After repeating the compression procedure , a second coating was performed , but this time water was pumped into the funnel by means of a peristaltic pump .

Both Millipore cellulose acetate and Nucleopore polycarbonate filters were coated by the method described but no resistive membrane was prepared . The Millipore filters

were then coated with agar gel in an attempt to present a more uniform , non-porous surface to the lipid monolayer , but this proved not to be succesful either . According to published work[98] , oxygen interferes with the photo-polymerisation of diacetylenes , and so experiments were performed under nitrogen to see if this was the reason for the failure of the experiments . Unfortunately this proved not to be the case .

The major problem with the funnel technique , as orignally conceived , was that there was no way of checking on the state of the monolayer as it was compressed .Therefore , there was no way of investigating the failure of the experiments attempted thus far . To alleviate this problem , an apparatus was devised that allowed the measurement of the surface pressure of the monolayer as it was compressed due to the falling water line . This basically consisted of a metal rod that supported a precision balance , and allowed a limited degree of vertical movement . The rod was calibrated by a Vernier scale to allow very small displacements , and was built in the mechanical support section of the Port Sunlight laboratory . The surface pressure was calculated from the change of weight of a Wilhelmy plate , measured by the precision balance . The Wilhelmy plate followed the water surface down the funnel by adjustment of the vernier scale . The submersion depth was kept constant for every reading by means of a travelling microscope . A π/A isotherm of diacetylenic lipid in the funnel was obtained , the molecular area being calculated from the volume of water removed from the funnel .

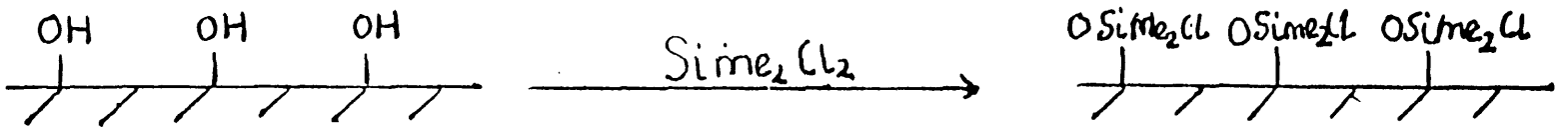

4.2 Silylation of Silica

It can be deduced from figure 4.3 that lipid molecules were adhering to the walls of the funnel as the surface pressure is lower than expected .

To counteract the adhesion of material to the surface of the funnel , a new material was selected . P.T.F.E. has a stronger hydrophobic nature than silylated glass and therefore may repel the molecules to a greater extent . The π/A isotherm of the new funnel was obtained in a similar manner to the glass one . The Wilhelmy plate again followed the water level down the funnel . This was achieved by finding the height of a marker a known distance above the Wilhelmy plate . The position of the water level could be calculated from the volume of water emerging from the funnel . The isotherm of diacetylenic lipids in the new funnel also showed molecules were adhering to the vessel walls .

An attempt to overcome the problem of molecules from the monolayer sticking to the funnel walls involved initially coating the vessel with a monolayer of lipid . This was done by loading a relatively compact monolayer onto the water surface and lowering the water level slowly . When a π/A isotherm of the treated funnel was obtained , it appeared that molecules were simply coming off the walls . This was confirmed when a π/A isotherm of pure water was obtained . It appeared there was no degree of permanance in the adsorption of molecules to the surface .

With the difficulties inherent to the funnel technique , it was decided to abandon it in favour of conventional Langmuir-Blodgett studies .

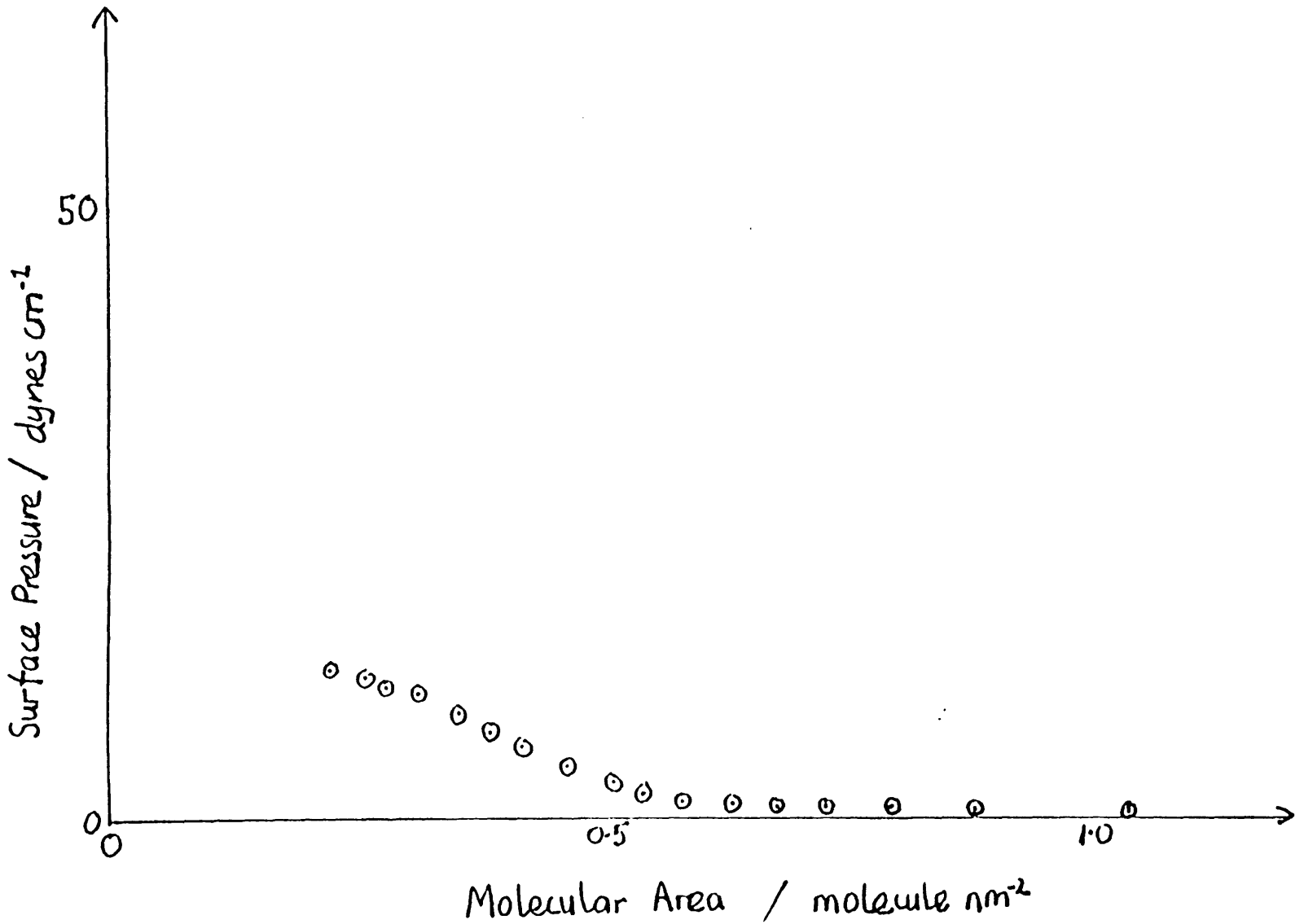

4.3 A π/A Isotherm of the Diacetylenic Lipid
Using the Funnel Technique

4.2.4 Langmuir-Blodgett Studies

A surface pressure / molecular area (Π/A) isotherm for a monolayer of pure diacetylenic lipid was obtained , (fig. 4.1) , by the technique described in section 3.2 . The photo-polymerisation and Langmuir-Blodgett coating characteristics of this monolayer were investigated .

4.2.4.1 Photopolymerisation Properties

It was observed that there was a shrinkage of the lipid monolayer on polymerisation .

Figure 4.4 shows a roughly linear dependence of polymerisation with respect to the quantity of photons incident on the monolayer , assuming the shrinkage of the monolayer is directly proportional to the extent of reaction. This linearity breaks down after a certain time , when the rate of polymerisation is less than that at lower exposure times . The reduction in the rate of polymerisation could be due to the fact that there are significantly less monomer units and so a greater degree of the photons do not lead to any reaction . Another factor to bear in mind is that there is a possibility of polymerised units joining together to form a closed unit , (fig. 4.5) . As the Wilhelmy plate measures the surface pressure at a particular region of the monolayer , the shrinkage inside the " closed circuits " of polymer will not be counteracted by barrier movement , i.e. holes will appear in the structure . This theory is backed up by the observation that the degree of shrinkage of a monolayer increases when lateral mobility is increased , (by adding non-polymerisable moeties to the monolayer) . This is

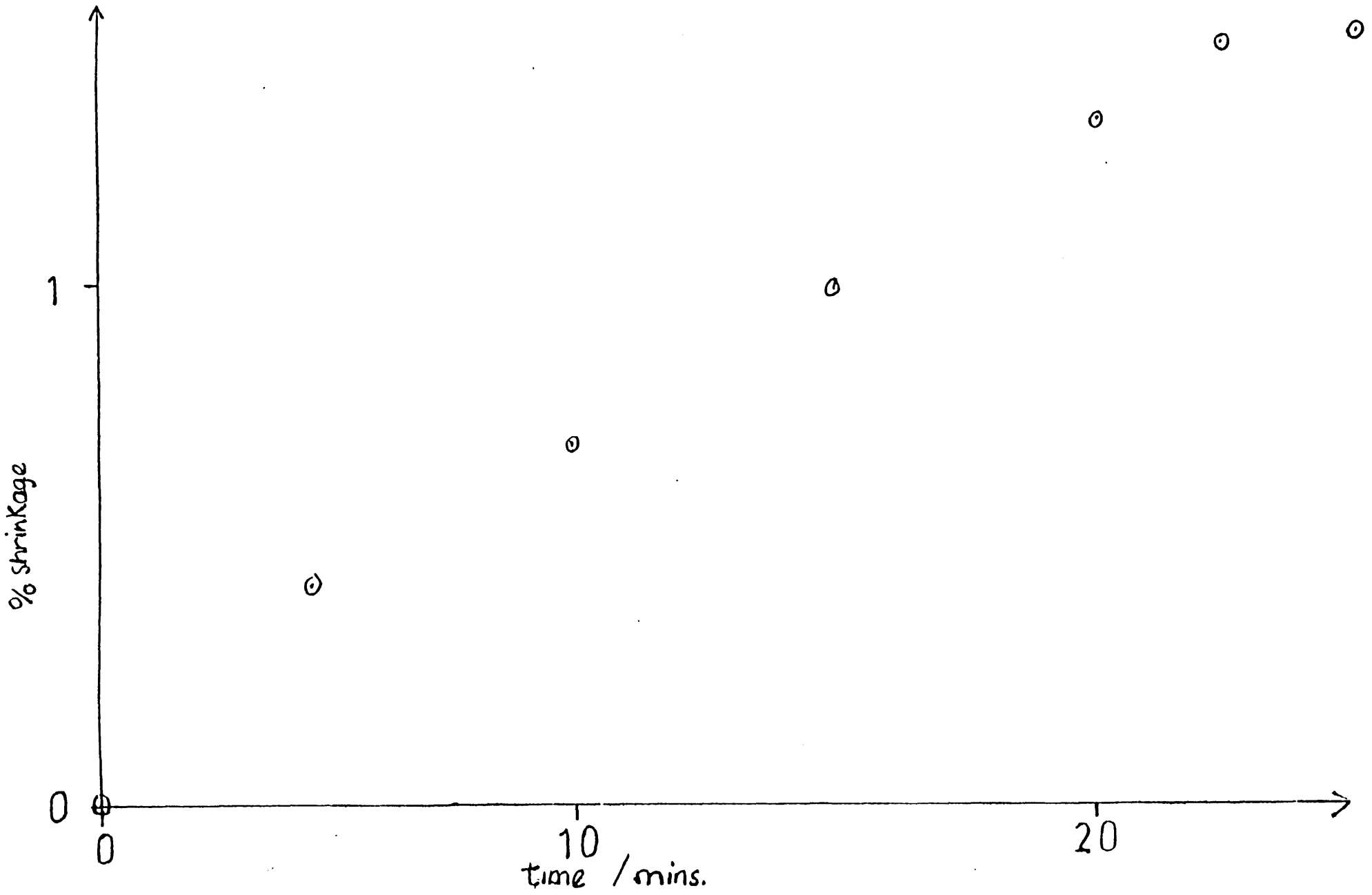

4.4 The % Shrinkage of a Lipid Monolayer versus UV exposure time

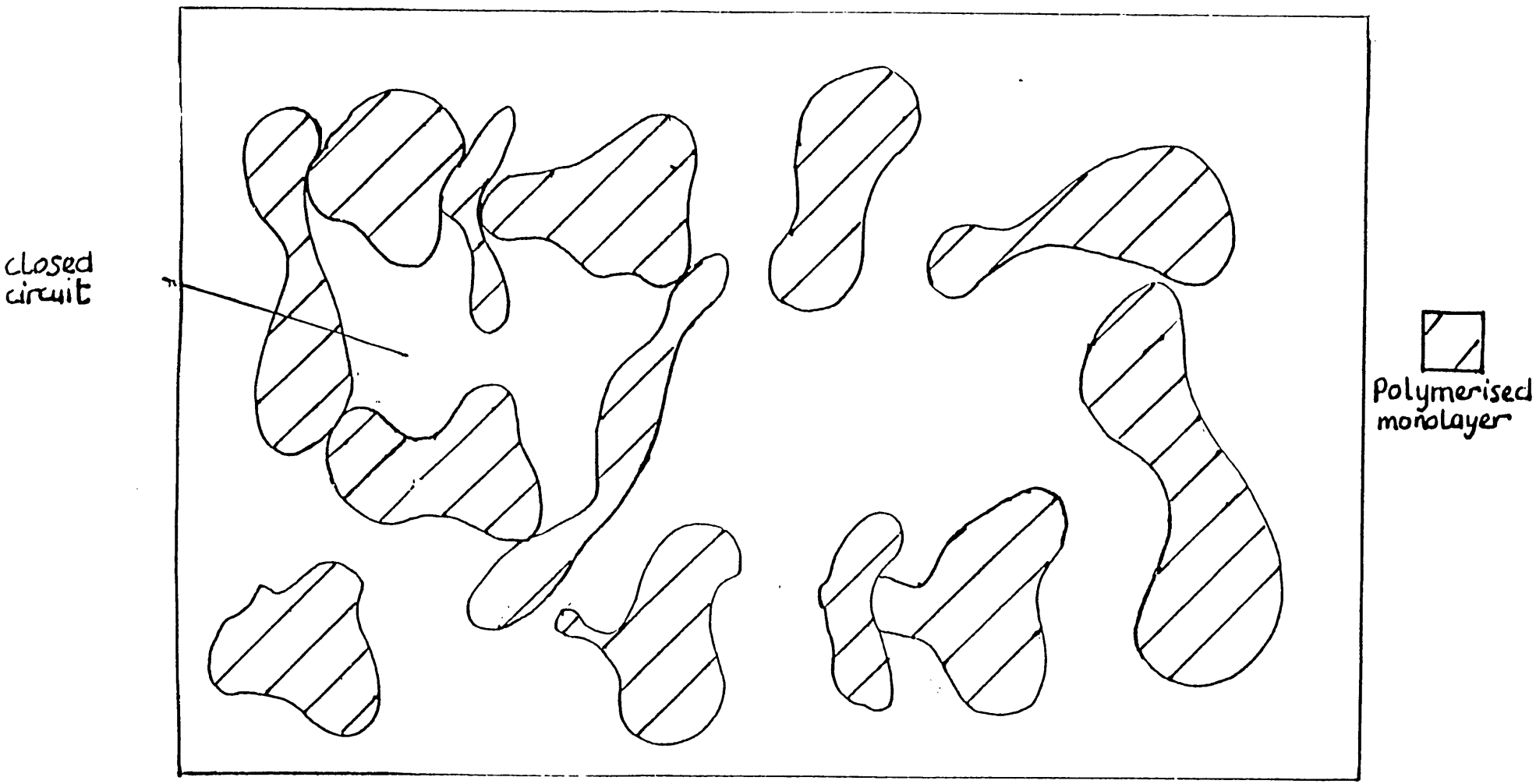

4.5 The Probable structure of Polymerised
Monolayers

discussed in section 4.3.1.2 .

The shrinkage on polymerisation was found to be dependent on the surface pressure of the monolayer prior to irradiation . A higher surface pressure lead to a lesser degree of shrinkage . Presumably , this is because the chances of forming a " closed circuit " of polymer are greatly enhanced when the molecules are more tightly packed .

For example

For a monolayer of diacetylenic lipids

when π = 33 dynes cm^{-1} % shrinkage was 0.3

when π = 16 dynes cm^{-1} % shrinkage was 1.7

It has been reported[98] , that oxygen exclusion is essential for diacetylenic photo-polymerisations as the ozone produced reacts with the unsaturated moeities , preventing polymerisation and leading to the breakdown of the orignal species . In this study , lipid monolayers were polymerised in air and in an inert argon atmosphere . No difference in shrinkage properties was observed .It must be interpretered that polymerisation is not affected by the presence of oxygen . Presumably the concentration of ozone produced by the irradiation is too low to have a significant effect .

4.2.4.2 Langmuir-Blodgett Coating Characteristics

The most convenient way of measuring the sucess of Langmuir-Blodgett coating is by the deposition ratio or transfer coefficient :-

$$\text{deposition ratio} = \frac{\text{area of monolayer removed}}{\text{area of the substrate}}$$

As with the photo-polymerisation , Langmuir-Blodgett coating is dependent on the surface pressure of the monolayer . The deposition ratio of Langmuir-Blodgett coating was found to be higher for greater surface pressures i.e. more tighly packed structures .

For example

For Millipore filter substrates

when π = 16.2 dynes cm^{-1} deposition ratio = 0.56

when π = 33.5 dynes cm^{-1} deposition ratio = 0.82

Initially Millipore cellulose acetate and Nucleopore polycarbonate and polyester filters were coated using the Kossi and Leblanc method (see section 1.2.) . The best transfer coefficients for any type of microfilter was 0.82 . The smoothness of the Nucleopore filters , with respect to the Millipore filters (fig. 4.6) , apparently does not improve its coating characteristics . To improve the morphology of the substrate , Millipore filters were coated with Agar gel This not only has the advantage of smoothness , but also presents an even surface throughout the cross-section of the substrate i.e. it is not porous . The failure of the Agar gel surface to significantly improve the value of the transfer coefficient lead to an investigation of the general coating characteristics of the diacetylenic lipid .

Conventional Langmuir-Blodgett coating was performed on metallic , polymeric and crystalline materials . A clean platinum surface gave a deposition ratio of zero , and hydrophillic materials (such as silica and polyethylene

glycol) gave deposition ratios of between 0.5 and 0.6 at best . On the other hand , hydrophobic PTFE gave a depostion ratio of 0.95 .

It would appear that the diacetylenic lipid coats better on hydrophobic surfaces rather than hydrophillic ones . This hypothesis was tested by altering the surface properties of selected substrates . The silica slides were treated with dichlorodimethyl silane to invoke a hydrophobic nature to their surfaces . A similar technique was used for polyester filters (initial pre-treatment with acid was required) . These substrates gave deposition ratios of 0.99 . Apparently lipids prefer to be coated in a "tails-down " fashion . This is backed up by the observation that the downward motions resulted in better transfer (i.e.X-type deposition) for both hydrophobic and hydrophillic substrates .

This is unfortunate from the point of view of creating a lipid bilayer . What is needed is an initial deposition in a " heads-down " fashion . With the Kossi and Leblanc method only 80% , at best , of the monolayer is deposited when this is attempted .

It was also noted that coating a substrate for a second or subsequent times resulted in better transfer . This was particurlarly notable for substrates with moderate transfer coefficients initially .

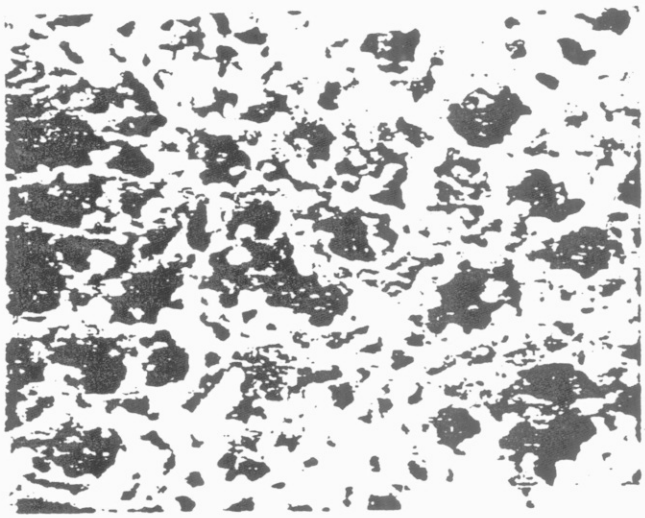

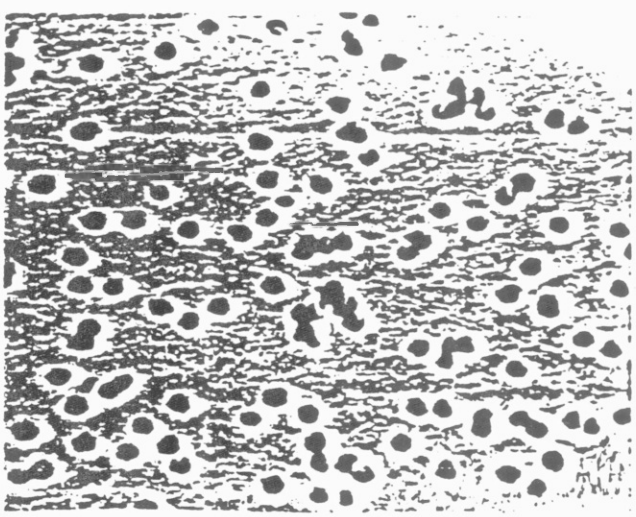

4.6 SEM Photographs of Millipore and Nucleopore Microfilters

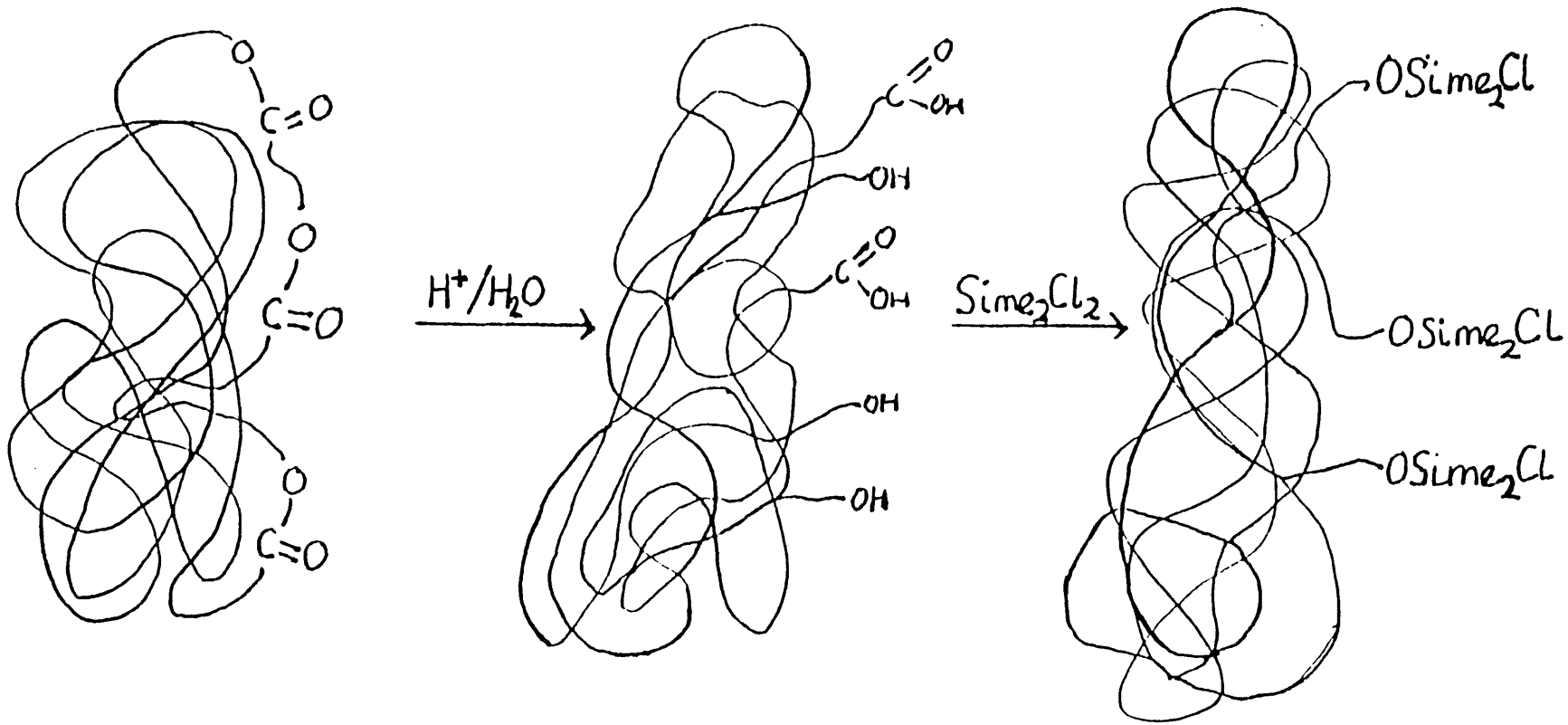

4.7 Silylation of a Polyester Microfilter

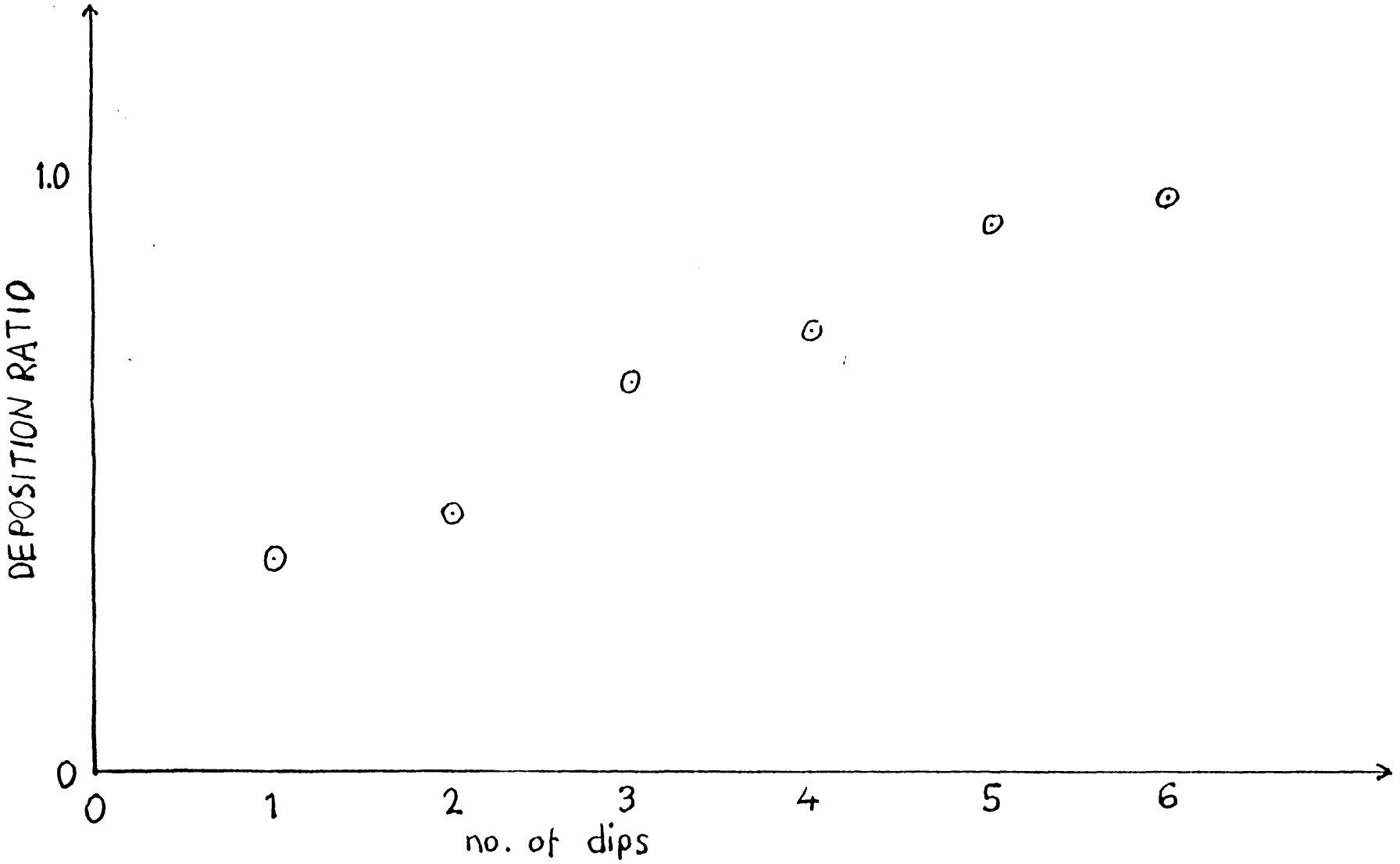

4.8 The Change of Deposition Ratio of lipid on a Microfilter with succesive coatings

4.3 Studies on Mixed Monolayers

4.3.1 Monolayers of DSPC (Distearoyl phospatidyl choline) and the Diacetylenic Lipid

Although deposition ratios very close to one can be obtained for diacetylenic monolayers , for selected substrates the coated lipid structure does not form a resistive layer. The major problem with the bilayers formed is presumably fractures resulting from the rigidity of the polymeric framework . A reduction in polymerisation would alleviate this difficulty . Reducing the intensity of U.V. irradiation was found to be impractical as removing the lamp to more than the 30-40 mm previously used resulted in no shrinkage of the monolayer , and presumably no polymerisation . Monolayers have been prepared using mixtures of polymerisable and non-polymerisable lipids in attempts to overcome this problem .

4.3.1.1 Miscibilty Properties

For a non-polymerisable lipid to increase the lateral fluidity of a polymerised monolayer , it must be miscible with the monomer units i.e there should not be separate regions of polymer and unpolymerisable lipid . Figure 4.9 demonstrates the miscibility of distearoyl phosphatidyl choline (DSPC) and the diacetylenic lipid . If the molecules were not miscible then the Π/A isotherm of the 50:50 mixture would separate into two distinct curves which could be super-imposed over the Π/A isotherms for pure DSPC and pure Diacetylenic lipid .

4.3.1.2 Photopolymerisation Properties

The initial rate of shrinkage of mixed monolayers was

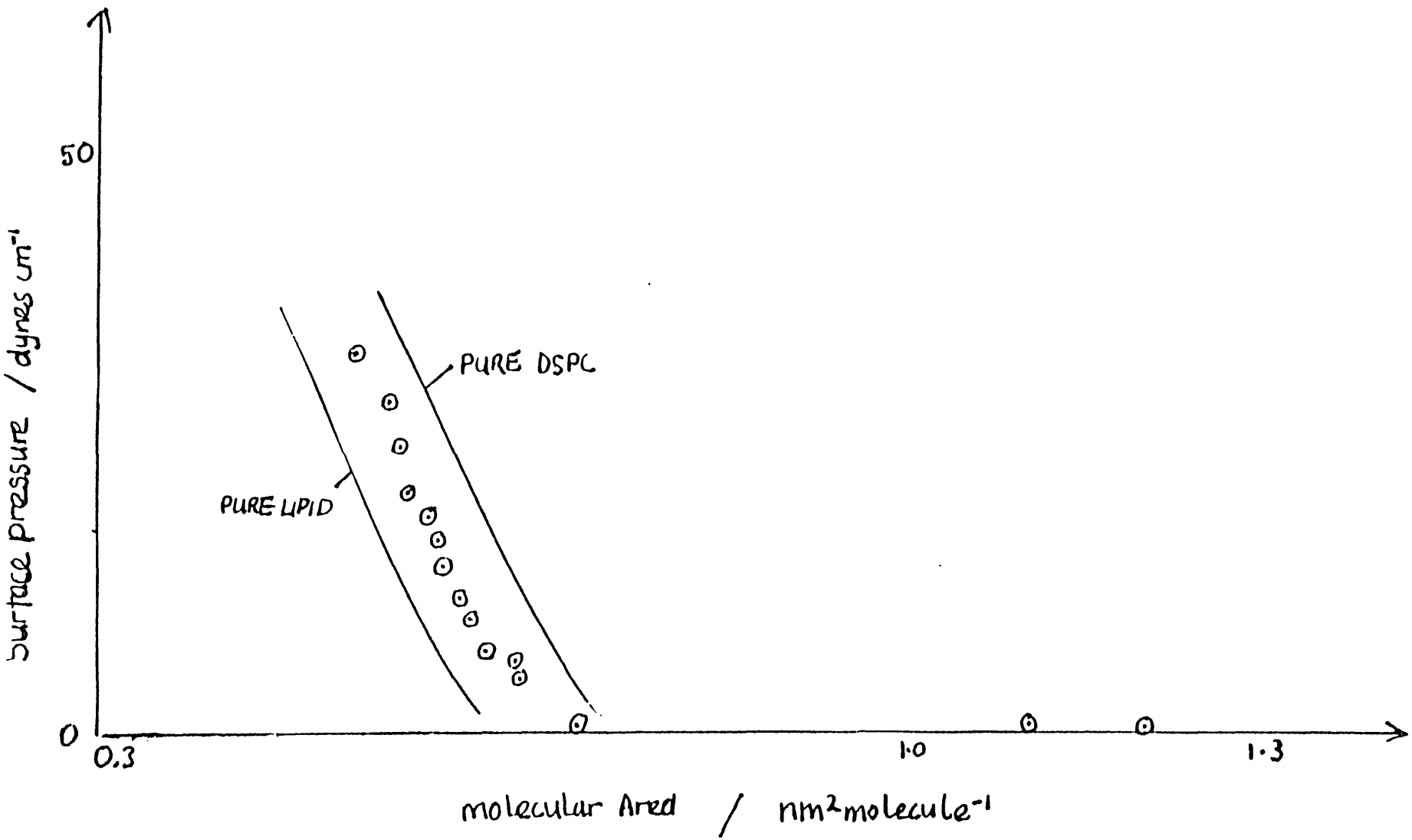

4.9 A π/A Isotherm of a Mixed DSPC/Diacetylenic Monolayer

less than that for 100% polymerisable lipid monolayers , but of the same order of magnitude . The total degree of shrinkage , however , was much larger than that for the pure diacetylenic monolayer . This effect is probably due the increased lateral mobility and the fact that this will close any fissures formed during polymerisation more effectively . The extent of polymerisation for mixed monolayers will be of the same order as the diacetylenic lipid monolayers as the time of irradiation was , in general , roughly double .

Again a dependence of shrinkage on surface pressure was observed .

For example

For monolayers of 50:50 mixtures of D.S.P.C. and diacetylenic lipid :-

when π = 32 dynes cm^{-1} %shrinkage was 1.7

when π = 16 dynes cm^{-1} %shrinkage was 9.4

4.3.1.3 Langmuir-Blodgett Coating Characteristics

The mixed monolayers produced consistently higher transfer coefficients for all substrates . Despite this observation bilayers with significant resistance were not obtained . There was a dependence of deposition ratio on surface pressure similar to that for pure diacetylenic lipid monolayers .

For example

For Millipore filter substrates

when π = 32 dynes cm^{-1} deposition ratio = 0.7

when π = 18 dynes cm^{-1} deposition ratio = 0.85

4.3.2 Mixed Monolayers of DPPC (Dipalmitoyl phosphatidyl choline) and DpPC (Diphytanyl phosphatidyl choline) and the diacetylenic Lipid

DSPC has a liquid-solid phase transition temperature above room temperature[99] . Consequently it should not improve the fluidity of the monolayer as much as similar lipids with phase transitions below room temperature .

DPPC and DpPC both fall into this category and were found to be miscible with the polymerisable lipid . Mixed monolayers of 50% diacetylenic lipid and 50% DPPC or DpPC gave high values of shrinkage and deposition ratios consistently very close to one . A summary of the percentage shrinkages for the various monolayers is shown in table 4.1 .

Small increases in resistance were observed for the bilayers formed on Millipore filters , (of the order of 2-3 fold increases) . Experiments using the silylated polyester filters were even more succesful . They resulted in truly resistive layers ; even for monolayers reistances of megaohms were recorded , which is equivalent to a 10^4 increase on uncoated , silylated filters . Despite the fact the bilayers could not be used as ion-selective membranes , the noticeable increase in resistance can be seen as evidence as the creation of high degree of perfection in the formed bilayer .

A summary of the data obtained from the Langmuir-Blodgett type coating experiments is shown in table 4.2 .

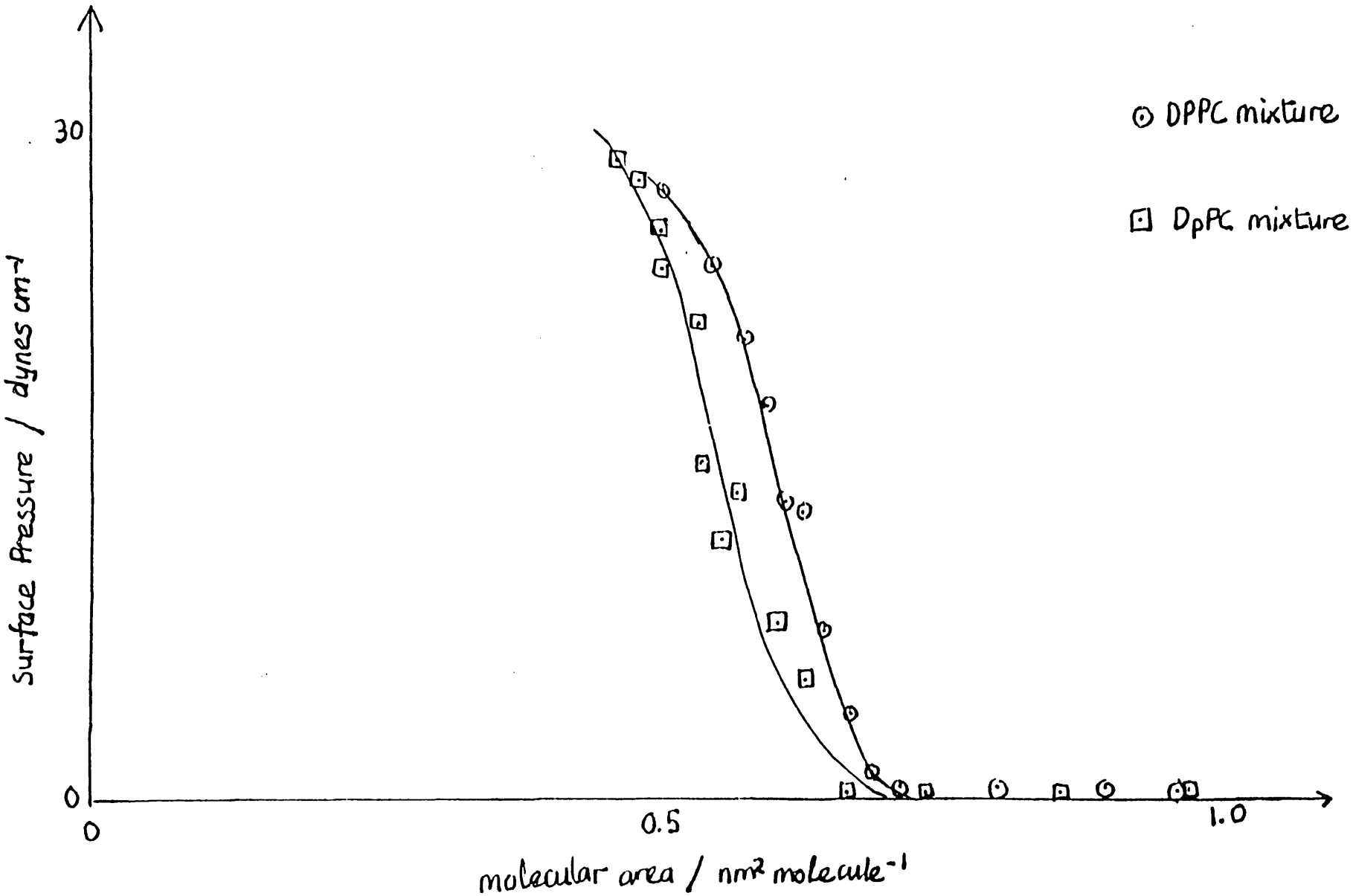

4.10 π/A Isotherms of Mixed Monolayers of DPPC and DpPC with Diacetylenic Lipid

COMPOSITION OF MONOLAYER	% SHRINKAGE
100% DIACETYLENIC LIPID	0.3-1.7 %
50:50 DSPC:DIACET.	1.7-9.4
50:50 DPPC:DIACET.	UPTO 10
50:50 DpPC:DIACET.	UPTO 10

TABLE 4.1 Langmuir-Blodgett Shrinkage Data

TECHNIQUE	SUBSTRATE	MONOLAYER COMP.	RESISTANCE / Ω	DEPOSITION RATIO
FUNNEL	MILLIPORE FILTER	DSPC MIX.	1-2 KΩ	N/A
"	NUCLEOPORE FILTER	DSPC MIX.	1-2 KΩ	N/A
"	AGAR GEL	DSPC MIX.	1.5-2.5KΩ	N/A
L-B	MILLIPORE FILTER	100% DIACET.	1-2 KΩ	0.56-0.82
"	NUCLEOPORE FILTER	DSPC MIX.	1-2 KΩ	0.7-0.85
"	"	DPPC MIX.	1.5-2.5KΩ	0.7+
"	"	DpPC MIX.	1-2.5 KΩ	0.7+
"	SILYLATED NUCLEOPORE FILTER	DPPC	10 MΩ	0.87-.95
"	"	DpPC	16.4 MΩ	0.87-1.0
L-B	SILYLATED SILICA	100% DIACET.	N/A	0.96-.98
"	SILICA	"	"	0.5-0.6
"	PLATINUM	"	"	0.0
"	PTFE	"	"	0.94-0.99
"	PEG	"	"	0.54

Table 4.2 Summary of Langmuir-Blodgett Deposition Data

4.4 The Closure of Pores in the Bilayer

The results from the previous section imply that a basic bilayer structure can be obtained from Langmuir-Blodgett coating but the membrane formed has fissures in it . Attempts were made to close the pores with filler molecules . This will also have the advantage of making the insertion of protein molecules easier .

Initially n-dodecane was used to fill the pores . Simple soaking resulted in an increase in bilayer resistance but the capacitance of the membrane would suggest that this is purely due to a soaked filter (i.e. the thickness of the membrane , from the parallel plate capacitor equation is too high) . Even when the n-dodecane was applied from a micro-syringe , no intermediate step occurred , the membrane went from having little resistance to a thick soaked filter paper .

Surfactants were then tried to plug the fissures in the structure . Long chain alcohols and the diacetylenic lipid were used but no significant change in resistance occured .

4.5 Miscellaneous Techniques

4.5.1 Liquid-Liquid Interfacial Systems

Experiments involving the creation of a diacetylenic lipid monolayer at a dodecane-water interface were attempted. The liquid-liquid interface has the advantage that it can be located in the pores of a microfilter , i.e. the disruption that Langmuir-Blodgett coating causes to a monolayer is avoided . The water-dodecane interface was set up in an

R.D.C. type of arrangement . A suspension of lipid was then added to the organic phase . The concentration of lipid was such that numerous compressed monolayers , (in the order of tens) , could be formed at the interface . This in fact was the saturation concentration .

Despite the irradiation of the formed monolayer no resistive layer could be detected after drying out the Millipore filter in air . The drying process may be the reason for this . Unfortunately it cannot be avoided as a second monolayer must be added to form the bilayer . The second monolayer would probably have been formed in a conventional Langmuir-Blodgett coating technique .

4.5.2 Electropolymerisation Studies

Electropolymerisation is advantageous as facile control of the kinetics of the initiation process , via the electrical potential , is possible . However , there may be problems finding a suitable conducting species to be used as the electrode to support the bilayer . Initial studies were carried out on a platinum electrode . Electropolymerisation was found not to be possible as the topochemical limitations applicable to photo-polymerisation also apply in this circumstance .

4.6 Future Work

The failure to get a resistive lipid bilayer by Langmuir-Blodgett coating was probably due to the degree of perfection needed in the final structure . The presence of very small fissures will lead to great reductions in the resistance of the membrane .

Uneven substrates will probably never coat to the accuracy required for an amperometric sensor . Langmuir-Blodgett coating may work on very flat surfaces though , if coating is made thermodynamically favourable .

The substrate may be made attractive to the lipid so that 100% coating is more likely . This attraction could be electrostatic , as has been used in cell biology[3] . Polylysine , a polypeptide , can be used to coat petri dishes to attract the phospholipids present in cell membranes . A suitable lipid must be used for this procces .

The treatment of the surface of the substrate in a similar way to that of the polyester filter in this work may provide a solution . It was found that if alkyl chains are placed on the surface of the substrate then the alkyl chains of the lipids will be attracted to it . If the silane has an end group that is attractive to the lipid head group then good " heads-down " deposition should result . This effect may be enhanced if the initial lipid monolayer could be bound directly , chemically to the substrate surface . A non-porous surface , e.g. a gel , must be used in the latter strategy . Unfortunately , these ideas could not be attempted satisfactorily in this study as they require a degree of organic synthesis not readily available .

Another possibilty is the use of a three-phase system . The lipid monolayer may be spread on a non-volatile , organic solvent , that is relatively polar , (e.g. an ether) , and the substrate may be made aqueous , (e.g. a gel) . The charged lipid head groups would preferentially locate on the

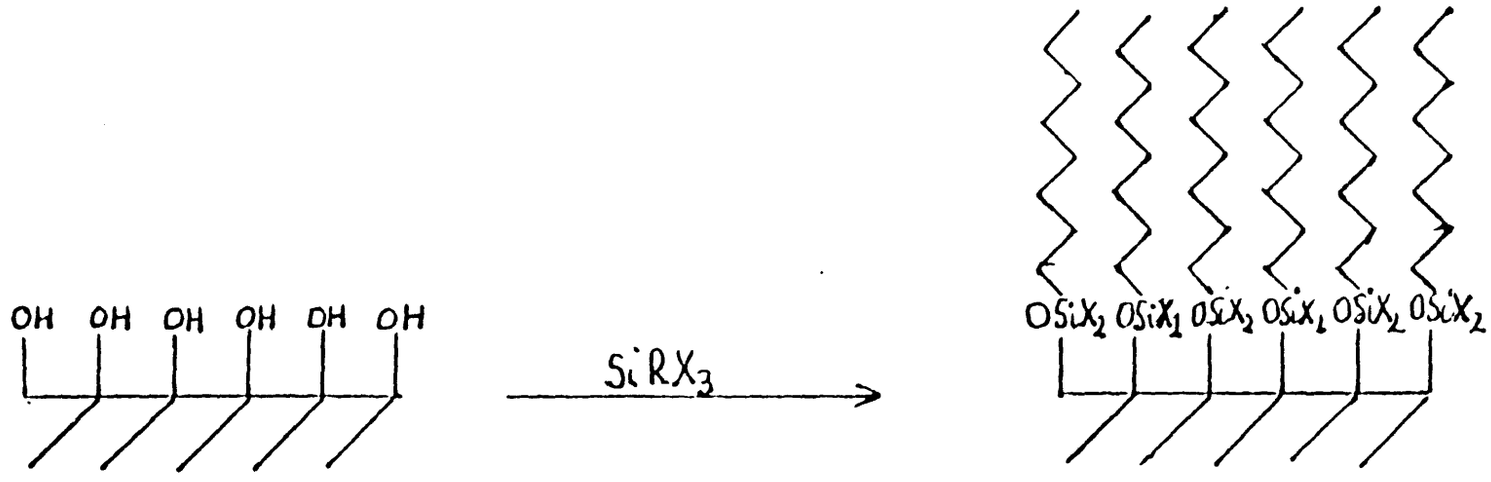

4.11 Silylation of a Substrate Surface

more polar aqueous substrate .

Problems with this approach include :-

i) The expense of the solvent (purity is essential) .

ii) Poor congregation of lipid at the surface , (i.e. the lipid may dissolve into the solvent , especially at low molecular areas) .

iii) The technique still retains the feature of the rigid , polymeric framework .

4.7 Black Lipid Membranes

It would appear that the Langmuir-Blodgett technique is too brutal a technique to achieve a lipid bilayer structure consistently . The black lipid membrane technique was used as a means of creating a lipid bilayer of diacetylenic molecules (plus 10% oxidised cholesterol) and U.V. irradiation was applied in an attempt to initiate photo-polymerisation .

4.7.1 A.C. Impedance Measurement

Black lipid membranes of the diacetylenic lipid (and oxidised cholesterol) consistently gave resistance values in the order of tens of megaohms per square centimetre . The capacitance values were in the order of tens of nanoFarads per square centimetre , which , assuming the bilayer acts as a parallel plate capacitor resulted in an average thickness of eight nanometres . This is the correct order of magnitude for a lipid bilayer[1] , but is slightly large . The error in the value of the bilayer thickness could be due to an

over-estimate of the relative permittivity of the central region of the bilayer (assumed to be five) , but is probably due , in part at least , to the presence of solvent in the bilayer structure .

4.7.2 The Electrochemistry of Diacetylene Bilayers

A current-voltage curve for a black lipid membrane exhibits a non-ohmic critical voltage , V_{CRIT} , (approximately 90 mV with respect to SCE) after which the current rises more rapidly than expected (fig. 4.12) . This effect is due to the formation of fissures in the bilayer , and is not observed for a solvent soaked microfilter .

It was noted that the critical voltage steadily drops , (roughly 5 to 10 mV) , after the formation of the BLM and then settles down . Presumably this is an indication of the solvent coming out of the bilayer and the resultant thinning.

The value of V_{CRIT} and the A.C. impedance value was found not to change on exposing the bilayer to U.V. irradiation . This observation , coupled with the fact that the membranes never lasted more than a few days , suggests that polymerisation of the bilayers did not take place to any significant degree . The failure of polymerisation was probably due to the solvent in the structure , which prevented the correct arrangement of molecules for polymerisation .

The effect of adding molecules to induce conductivity across a bilayer was followed for diacetylenic membranes . The critical voltage was removed (i.e. ohmic behaviour was restored) , on addition of any carrier molecules ,e.g.

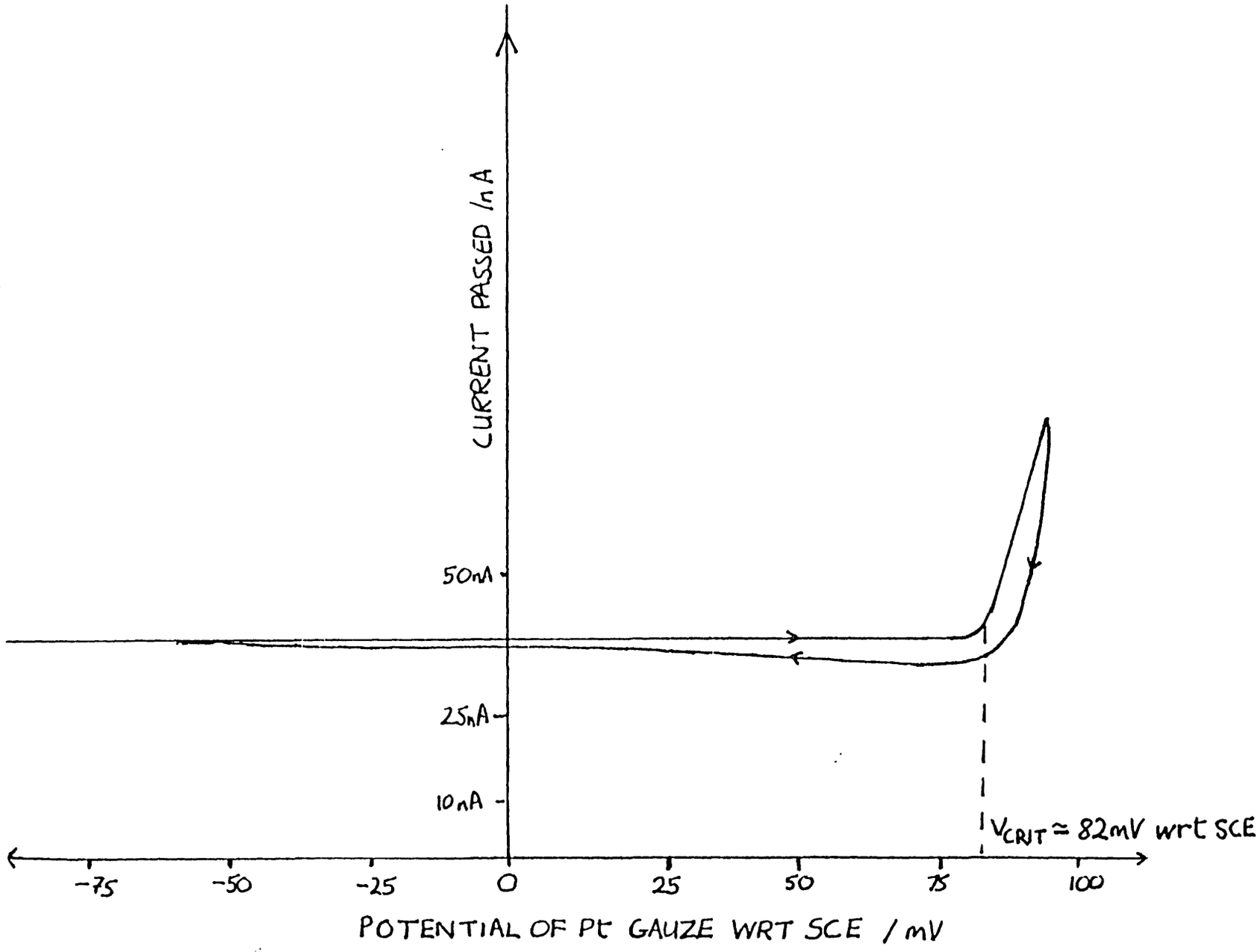

4.12 An IV Curve for a BLM of Diacetylenic Lipid

valinomycin . There was no effect , though , when channel formers , such as phloretin , were added . This effect was also probably due to the level of solvent in the bilayer .

4.8 Summary of BLM Work

The failure of the polymerisation of BLM`s was probably due to the prescence of solvent . This would preclude the reaction on topochemical grounds . Therefore , the lipid polymerisation cannot be made facile as the polymerisation must not trap solvent molecules inside the membrane . When a BLM is formed it must be left for at least a quarter of an hour to allow for solvent evaporation . In general , BLM`s have limited usefulness because of the presence of the solvent as this hampers the functioning of the membrane .

CHAPTER 5 THE DEVELOPMENT OF A NOVEL TECHNIQUE FOR STUDYING DIFFUSION THROUGH LIQUID MEMBRANES

5.1 Liquid Membranes

Liquid membranes are generally oily , hydrophobic phases supported by polymeric frameworks , such as microfilters . The ion-selective nature of liquid membranes comes from the chemistry of the ions or molecules dissolved in the organic phase .

The rate at which ions diffuse through liquid membranes and the mechanism of the ion-selective process have generally been studied by A.C. impedance methods[99,100] . These studies have yielded information on the fundamental chemistry of the ionophores , which may improve the efficiency or reduce the cost of ISE`s .

5.2 Valinomycin as an Ionophore for Potassium Ions

Figure 5.1 shows the response of two calomel electrodes placed either side of a liquid membrane containing valinomycin to changing the concentration of potassium chloride on one side of the membrane . The difference in the electrode potentials varies linearly with the logarithm of the concentration of the test solution up to a value of concentration of roughly 0.5 M . This suggests that the valinomycin membrane , as expected , is acting as a ion-selective membrane .

5.3 Measurement of Halide Fluxes

At present there is no potassium ion-selective electrode that provides an immediate response . Therefore the flux of potassium ions cannot be measured directly as the change in

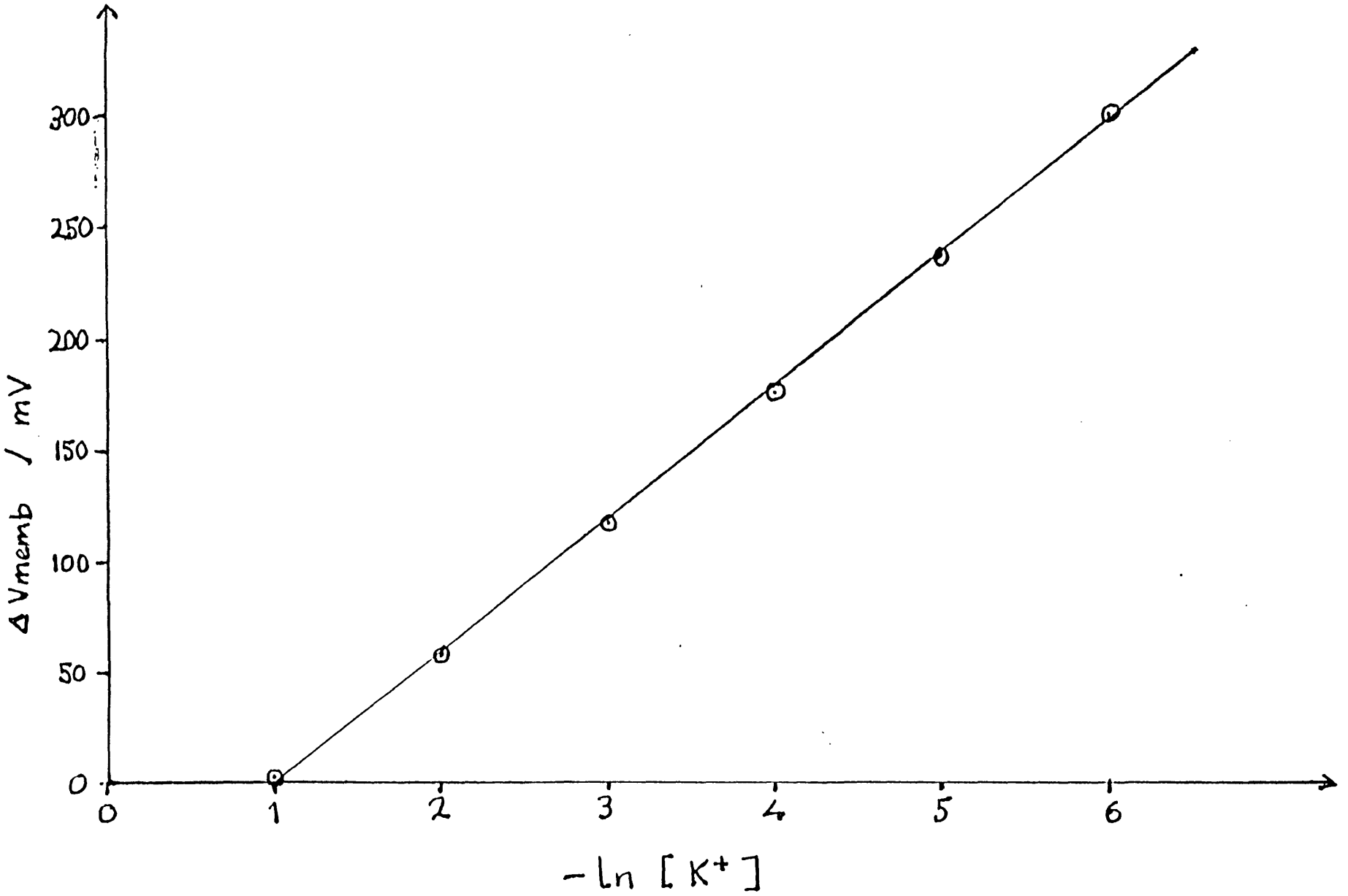

5.1 ΔV_{memb} versus $\ln[K^+]$ for a Valinomycin Based Liquid Membrane

potential of the ISE would be at least partly due to kinetics of the ion-selective process .

The accepted mechanism of selective potassium ion conduction[38] involves the formation of an ion pair $KVAL^{+}A^{-}$ inside the membrane (fig.5.2) . Where $KVAL^{+}$ is the potassium / valinomycin complex and A^{-} is the counterbalancing anion . Therefore the flux of potassium ions passing through the liquid membrane can be measured by obtaining the flux of the A^{-} species .

If the counter balancing ion is a halide , (Cl^{-} , Br^{-} or I^{-} only) , then a silver / silver halide arc electrode can be used ,(section 2.2.2) with the liquid membrane being positioned on the central porous disc of a rotating diffusion cell . The flux of halide (or potassium ions) may be obtained from the potential of the silver / silver halide electrode in conjunction with equation 2.18 .

The flux of potassium ions obviously was towards the solution of lower concentration . The potential of a Ag/AgCl electrode is dependent on background halide concentration , (the higher the concentration the lower the potential) . Consequently the response to changes in halide concentration is dependent on the background concentration . It was found that a halide concentration of less than 10^{-3}M was required to obtain an easily detectable response to the fluxes obtained from a valinomycin liquid membrane .

5.3.1 The Kinetic Model

The general mechanism of the transport of potassium and halide ions through liquid membranes is shown figure 5.2 . An expression for the flux of ions through the liquid membrane can be obtained by considering the processes shown in 5.2 separately .

$$j = k_1[K^+]_0[L]_0 - k_{-1}[KL^+]_0 \qquad (5.1)$$

$$= k_2[KL^+]_0[x^-]_0 - k_{-2}[KLX]_0 \qquad (5.2)$$

$$= D_{IP} / L ([KLX]_0 - [KLX]_1) \qquad (5.3)$$

$$= k_{-2}[KLX]_1 - k_2[KL^+]_1[X^-]_1 \qquad (5.4)$$

$$= k_{-1}[KL^+]_1 - k_1[K^+]_1[L]_1 \qquad (5.5)$$

$$= D_L / L ([L]_1 - [L]_0) \qquad (5.6)$$

0 and 1 signify opposite sides of the membrane

L is the unchelated and KL the chelated ligand

KLX indicates the ion pair

An expression for the total ligand concentration can be obtained :

$$[L]_\Sigma = 1/2 ([L]_1 + [L]_0 + [KLX]_1 + [KLX]_0) \qquad (5.7)$$

The halide fluxes can be measured so that the bulk potassium concentration at the effluxing side of the membrane (1) is neglible . This is achieved by having equal concentrations of KX and NaX at either side of the membrane . This condition allows the second term in 5.5 to be ignored , i.e. $[K^+]_1 = 0$.

A general term for the flux of ions can now be obtained by solving 5.1 to 5.7 simultaneously :-

$$\frac{[L]_\Sigma}{j} = \frac{L}{2D_L} + \frac{2}{k_1[K^+]_0} + \frac{2}{k_1k_2[K^+]_0[X^-]} + \frac{L}{k_1k_2D_{IP}[X^-][K^+]_0}$$

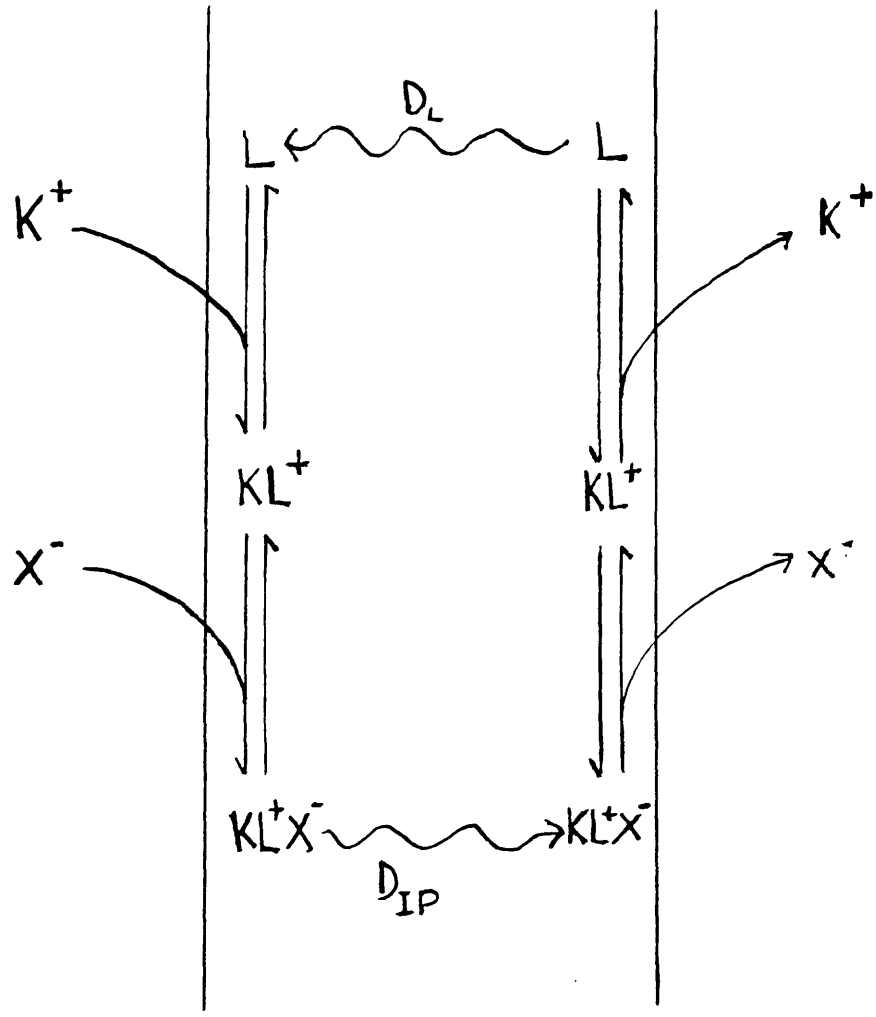

5.2 The Mechanism of K^+ Transport

$$+ \frac{L}{2D_{IP}} + \frac{1}{k_{-2}} + \frac{K_2[X^-]}{k_{-1}} \qquad (5.8)$$

Equation 5.8 describes a variety of kinetic effects :-

i) The first term describes the diffusion of the unchelated ion to side 0 .

ii) The second term describes the simple chelation of potassium by the ligand .

iii) The third term accounts for the chelation of the potassium ion to form an ion pair , i.e. a combination of the first and second equilibria which assumes the halide ions are present in the membrane .

iv) The fourth term describes a simultaneous chelation of K^+ and the formation of the ion pair . This basically assumes the $KVAL^+$ complex is a reactive intermediate .

v) The fifth term takes account of the diffusion of the ion pair through the membrane .

vi) The sixth term takes care of the diffusion of the halide ions into the membrane to form an ion pair with the chelated ligand .

vii) The seventh term describes the situation of K^+ ions being excreted from the membrane coupled with an equilibrium of the ion pair and the chelated ligand .

Equation 5.8 describes a thorough kinetic model . A more applicable model can be obtained by assuming only mass transport , the diffusion of the potassium and halide ions into the membrane and diffusion of the ion pair through the membrane are separately significant .

The concentration of K^+ and X^- ions at the surface of the membrane can be obtained from 2.7

$$[K^+]_0 = [K^+]_\infty - j / k_D = c \qquad (5.9)$$

$$[X^-]_0 = [X^-]_\infty - j / k_D = c \qquad (5.10)$$

$$[X^-]_1 = j / k_D \qquad (5.11)$$

$$\frac{1}{j} = \frac{1}{k`_0} + \frac{1}{k`_1 c} + \frac{1}{k`_2 c^2} + \frac{K_2^{III}}{k_D k`_3 \omega^{-1/2}} \qquad (5.12)$$

$k`_0$ , $k`_1$, $k`_2$ and $k`_3$ are the rate constants for ligand / ion pair diffusion , K^+ chelation , X^- diffusion and mass transport respectively .

From 5.12 a series of diagnostic plots can be obtained if it is assumed that two and only two steps are rate determining . These plots are shown in table 5.1 .

5.3.2 Flux Measurements For Valinomycin in Diphenyl Ether

The variation of the flux of halide ions through a membrane , containing 10^{-3}M valinomycin , with rotation speed was obtained . It would appear that the diffusion of the halide ion into the membrane and the diffusion of the ion pair through the membrane are rate determining , (fig.5.3) .

At lower concentration of valinomycin the picture is not as clear and the simple mathematical model is not valid . This arises presumably as the flux of species through the liquid membrane is now dependent on the step involving potassium ion chelation as well .

It was found that with no valinomycin present in the

	I	II	III
0	$1/j$ vs. $1/c$	$1/j$ vs $1/c^2$	$1/j$ vs. $j/\omega^{1/2}$
I	-	c/j vs. $1/c$	c/j vs. $cj/\omega^{1/2}$
II	-	-	c^2/j vs. $c^2j/\omega^{1/2}$

Table 5.1 The Diagnostic Plots for Determining the Rate Determining Steps in the Diffusion of Ions Through Liquid Membranes

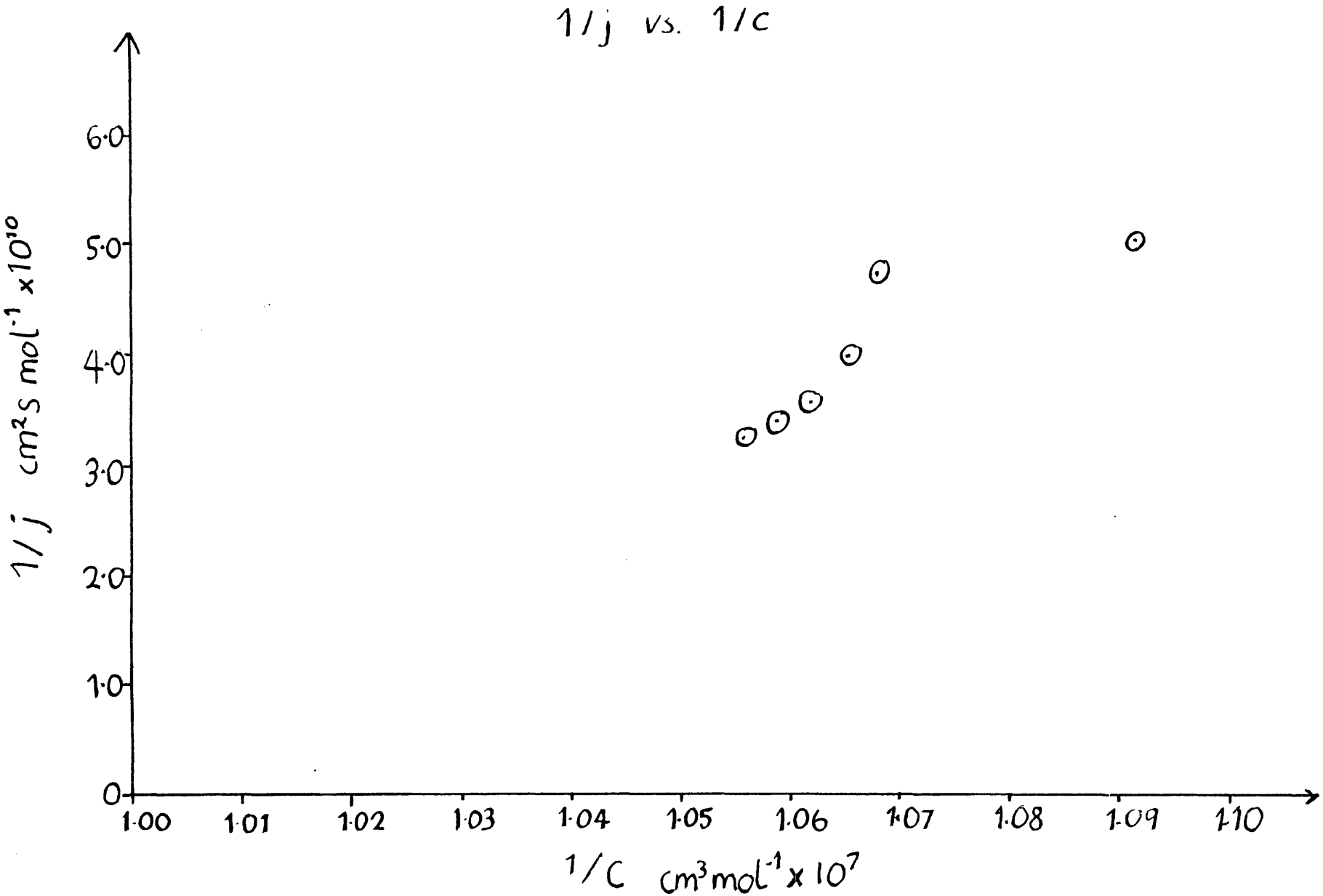

5.3 Diagnostic Plots for 0.001 M Valinomycin Membranes

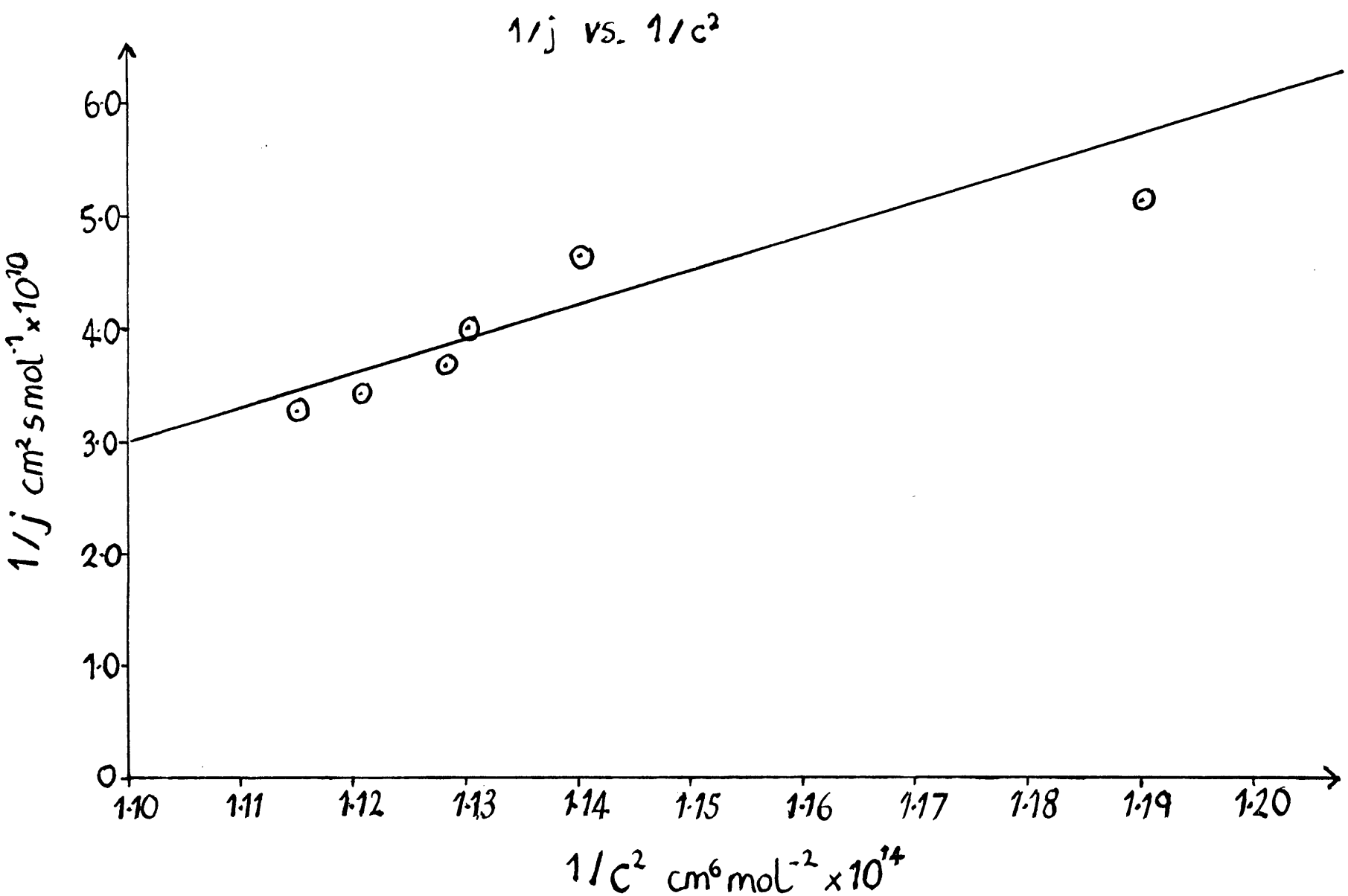
1/j vs. 1/c²
1/j cm² s mol⁻¹ x 10¹⁰
6·0
5·0
4·0
3·0
2·0
1·0
0
1·10
1·11
1·12
1·13
1·14
1·15
1·16
1·17
1·18
1·19
1·20
1/c² cm⁶ mol⁻² x 10¹⁴

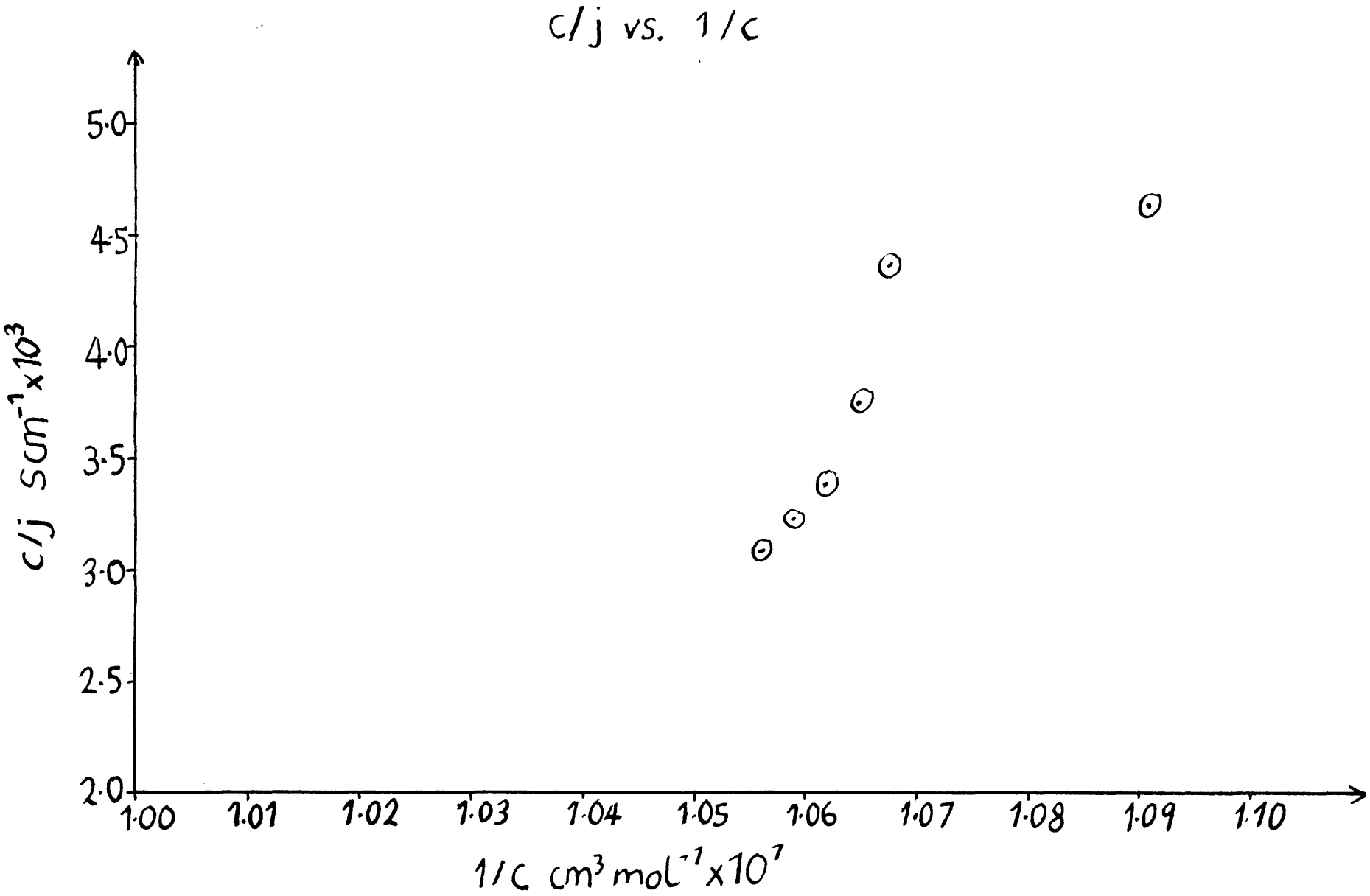
c/j vs. 1/c
c/j S cm⁻¹ x 10³
5·0
4·5
4·0
3·5
3·0
2·5
2·0
1·00
1·01
1·02
1·03
1·04
1·05
1·06
1·07
1·08
1·09
1·10
1/c cm³ mol⁻¹ x 10⁷

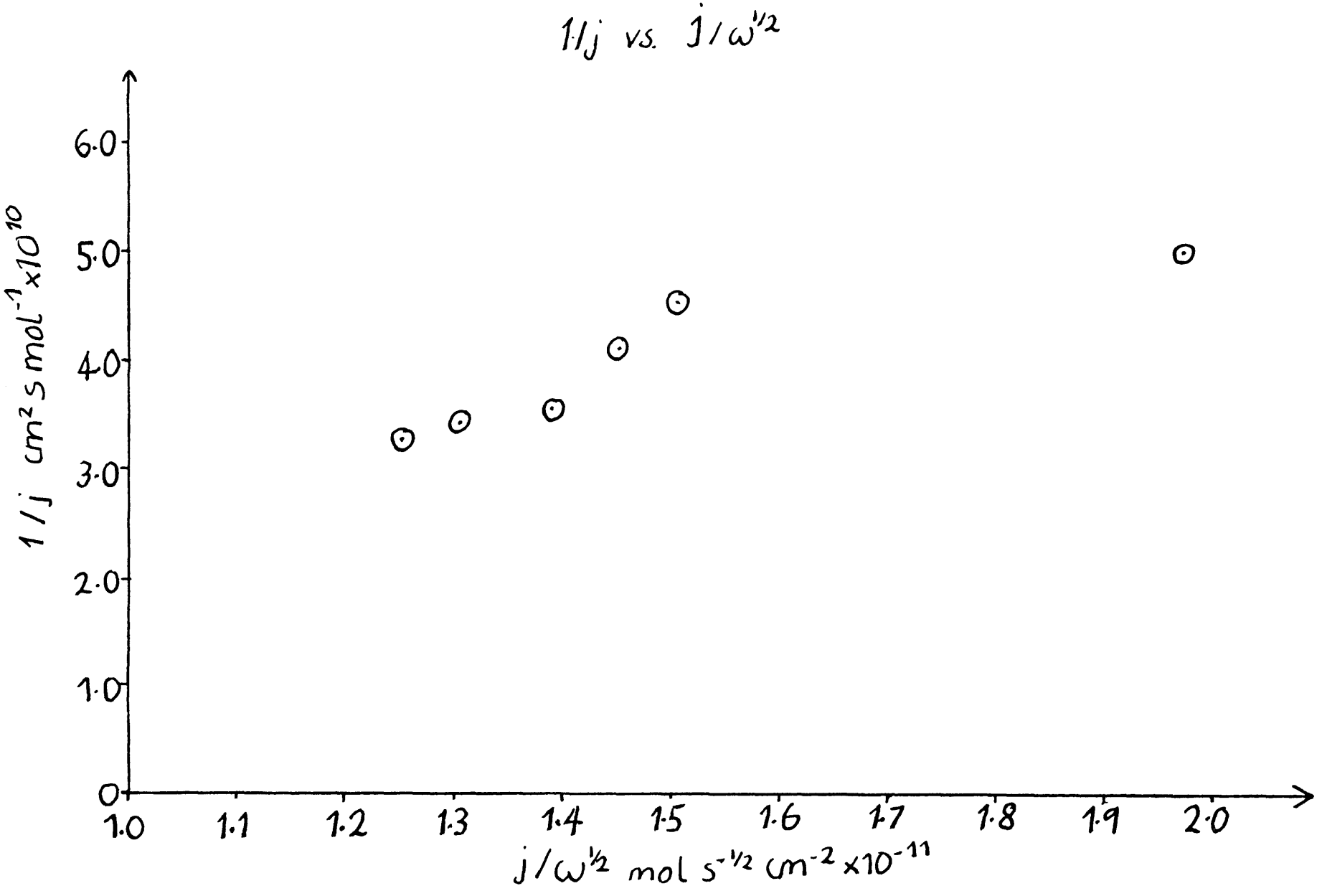
1/j vs. j/ω^1/2
1/j cm² s mol⁻¹ x10¹⁰
6·0
5·0
4·0
3·0
2·0
1·0
0
1·0
1·1
1·2
1·3
1·4
1·5
1·6
1·7
1·8
1·9
2·0
j/ω½ mol s⁻½ cm⁻² x10⁻¹¹

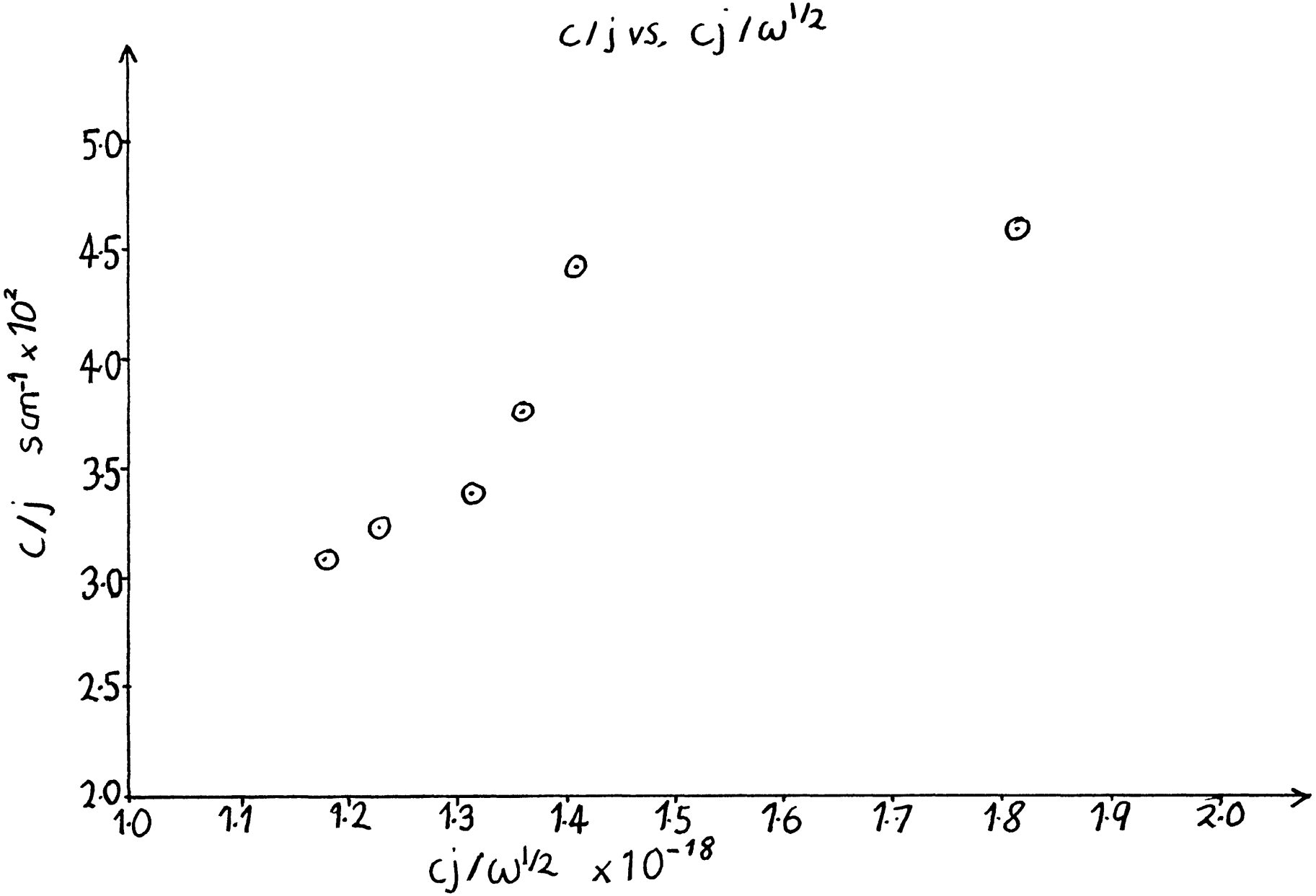
c/j vs. cj/ω^1/2
c/j S cm^-1 x 10^2
5·0
4·5
4·0
3·5
3·0
2·5
2·0
1·0
1·1
1·2
1·3
1·4
1·5
1·6
1·7
1·8
1·9
2·0
cj/ω^1/2 x 10^-18

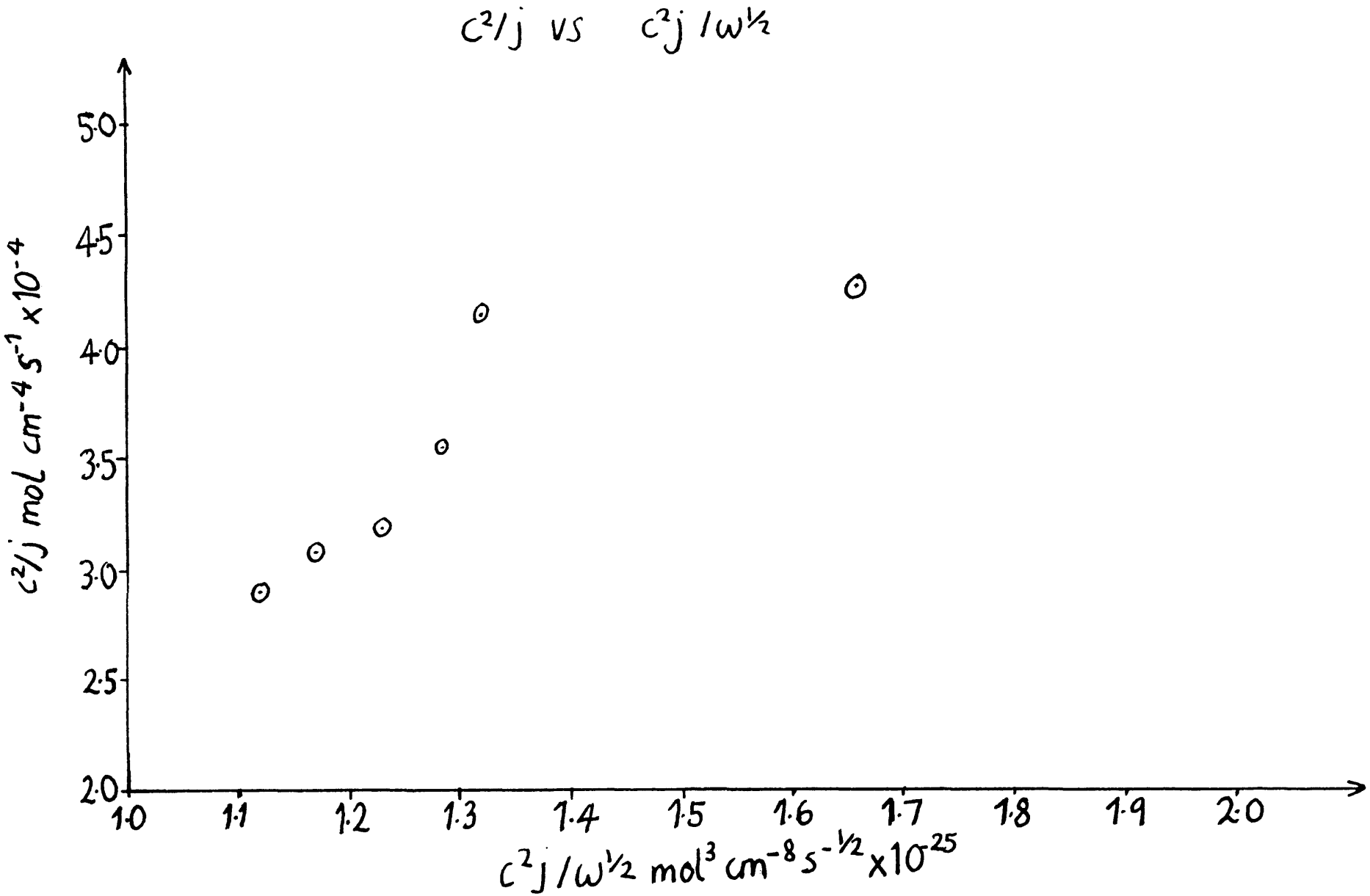
C^2/j vs $C^2j/\omega^{1/2}$
C^2/j mol cm^{-4} s^{-1} $\times 10^{-4}$
5·0
4·5
4·0
3·5
3·0
2·5
2·0
1·0
1·1
1·2
1·3
1·4
1·5
1·6
1·7
1·8
1·9
2·0
$C^2j/\omega^{1/2}$ mol^3 cm^{-8} $s^{-1/2}$ $\times 10^{25}$

membrane that no flux of ions could be observed with the Ag/AgCl sensor , (no change in potential) .

5.3.3 Flux Measurements for Membranes Containing Sodium Tetraphenylborate and Valinomycin in Diphenyl Ether

Another set of experiments involved the preparation of liquid membranes containing sodium tetraphenylborate . It has been reported[99,100] that the tetraphenylborate ion can act as the counterion to the potassium / valinomycin complex . Its less polar nature tends to make the tetraphenylborate ion soluble in organic solvents .This hypothesis was substantiated by the reduction of halide fluxes , through liquid membranes containing the tetraphenylborate ion , to neglible values .

5.3.4 The Ageing Effects of the Valinomycin Membranes

It was observed that the values of the flux of halide ions , through the liquid membranes , were reduced by a factor of roughly five over a period of twenty four hours from the preparation of the membrane . This contradicts observations[101] that the membrane resistance goes down during this period in the lifetime of the membrane . The explanation may lie in the hypothesis that pools of water enter the membrane[101] , and a consequent alternative method of potassium ion transport not involving the creation of the ion pair , i.e. the transport of K^+ or $KVAL^+$ in the pools of water .

5.3.5 Flux Measurements for Membranes Consisting of 18-Crown-6 Dissolved in Diphenyl Ether

The measurement of the flux of halide ions emerging from a liquid membrane consisting of 18-crown-6 (a crown ether selective for potassium ions) in a diphenyl ether solution was made . Figure 5.4 shows that these membranes have similar kinetics to the valinomycin membranes . The diffusion of the halide ions into the organic phase and the diffusion of the ion pair through the membrane are rate determining .

5.3.6 Variance in the Halide Counterion

It was found that the flux of halide ion through any kind of liquid membrane was independent of the actual halide ion used . This is not particularly surprising since the diffusion coefficients of chloride , bromide and iodide ions are similar[95] .

5.4A.C Impedance Studies

5.4.1 The Nature of the Impedance Spectra for Liquid Membranes

The equivalent circuit for membranes containing valinomycin is shown in figure 5.5 . Typical A.C. impedance spectra obtained from valinomycin / diphenyl ether membranes is shown in figure 5.6 . There are two basic processes that can be observed with A.C. impedance studies on liquid membranes . The bulk membrane resistance and geometric capacitance (R_b and C_g) yield information on the transport of species through the membrane . The charge transfer resistance and double layer capacitance (R_{ct} and C_{dl}) give an indication of processes ocurring at the membrane-solution

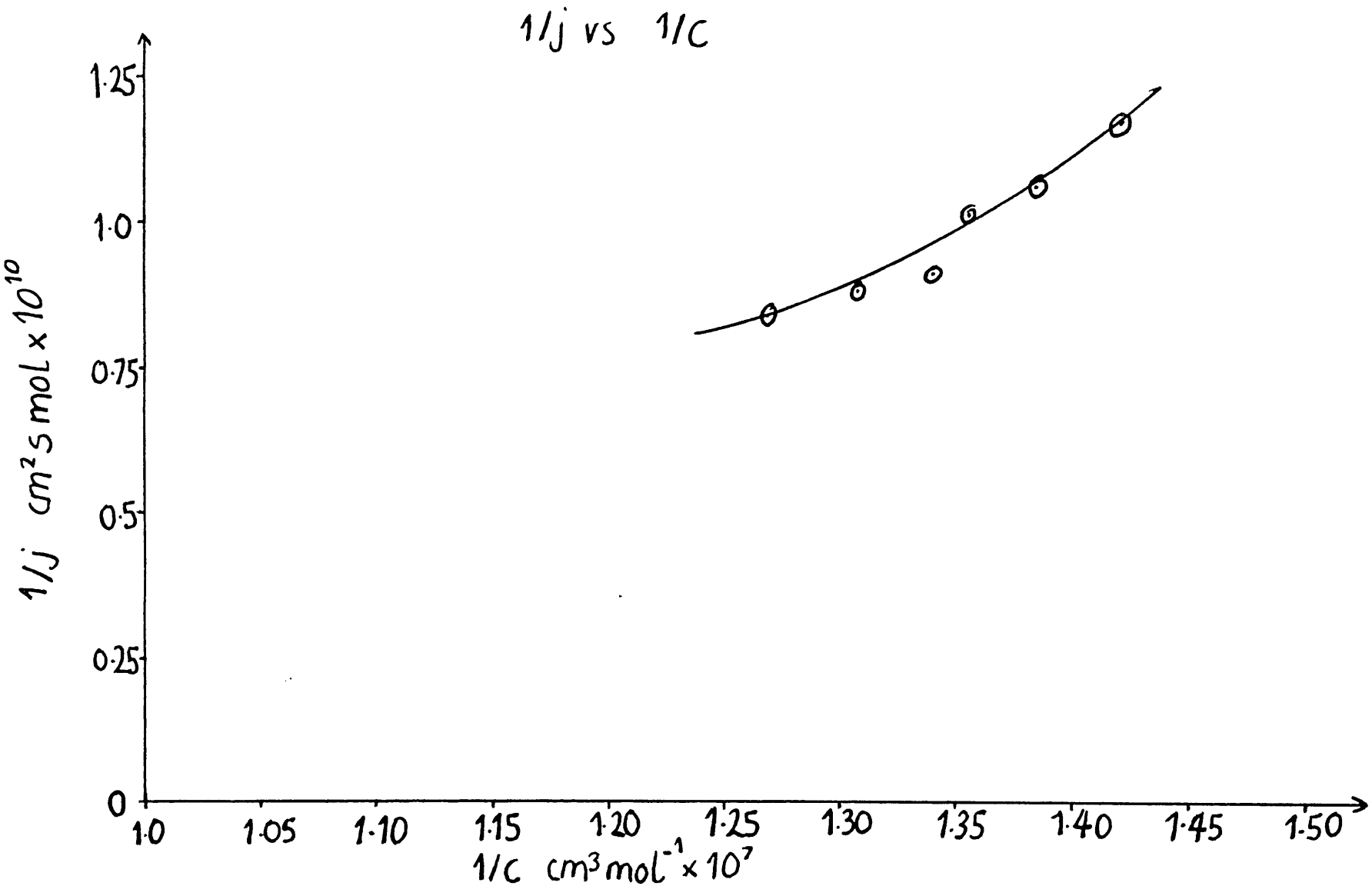

5.4 Diagnostic Plots for 0.001 M 18-Crown-6 Membranes

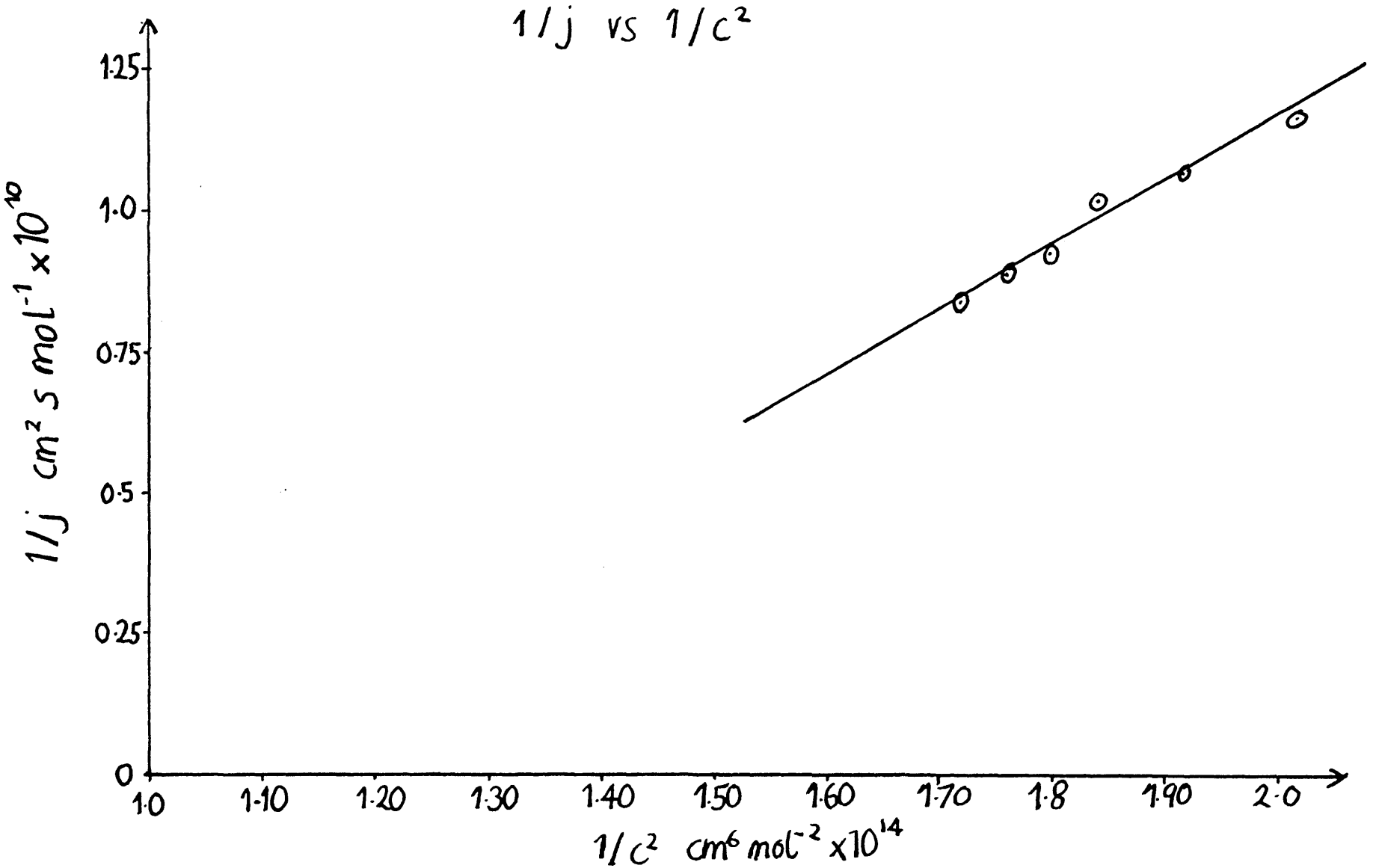
1/j vs 1/c²
1/j cm² s mol⁻¹ x 10¹⁰
1·25
1·0
0·75
0·5
0·25
0
1·0
1·10
1·20
1·30
1·40
1·50
1·60
1·70
1·8
1·90
2·0
1/c² cm⁶ mol⁻² x 10¹⁴

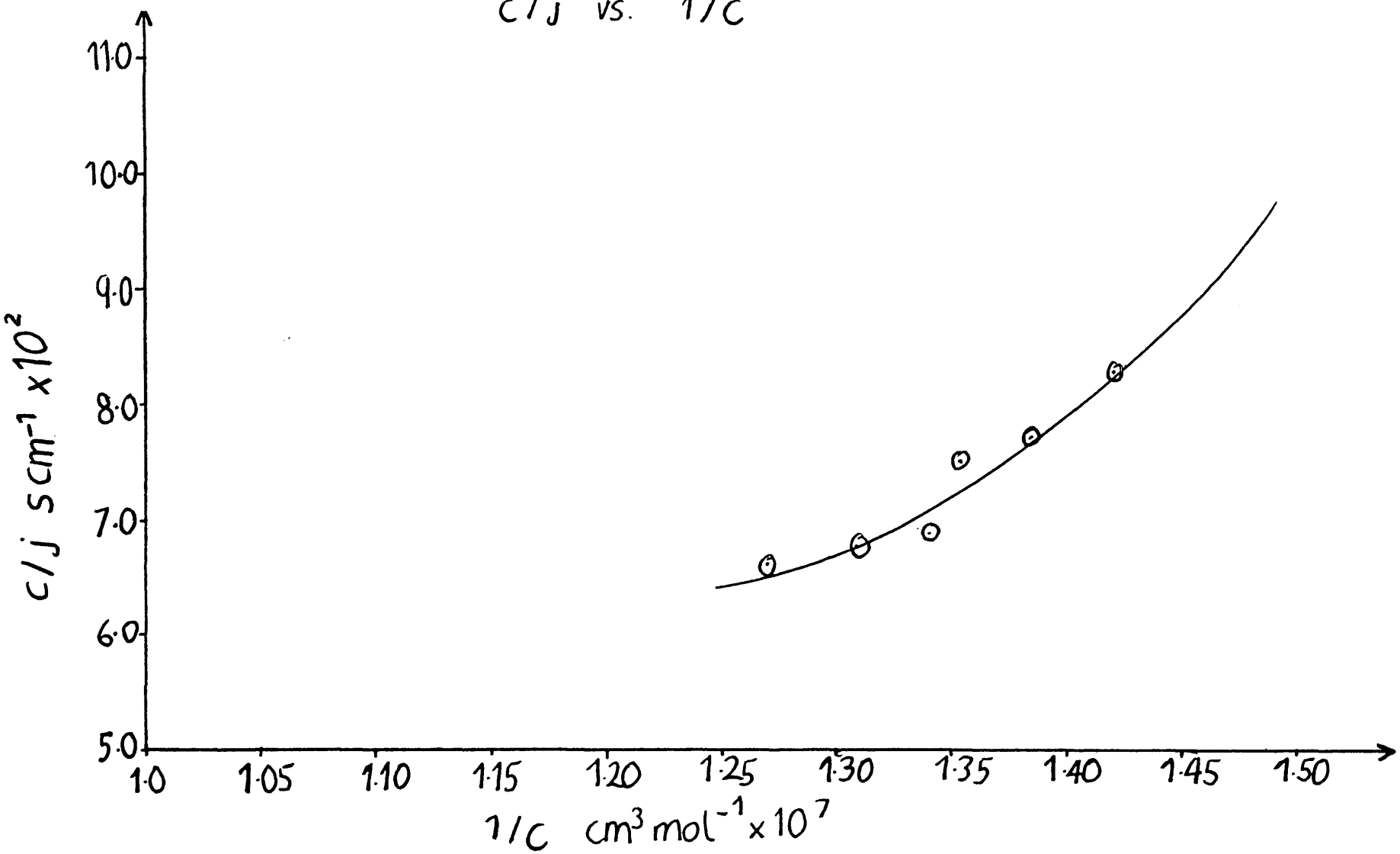
c/j vs. 1/c
11·0
10·0
9·0
8·0
7·0
6·0
5·0
c/j S cm⁻¹ x10²
1·0
1·05
1·10
1·15
1·20
1·25
1·30
1·35
1·40
1·45
1·50
1/c cm³ mol⁻¹ x10⁷

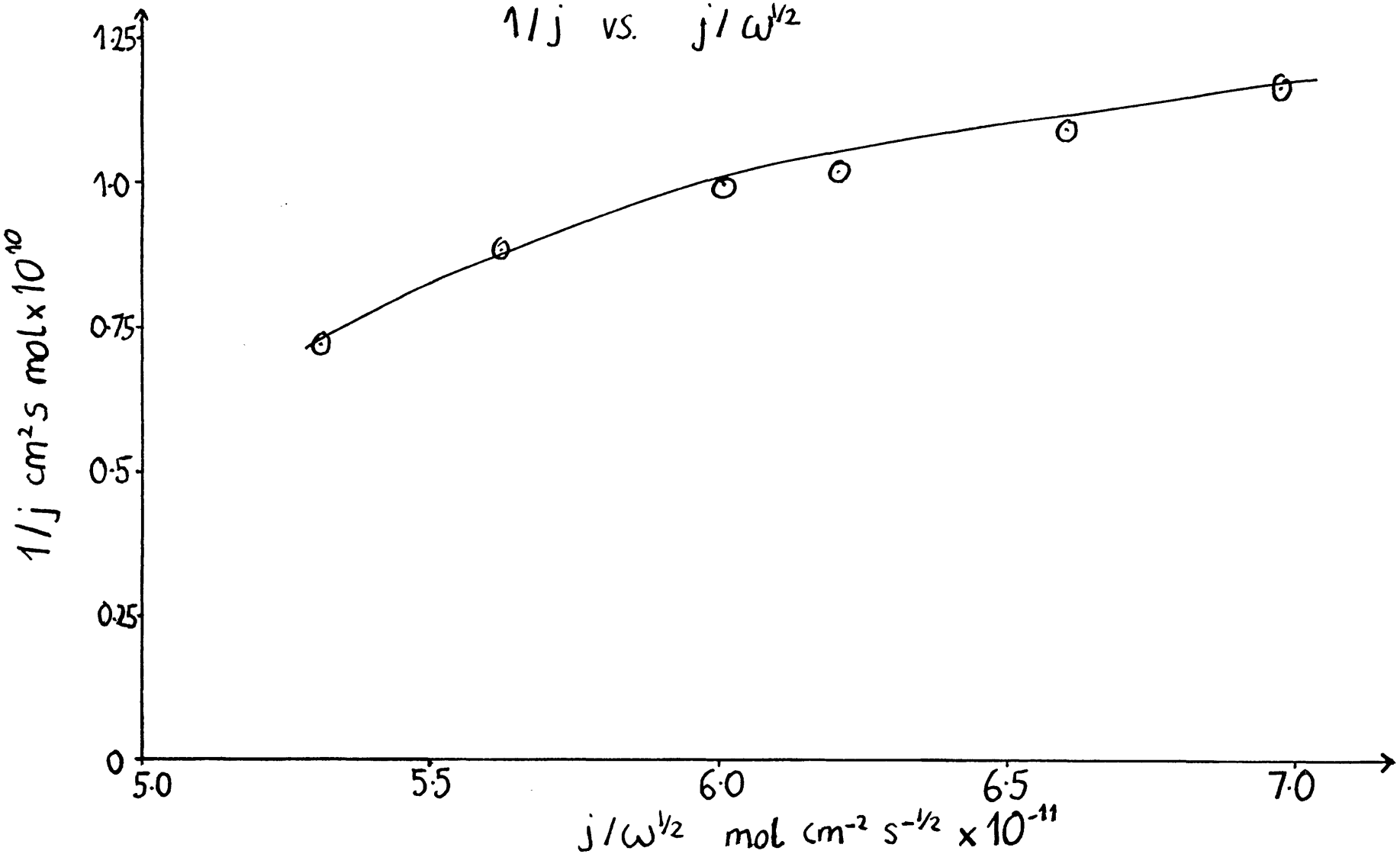
1/j vs. j/ω^1/2
1.25
1.0
0.75
0.5
0.25
0
1/j cm² s mol x 10^10
5.0
5.5
6.0
6.5
7.0
j/ω^1/2 mol cm^-2 s^-1/2 x 10^-11

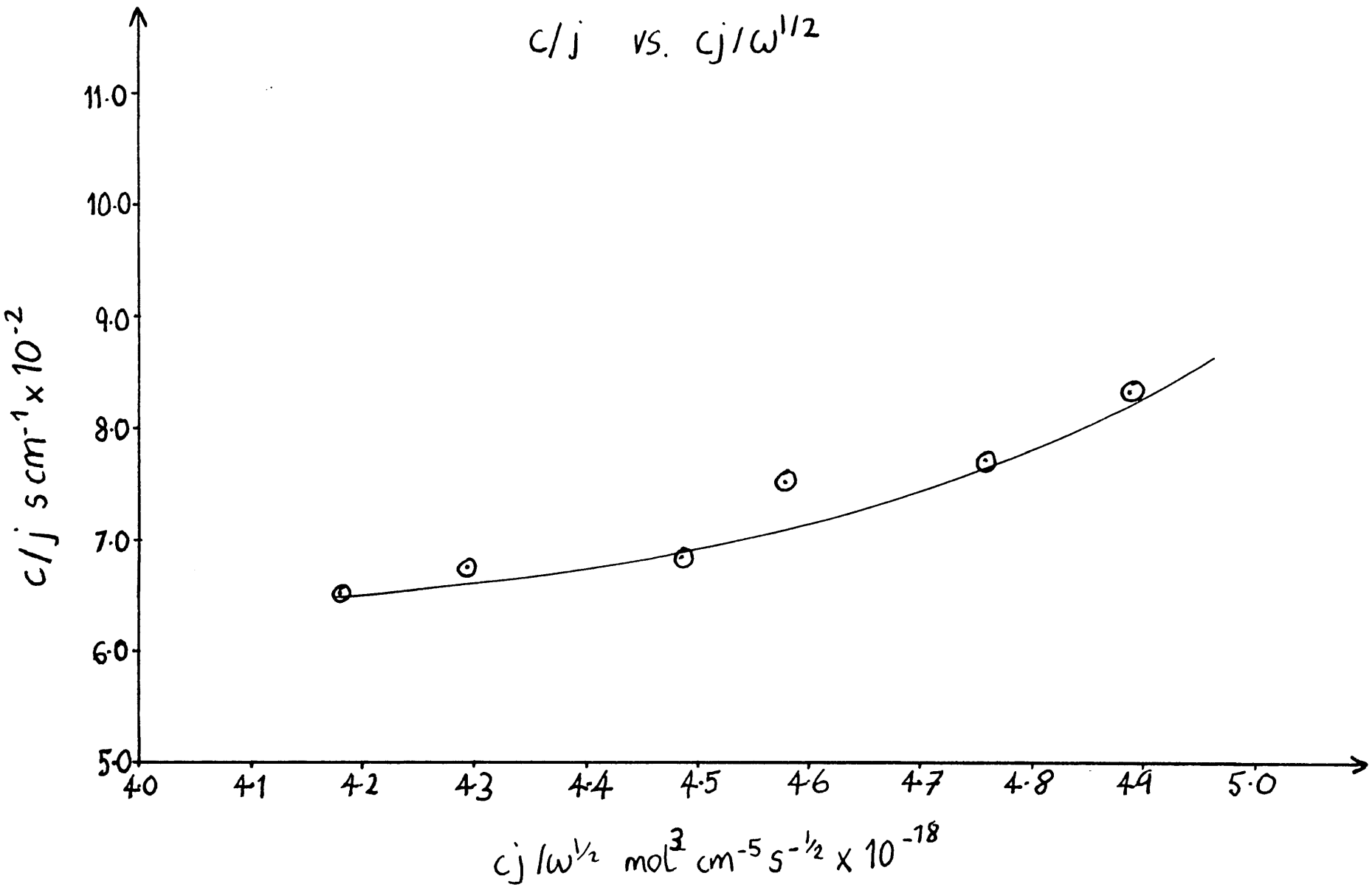
c/j vs. cj/ω^1/2
11·0
10·0
9·0
8·0
7·0
6·0
5·0
c/j s cm⁻¹ x 10⁻²
4·0
4·1
4·2
4·3
4·4
4·5
4·6
4·7
4·8
4·9
5·0
cj/ω½ mol³ cm⁻⁵ s⁻½ x 10⁻¹⁸

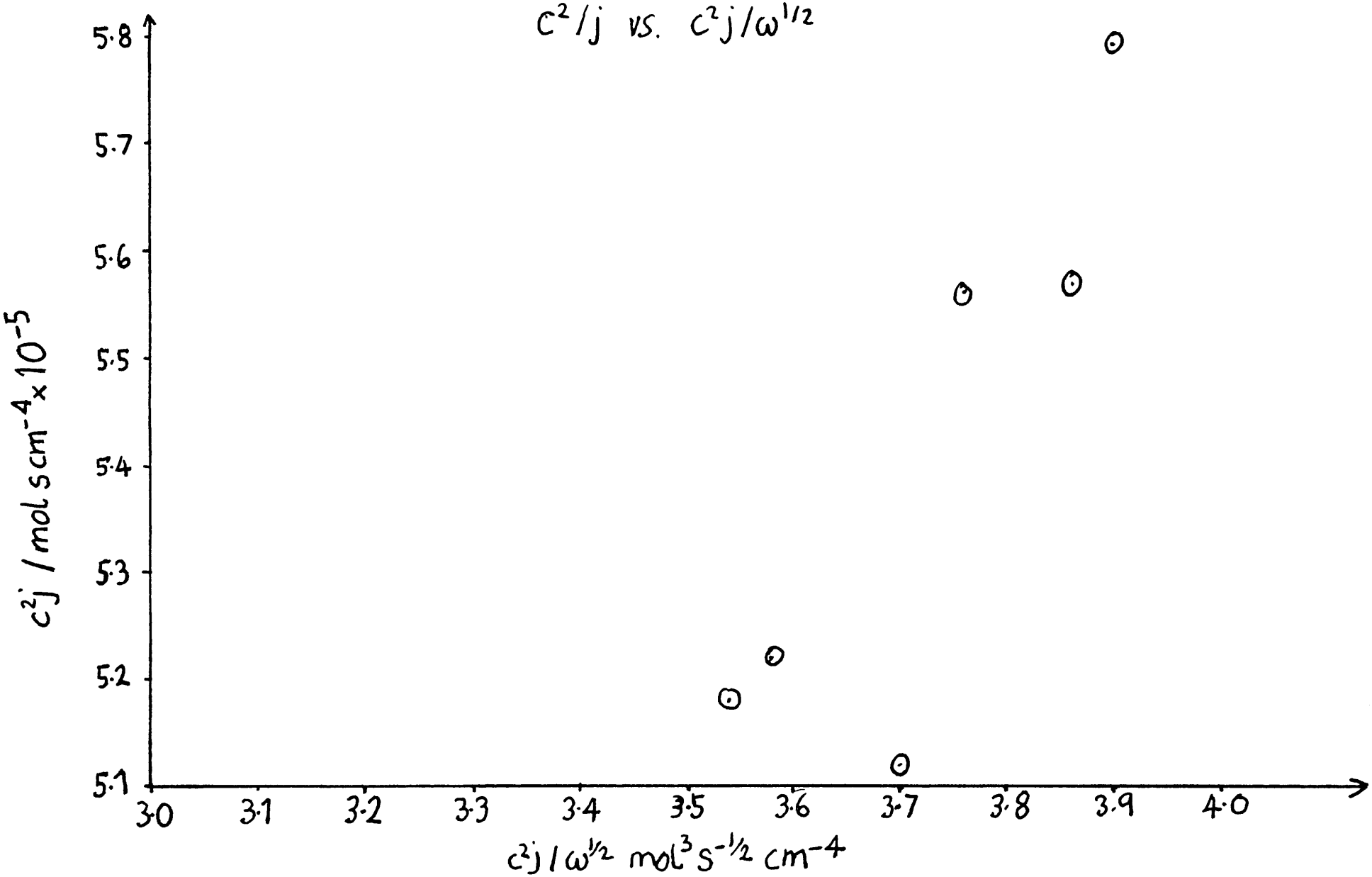
C^2/j vs. $C^2j/\omega^{1/2}$
5·8
5·7
5·6
5·5
5·4
5·3
5·2
5·1
c^2j / mol s cm^{-4} x 10^{-5}
3·0
3·1
3·2
3·3
3·4
3·5
3·6
3·7
3·8
3·9
4·0
$c^2j/\omega^{1/2}$ mol^3 s$^{-1/2}$ cm^{-4}

interface .

5.4.2 Processes Occuring Inside the Membrane

The bulk membrane resistance of a membrane can be obtained by noting the intercept of the first semicircle of the A.C. impedance spectrum . The geometric capacitance can then be calculated by obtaining the frequency at the maximum of the semicircle (i.e. finding the value of the time constant , τ) .

The variation in R_b with the concentration of valinomycin in the liquid membrane is shown in figure 5.7 . There is a massive increase in the value of R_b when the ionophore concentration drops , which is indicative of the switch over point between mass transfer and kinetic control of the halide flux values .

5.4.3 Interfacial Processes

Armstrong et al.[101] obtained a second semicircle in their impedance spectra of liquid membranes containing valinomycin. The failure to record this part of the spectrum , in this study , was probably due to the unsuitability of the electronics employed .

The value of charge transfer resistance obtained by Armstrong et al. , for a valinomycin concentration of 10^{-3}M was 8.8×10^{3} ohms per square centimetre . The value of the exchange current , I_o , (i.e. the flux of species across either interface) obtained from equation 2.27 is 2.9×10^{-6} amps per square centimetre . This value is equivalent to a flux of monovalent ions of 3×10^{-11} moles per square

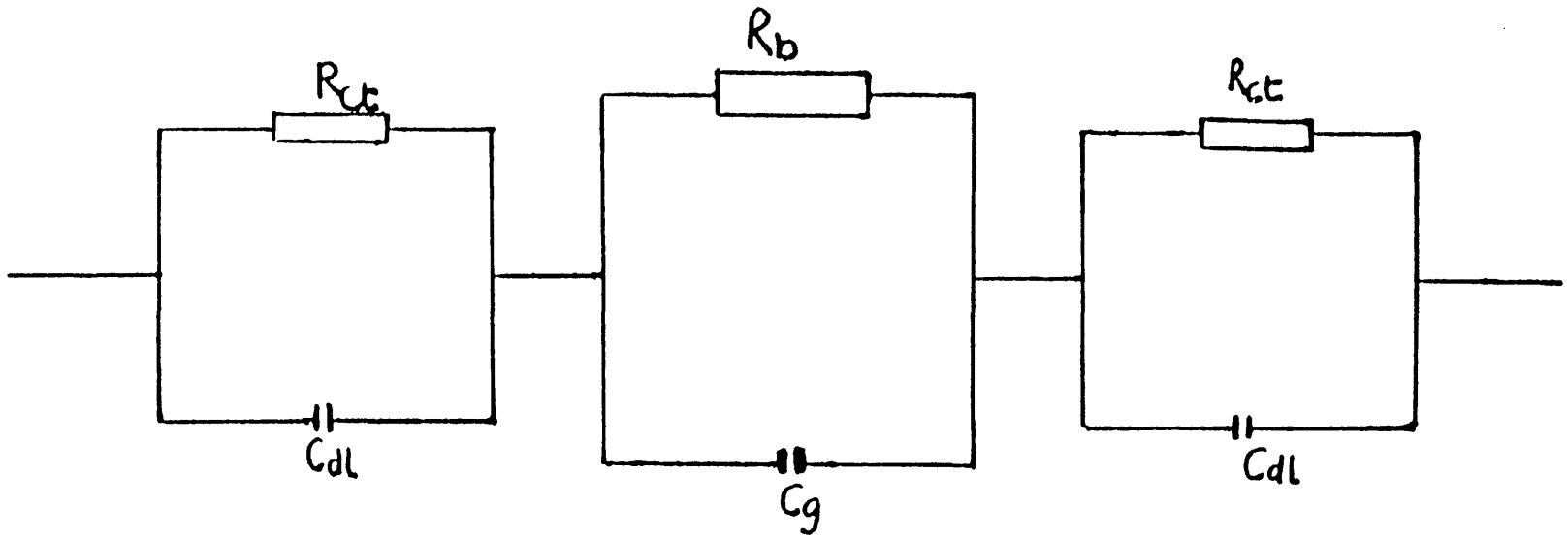

5.5 The Equivalent Circuit for a Valinomycin Based Liquid Membrane

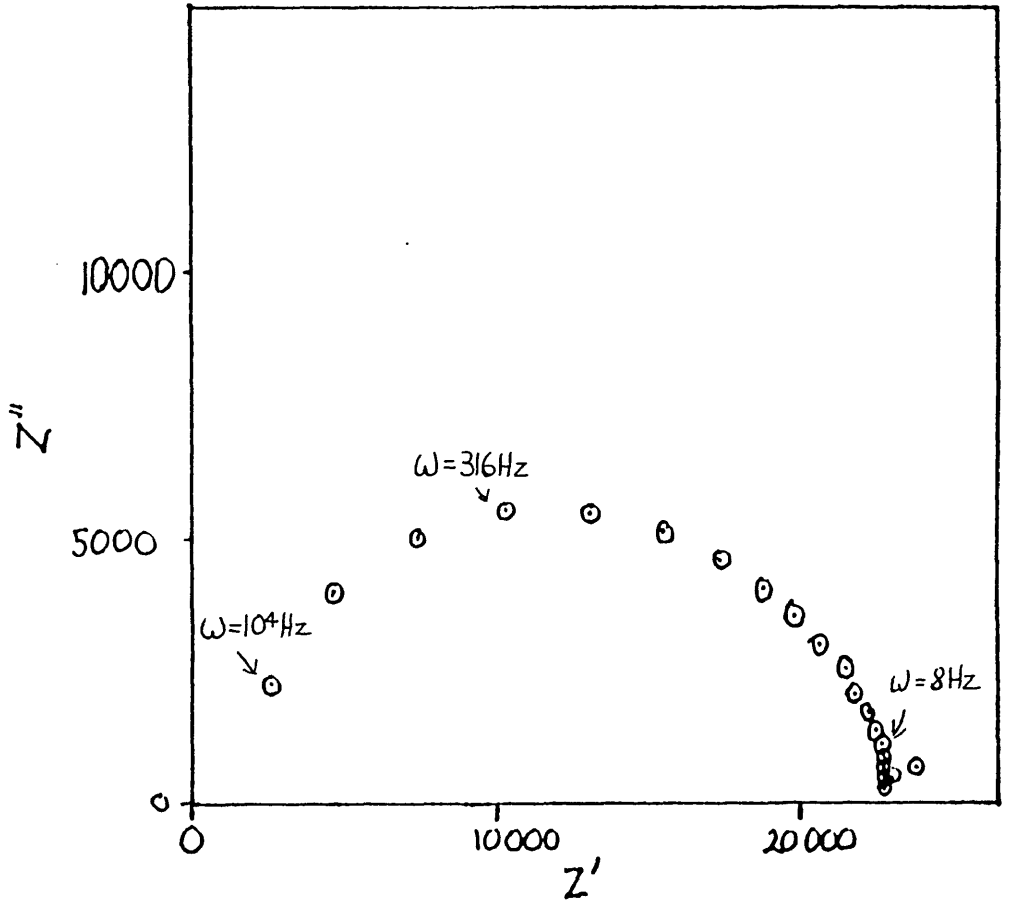

5.6 The AC Impedance Spectrum of the Membrane

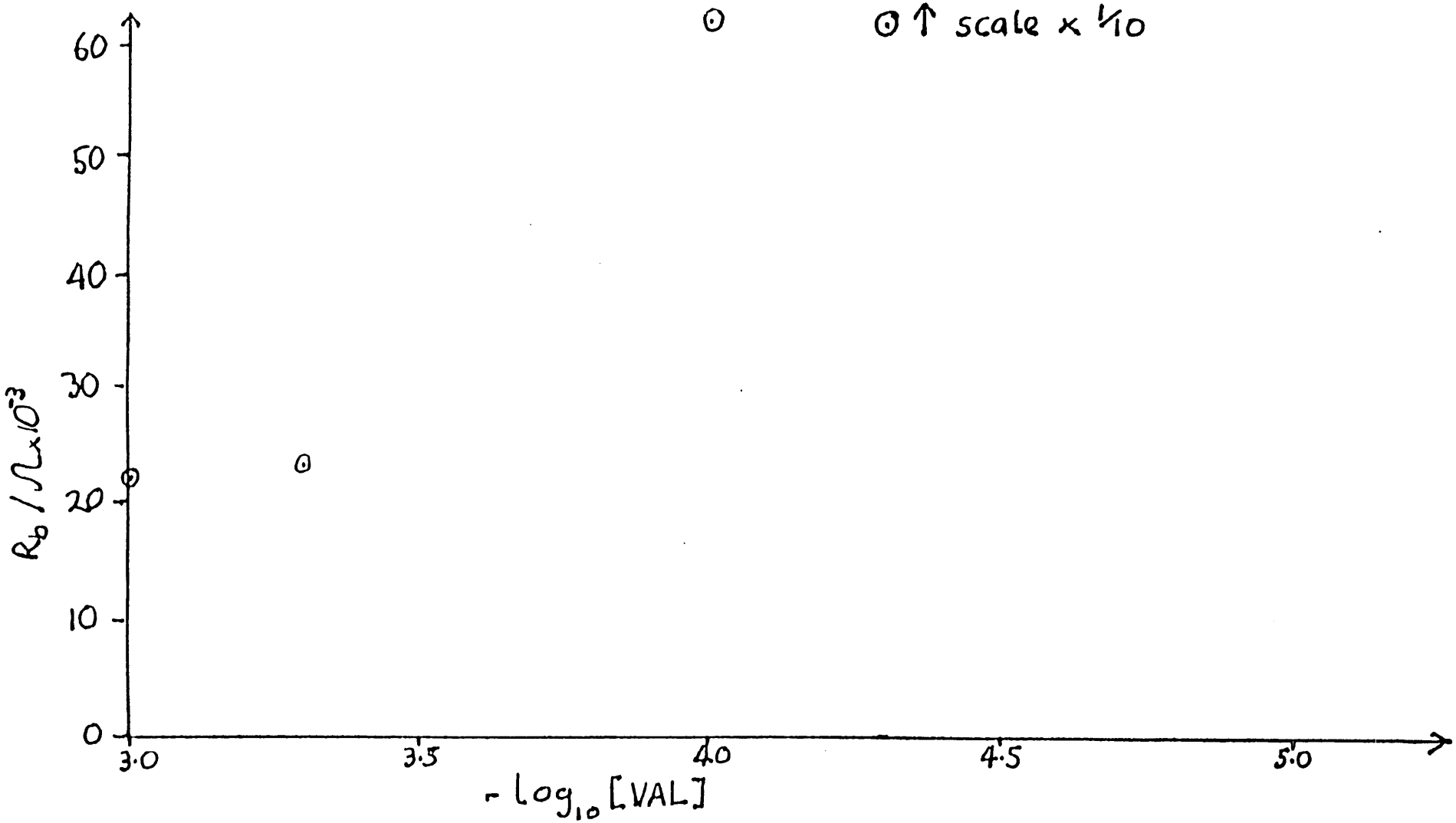

5.7 R_B versus $-\ln[Val]$

centimetre per second . This value is of the same order of magnitude as that obtained from the silver / silver halide electrode studies . This would tend to indicate that the mechanism involving the formation of an ion pair is correct , although it must be emphasised that strictly quantitative measurements of halide ion flux at zero rotation speed are unviable , and A.C. impedance spectra values were not obtained for a rotating liquid membrane .

5.5 Summary

i) The arc electrode system is a reliable method for detecting the small fluxes of ions diffusing through liquid mebranes .

ii) For a valinomycin liquid membrane , and presumably for uncharged ionophore systems in general , ion pairs , such as $KVAL^{+}A^{-}$ are formed inside the organic phase . A^{-} can either come from the external solution , or preferably be present inside the membrane . Obviously , for the latter case A^{-} must be a relatively hydrophobic ion .

iii) It would appear that the structure of the liquid membranes is subject to breakdown with time . The hypothesis that water droplets can enter the organic phase means that the long term usuage of liquid membranes in ion-selective electrodes is not viable .

iv) Commercial ion-selective electrodes , including valinomycin based potassium selective electrodes , get round the previously mentioned problem by locating the ionophores in solid , PTFE frameworks . Future work must include the setting up of experimental apparatus that enables the arc

electrode sensor to measure the flux of ions through these commercial , polymeric systems .

CHAPTER 6 THE DEVELOPMENT OF A TECHNIQUE FOR MEASURING INTERFACIAL POLYMERISATION RATES

6.1 The Arc Electrode Technique Applied to Interfacial Chemistry

The arc electrode technique , mentioned in the last chapter , can be used to study reactions occurring at an interface , set up on the Millipore filter disc . The pre-requisite for the applicability of this technique is that the interfacial reaction should produce a species that can be sensed spontaneously at an ion-selective arc electrode .

An example of such a reaction is the condensation reaction producing an amide . This reaction involves an amine from the aqueous phase reacting with an acid chloride from the organic phase :

$$RCOCl + R`NH_2 \longrightarrow RCONHR` + HCl$$

The side product , hydrogen chloride , goes into the aqueous phase as protons and chloride ions . The chloride ions can be detected by a Ag/AgCl arc electrode as described in section 2.2.2

6.2 Nylon Polymerisation

6.2.1 The Experimental Conditions

A well documented[68,69,71] interfacial amide reaction is the production of nylon , a polyamide . The polymerisation of sebacoyl chloride and diamine hexane , (to form 6,10-nylon) was carried out in a rotating diffusion cell apparatus . A Ag/AgCl arc electrode was used to measure the flux of chloride ions produced by this reaction . The acid chloride was added to heptane in the inner compartment (Fig.2.4) .

The diamine was added to an aqueous solution of sodium hydroxide . The hydroxyl ion is a proton acceptor which is required for the polymerisation . As the reactants were added simultaneously , the potential of the arc electrode was noted . The rotation speed of the RDC was varied so as to control the effective concentration of reactants at the reaction site .

6.2.2 Chloride Flux Measurements During Interfacial Polymerisation

Due to the relatively low interfacial area , (in the order of square centimetres) , the concentrations of reactants used in other studies[68,69,70,74,75] , i.e. roughly molar , resulted in the blockage of the interface within seconds . Consequently the potential of the arc electrode did not vary significantly . When lower concentrations were used however , a "transient-type" behaviour was observed on V_{arc} (Fig.6.1) . This gradual reduction in the rate of production of chloride ions , (the "transient lasted for 20-30 minutes) was roughly exponential . This is in agreement with other studies[75] , and suggests there is a blocking of the interface with a porous polymeric film which terminates the reaction when it grows to a certain thickness .

At a particular point in the "transient" the flux of chloride ions obeys the Levich equation (Fig.6.2) . The straight line to the flux versus the square root of the rotation speed at the initiation of the polymerisation suggests that the reaction is mass transport controlled . The

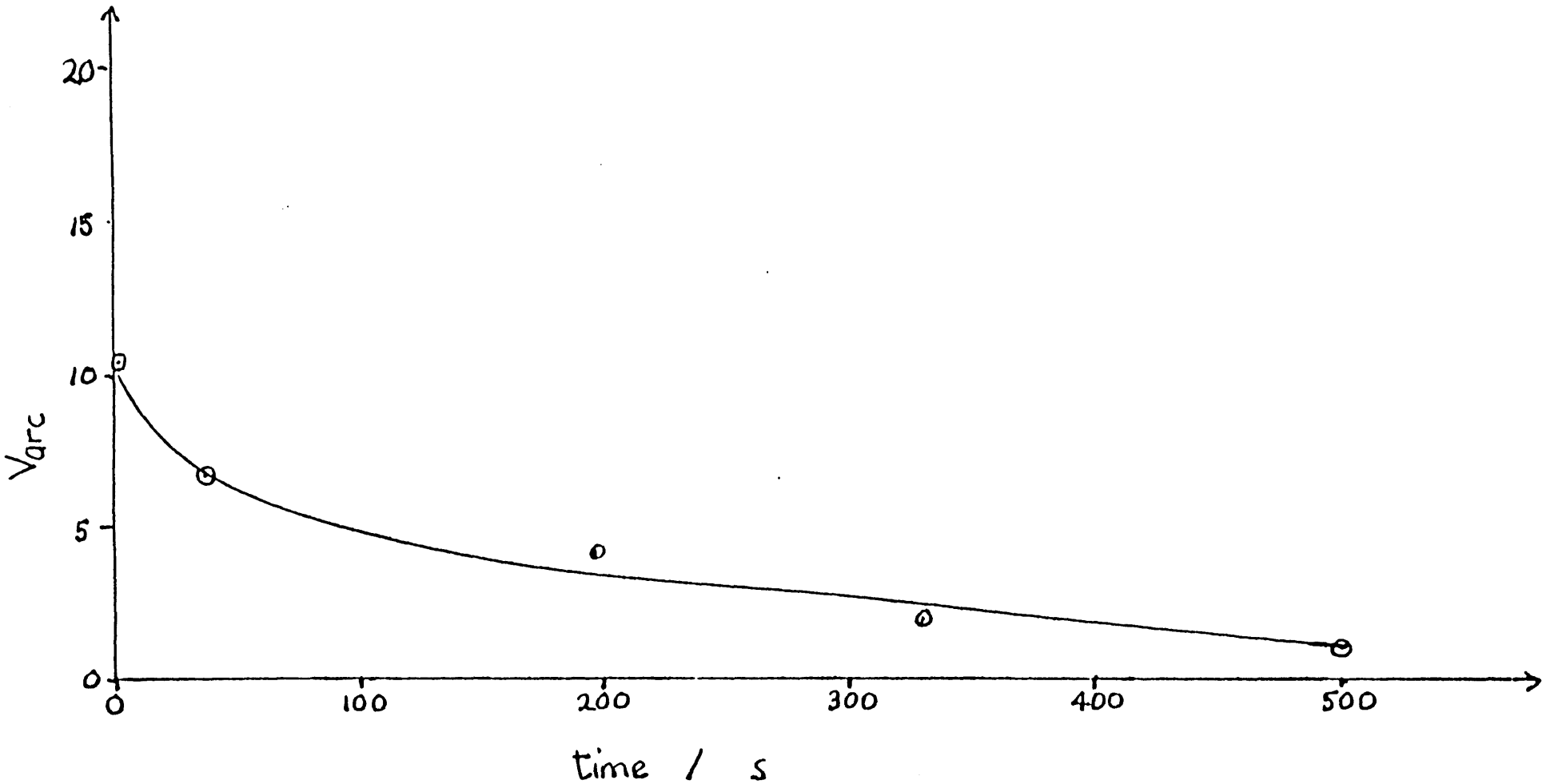

6.1 V_{arc} vs. Time

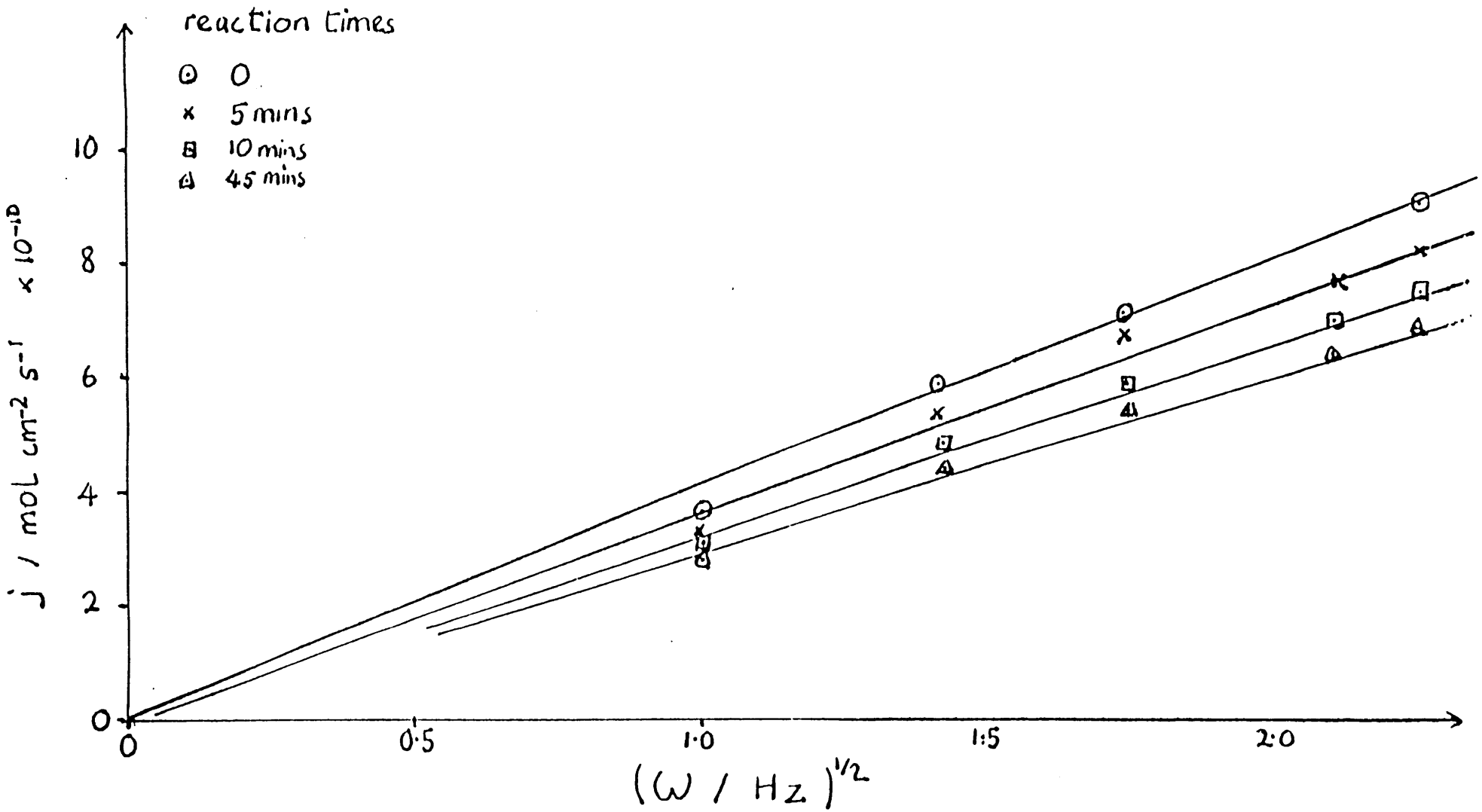

6.2 The Family of Levich Slopes

gradient of these plots is reduced as the reaction progresses (Fig.6.2) , and this effect is plotted in figure 6.3 . Presumably this is due to the decrease in the effective area of reaction . This hypothesis is backed up by the observation that the plot is similar to the change in conductance versus time plot in reference 75 , for the same reaction and conditions .

6.3 Following the Reaction Between Hexane Diamine and PP563

The reaction between sebacoyl chloride and hexane diamine was observed to be facile . The previous section has dealt with the study of how the polymerisation is slowed by the formation of a polymer film . Although this is of interest to polymer chemistry , it was decided to pursue a reaction with a slower chemical rate constant and so investigate whether or not a study of chemical kinetics was possible with the arc electrode technique .

PP563 (Fig.6.4) tends to react considerably slower than striaght chain acid chlorides[102] . This is presumably due to steric considerations . A similar technique to that employed in section 6.2.1 was employed for the study of the reaction between PP563 and hexane diamine at a water heptane interface .

It was observed that changes in V_{arc} were considerably slower than the equivalent values for the polymerisation . The rotation speed dependence was observed to be of a Koutecky-Levich nature (Fig.6.5). This suggests that mass transport was not the only rate determining step but a chemical reaction was also important .

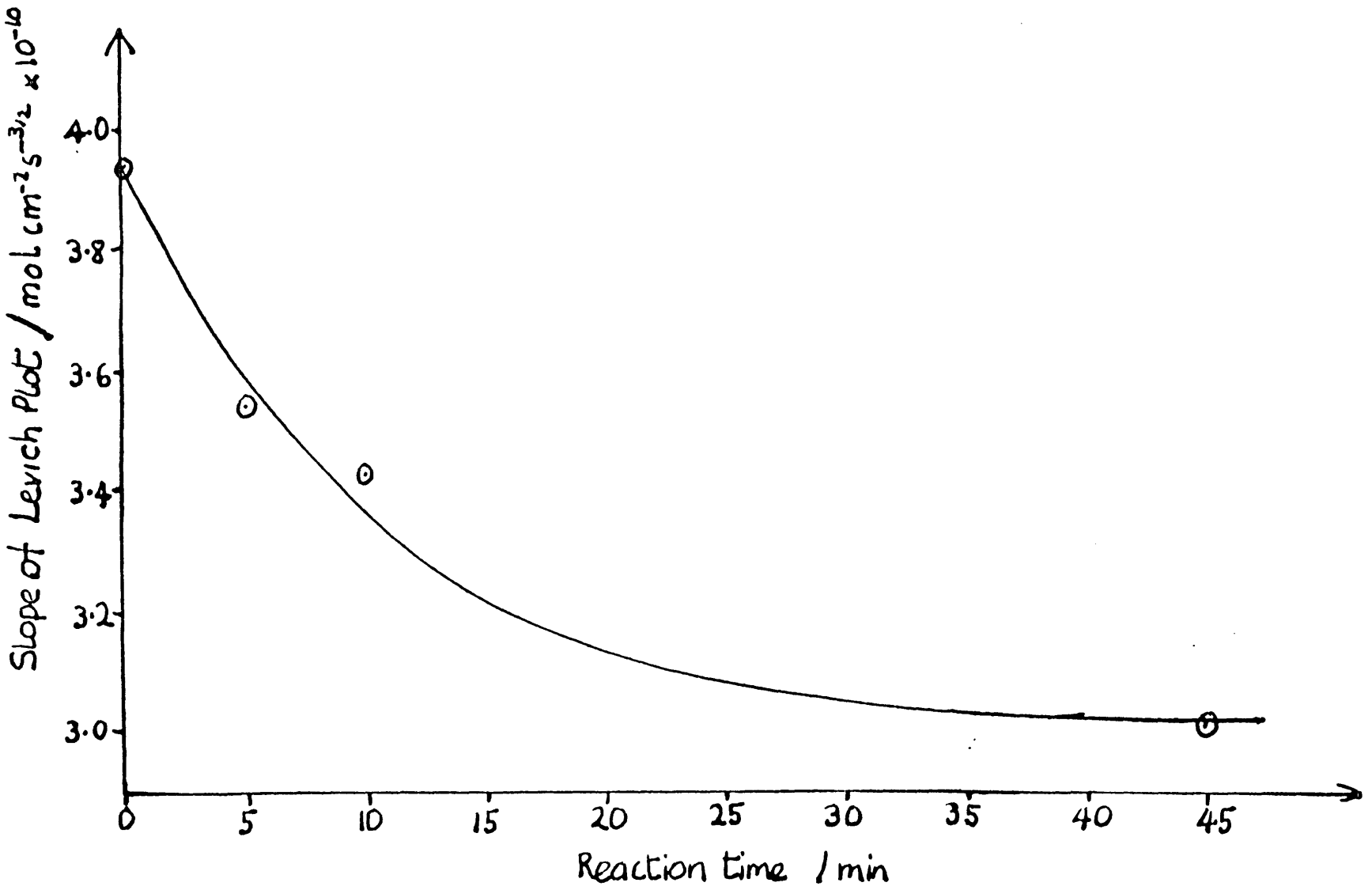

6.3 The Slopes of the Levich Equations vs. Reaction Time

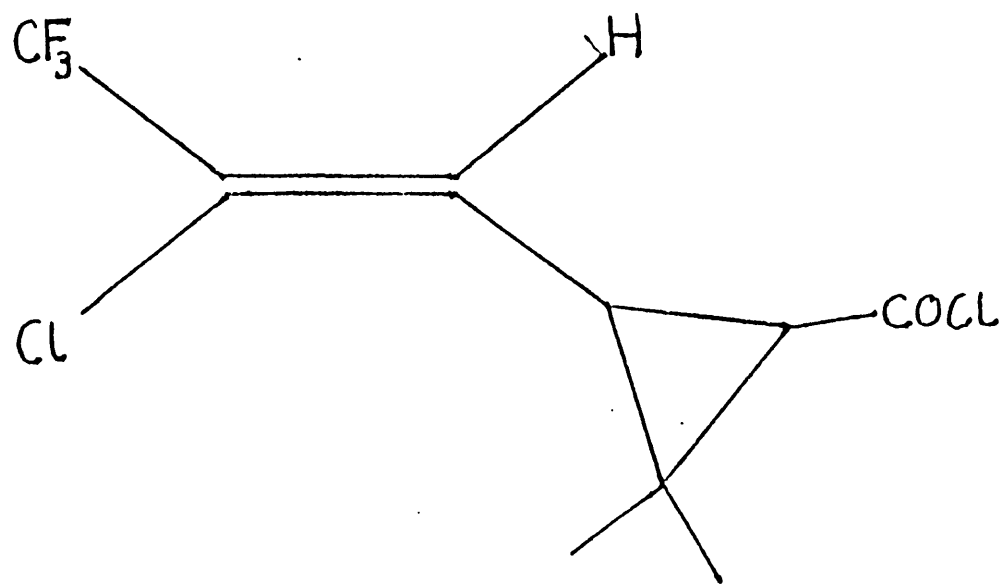

6.4 PP563

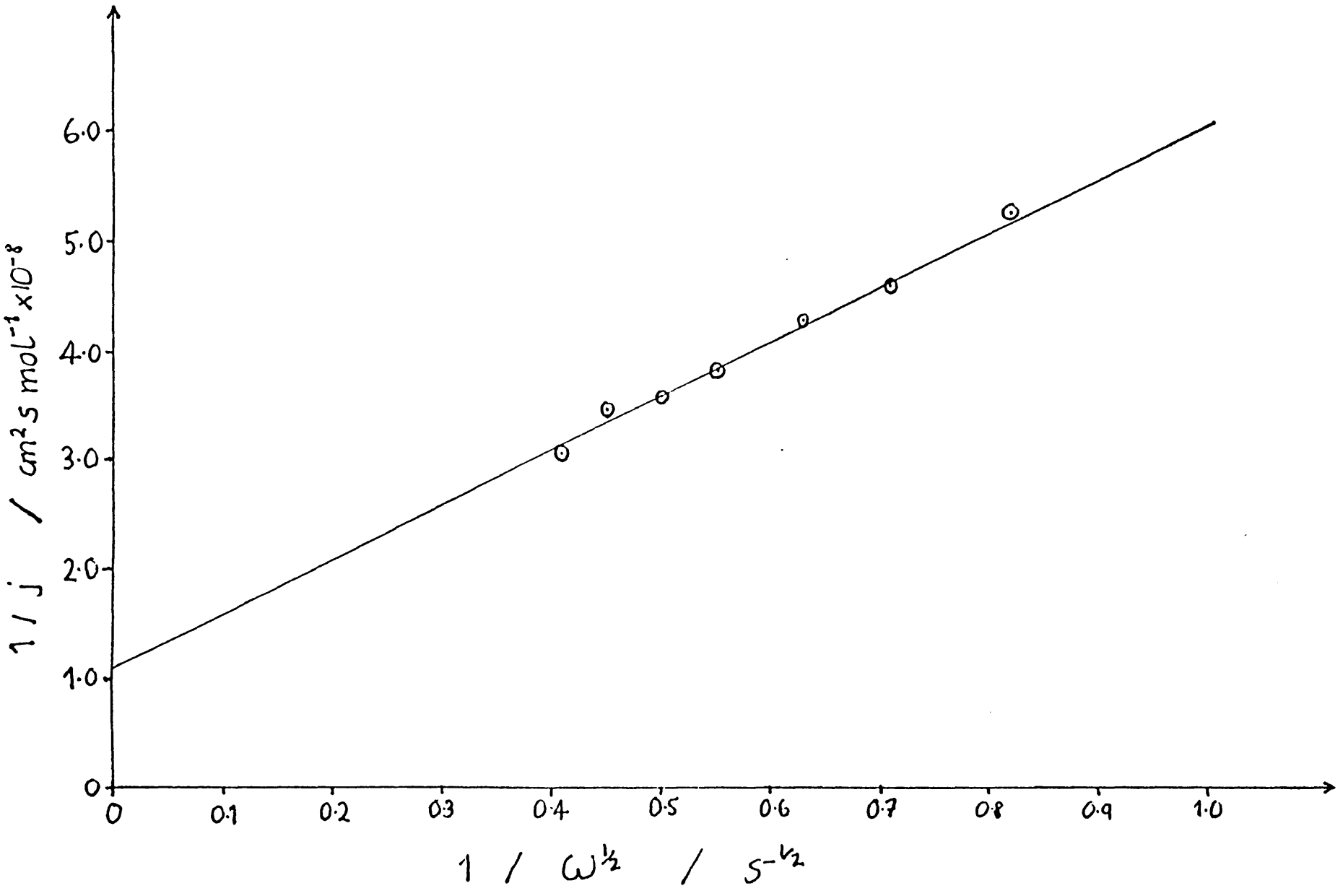

6.5 1 / j vs. 1 / $w^{1/2}$ for the PP563 Reaction

From equation 2.13 the intercept of the Koutecky-Levich plot , (i.e. when $\omega \longrightarrow \infty$) should give a rate constant for the chemical reaction . This was calculated to be 9.1×10^{-7} mol cm^{-2} s^{-1} . No literature value for this rate constant could be found , but it two orders of magnitude greater than the the hydrolysis of PP563 at the same pH[102] .

6.4 Summary and Future Work

The arc electrode technique has been proven to be a convenient and accurate technique for measuring small fluxes at liquid-liquid interfaces . Further work on the amidation reaction includes :-

i) Investigating how the pH affects the rate constant , (hydroxyl ions are used to drive the equilibrium to the products side) .

ii) Varying the concentrations of the reactants , i.e. so they are in unequal proportions . The current study has solely looked at equal concentrations .

iii) Investigating the effect of inhibitors such as surfactant molecules .

iv) Studying other amidation reactions

The arc electrode technique can also be extended to the study of other interfacial processes :-

i) solvent extraction .

ii) The sequestering of ions from aqueous solutions .

iii) Surfactant aggregation .

iv) Organic interfacial reactions .

REFERENCES

1) H.Ti Tien "Bilayer Lipid Membranes" Marcel Dekker 1974

2 a) B.Hupfer and H.Ringsdorf ACS S Series 175 103 209 (1981)
b) H.Bader , K.Dorn , B.Hupfer , H.Ringsdorf Advances in Polymer Science 1 1 (1985)

3) C.Avers "Cell Biology" Van Nostrand 1976

4) A.L.Lehninger "Biochemistry" Worth 1975

5) C.Stryer "Biochemistry" W.H.Freeman 1975

6) G.Gregoriadis , A.C.Alliom "Liposomes in Biological Systems" Wiley 1980

7) L.Gros , H.Ringsdorf , H.Schupp Angew.Chem.Intl.Ed.Engl.20 (1981)

8) B.Franklin Philosophical.Trans. 64(1) 445 (1774)

9) A.Pockels Nature 48 152 (1893)

10) Lord Rayleigh Phil.Mag. 48 321 (1899)

11) W.B.Hardy Proc.Roy.Soc.(Lond.) A86 610 (1912)

12) I.Langmuir J.Proc.Amer.Chem.Soc. 39 1848 (1917)

13) K.Blodgett J.Amer.Chem.Soc. 57 1007 (1935)

14) I.Frankuchen Phys.Rev. 53 909 (1938)

15) S.Bernstein J.Amer.Chem.Soc. 60 1511 (1938)

16) I.Langmuir , J.Schaefer , H.Sobotka J.Proc.Amer.Chem.Soc. 59 1751 (1937)

17) M.Montal and P.Mueller Proc.Nat.Acad.Sci.USA 69(12) 3561 (1972)

18) R.H.Tredgold and M.Elgamal Biochim.Biophys.Acta 555 381 (1979)

19) C.N.Kossi and R.M.Leblanc J.Coll.Int.Sci. 80(2) 426 (1981)

20) K.Heckman et al E.P. 059393

21) P.Mueller , D.O.Rudin , H.Ti Tien , W.C.Westcott Nature 194 979 (1962)

22) R.H.Guy and R.Fleming J.C.S.Chem.Commun. 729 (1974)

23) S.L.Regen , P.Kirszensztejn , A.Singh **Macromolecules** 16 335 (1938)

24) J.H.Fendler **Science** 223 888 (1984)

25) D.S.Johnston , S.Sanghera , M.Pons , D.Chapman **Biochim.Biophys.Acta** 602 57 (1980)

26) R.Elbert , A.Laschewsky , H.Ringsdorf **J.Am.Chem.Soc.**107 4134 (1985)

27) D.Bloor and R.R.Chance "**Polydiacetylenes**" **NATO ASI Series E Martinus Nijhoff** (1985)

28) H.H.Hub , B.Hupfer , H.Koch , H.Ringsdorf **J.Macromol.Sci. Chem.** A15(5) 701 (1981)

29) R.Elbert , A.Laschewsky , H.Ringsdorf **J.Amer.Chem.Soc.** 107 4134 (1985)

30) D.W.R.Gruen , D.A.Haydon **Biophys.J.** 30 129 (1980)

31) H.Ti Tien **Membr.Transport** 1 165 (1984)

32) R.Fettiplace , D.A.Haydon **J.Physiol.Rev.** 60 510 (1980)

33) V.F.Antonov , Y.G.Rovin , L.T.Trifmov "**A Bibliography of Bilayer Lipid Membranes : 1962-1975**" All Union Institute for Scientific Information , Moscow

34) Y.A.Chizmadzev , I.G.Abidor , V.F.Pastushev , V.B.Arakelya **Bioelectrochem.Bioenerg.** 6 37 (1979)

35) R.Benz , K.Janko , P.Lauger **Biochim.Biophys.Acta** 551 236 (1979)

36) Y.A.Shchipanov and G.Y.Drachev **Biofizika** 25 921 (1980)

37) K.R.Rohr and J.A.Rooney **Biophys.J.** 23 33 (1978)

38) W.Ostwald **Z.Physik Chem.** 6 71 (1890)

39) E.Overton **Pfluger's Arch.Ges.Physiol.** 92 346 (1902)

40) J.Bernstein **Pfluger's Arch.Ges.Physiol** 92 521 (1902)

41) B.Lengyel and E.Blum **Trans.Faraday soc.** 30 461 (1934)

42) E.Pungor and E.Hallos-Rokosinyi **Acta Chim.Hung.** 27 63 (1961)

43) M.S.Frant and J.W.Ross **Science** 154 1553 (1966)

44) K.Sollner and G.M.Shean **J.Amer.Chem.Soc.** 86 190 (1964)

45) J.W.Ross **Science** 156 1378 (1967)

46) G.G.Guilbault Pure Appl.Chem. 25 727 (1971)

47) G.A.Rechnitz , T.L.Riechel , R.K.Kobos , M.E.Meyerhoff Science 199 440 (1978)

48) M.A.Arnold and G.A.Rechnitz Anal.Chem. 52 1170 (1980)

49) J.A.M.Hinke "Cation-selective Microelectrodes fof Intracellular Use" Chapter17 of "Glass Electrodes for Hydrogen and Other Cations" Ed. G.Eisenman Marcel Dekker (1969)

50) L.S.Kelday , D.J.F.Bowling , M.G.Penny J.Exp.Bot. 28 31 (1977)

51) J.L.Walker Anal.Chem. 43 89A (1971)

52) P.M.Whelan , M.J.Hodgson "Essential Principles of Physics" John Murray 1982

53) R.P.Buck , D.E.Hackleman Anal.Chem.52 1935 (1980)

54) J.Janata , S.D.Moss Biomed. Eng. 11 241 (1976)

55) P.T.McBride , J.Janata , P.A.Comte , S.D.Moss , C.C.Johnson Anal.Chim.Acta 101 239 (1978)

56) S.D.Moss , J.Janata , C.C.Johnson Anal. Chem. 47 2238 (1975)

57) S.Caras , J.Janata Anal.Chem. 52 1935 (1980)

58) T.B.Grimley Proc.Roy.Soc. (A) 201 40 (1950)

59) P.K.C.Tseng and W.F.Gutknecht Anal.Lett. 9 795 (1975)

60) A.Hulanicki , R.Lewandowski , A.Lewenstam Anal.Chim.Acta 110 197 (1979)

61) M.Mascini Anal.Chim.Acta 62 29 (1972)

62) E.Pungor , L.Stehli , L.Andre , J.Gyorgy Anal.Chim.Acta 46 318 (1969)

63) K.Toth , E.Pungor Anal.Chim.Acta 51 221 (1970)

64) M.H.Hebb J.Chem.Phys. 20 185 (1952)

65) C.Wagner J.Chem.Phys. 21 1819 (1953)

66) J.W.Ross "Solid State and Liquid Membrane ISE`s" Ch.2 of "ISE`s" NBS special publication No.317 Washington 1969

67) A.Zalkin , D.H.Tompleton J.Am.Chem.Soc.75 2453 (1953)

68) T.Anfalt , D.Jagner Anal.Chem.Acta 50 23 (1970)

69) K.Schwabe , H.Dahms Z.Electrochemie 65 518 (1961)

70) H.J.Nielsen , E.H.Hansen Anal.Chim.Acta 85 1 (1976)

71) T.P.Hadjuoanou , E.P.Diamandis Anal.Chim.Acta 94 443 (1977)

72) H.Staudinger "Die Hochmolekularen Verbindungen" Springer-Verlag OHG Berlin 1932

73) W.H.Carothers Collected Papers : High Polymers Vol.1 Wiley 1940

74) P.J.Flory "Principles of Polymer Chemistry" Cornell University Press 1953

75)R.B.Seymour "Introduction to Polymer Chemistry" McGraw Hill 1971

76) P.W.Morgan , S.L.Kwolek J.Chem.Ed. 36 182 (1959)

77) P.W.Morgan "Condensation Polymers" Interscience Wiley 1965

78) M.L.Bender , J.M.Jones J.Org.Chem. 27 3771 (1962)

79) J.F.Norris , V.W.Ware J.Am.Chem.Soc. 61 1418 (1939)

80) E.M.Hodnett , D.A.Holmer J.Polm.Sci. 58 1415 (1962)

81) E.Z.Fainberg , N.V.Mikhailov Polym.Sci.USSR 3 222 (1962)

82) W.A.H.Haffman , R.W.Smith , W.T.Dye Chem.Abstr. 58 9254 (1963)

83) J.Davies Private Communication

84) W.J.Albery , M.L.Hitchman "Ring Disc Electrodes" Clarendon Press 1971

85) R.A.Choudhery Ph.D.Thesis London 1985

86) W.G.Cochran Proc.Camb.Phil.Soc.Math.Phys.Sci. 30 365 (1954)

87) V.G.Levich "Physicochemical Hydrodynamics" Prentice Hall (1962)

88) W.J.Albery Trans.Faraday Soc. 62 1915 (1966)

89) W.J.Albery , S.Bruckenstein ibid. 62 1920 (1960)

90) D.Midgeley , K.Torrance "Potentiometric Water Analysis" Wiley 1971

91) J.Katin , S.Szpak , P.N.Dennion J.Electrochem.Soc. 120 883 (1973)

92) W.J.Albery , S.Bruckenstein , D.T.Napp Trans.Faraday Soc. 62 1932 (1966)

93) W.J.Albery , A.R.Mount to be published

94) Southampton Electrochemistry Group "Instrumental Methods in Electrochemistry" J.Wiley 1985

95) K.Snook Ph.D. Thesis London 1983

96) P.Fisk D.Phil Oxford 1978

97) N.Wagner , K.Dose , H.Koch , H.Ringsdorf Febs.Lett. 132(2) 313 (1981)

98) D.R.Day , H.Ringsdorf Makromol.Chem. 180 1059 (1979)

99) W.R.Redwood , F.R.Pfeiffer , J.A.Weisbach , T.E.Thompson Biochim.Biophys.Acta 233 1 (1979)

100) R.D.Armstrong , J.C.Lockhart , M.Todd Electrochimica Acta 31(5) 591 (1986)

101) R.D.Armstrong , A.K.Covington , G.P.Evans Electroanal.Chem. 159 33 (1983)

102) R.D.Armstrong , A.K.Covington , G.P.Evans , T.Handyside

Electrochimica Acta 29(8) 1127 (1984)

103) J.Davies Personal Communication